Se

\CE PLASMON POLARITONS AND DETERMINATIO
X DIELECTRIC PERMITTIVITY AND THICKNESS
THIN METAL (SEMICONDUCTOR) FILMS

By

ABDURAHMAN AHMED

A Thesis

Presented to the

School of Graduate Studies

and

The Faculty of Science

Addis Ababa University

In Partial Fulfillment of the

Requirement for the Degree

Master of Science in Physics

June, 1989

Abstract

Surface plasmon-polaritons (SPlP) which can be excited on dielectric/metal (dielectric/semiconductor) interface can be used as highly sensitive non distructive probe for the determination of the dielectric constant $\varepsilon(w) = \varepsilon'(w) + i\varepsilon''(w)$ and thickness h of a metal semiconductor) film without a preset expression for $\varepsilon(w)$.

The theoretical background of the method [3] is based on the solution of the Maxwell's equations which provides the disperssion equation of SPlP at the surface of a thin metal (semiconductor) film and its interpretation in terms of attenuated total reflection (ATR) characteristics. The physical sense of the solution is demonstrated through the power flows and the field distributions of SPlP and other possible excitations.

It is shown that for strong absorbing metals (semiconductors) low radiative SPlP can exist at frequencies higher than the plasma frequency W_p. The analysis of the approximate solution of the approximate solution of dispersion equation for thin metal (semiconductor) film [3] established a well-defined limited frequency range of its applicability. It was found that the upper frequency limit depends upon the thickness of the film and falls down from $W_p/\sqrt{2}$ to $\sim 0.35\ W_p$ as $h \to 0$.

A computer model simulating realistic experimental conditions of measurement ATR characteristics is discussed. The accuracy of $\varepsilon'(w)$, $\varepsilon''(w)$ and h determination is established.

Acknowledgement

I would like to express my deepest gratitude and respect to my advisor and instructor Dr. D.A. Letov for paying series attention to the work accomplished, and his persistent assistance and guidance in the computer program. In addition, I owe a debt to him who aroused my interest, for further research (in his field, and from whose lectures I benefited much.

I am also grateful to Dr. P. Hurshka for his guidance in applying numerical analysis and the basic aknowledge of a computer. My gratitude also goes to W/o Shenaz Ahmed who undertook to type this paper work in devoting her valuable time.

Finally the Swedish Agency for Research Cooperation with Developing Countries (SAREC) is gratefully acknowledged for a financial support obtained through the Ethiopian Science and Technology Commission.

Abdurahman Ahmed

INTRODUCTION

The internal degrees of freedom of a medium generally excited by the passage through it of an electromagnetic wave. Infact because of the medium, the electromagnetic wave becomes a new type of wave in which the original electromagnetic field is modified by the induced polarization of the medium. This new mode of excitation is known as a polariton. For example, a photon coupled to the elementary excitation of an electron plasma in metals or semiconductors is called a plasmon polariton. A photon coupled to the lattice vibration in a crystal is called a phonon polariton, and so on.

Under certain conditions plasmon polariton propagates along the boundary of metals or semi-conductors with dielectric medium (discussed in Chapter I).

This type of elementary excitations is called a surface plasmon polariton (SPlP). The electric and magnetic fields of SPlP are taking maximum values at the interface metal or semiconductor/dielectric medium and are exponentially decaying with distance from a boundary in the direction of normal.

Concentration of the electromagnetic field near the metal or semi-conductor surface makes SPlP very sensitive to minor changes in characteristic quantities of interfacing media (like complex dielectric permittivity $\varepsilon = \varepsilon' + i\varepsilon''$) and to the state of roughness of the boundary.

Therefore SPlP constitutes a highly sensitive non-destroying probe for measuring purposes, particularly in the optical and infra-red range of frequencies.

Chapter I

1.1 Derivation of SPLP dispersion equation semiinfinite media case.

Suppose a TM polarization $\vec{H} = \vec{H}_z$ wave is incident on the interface n_1/n_2 of two media as shown in Fig.(1.1).

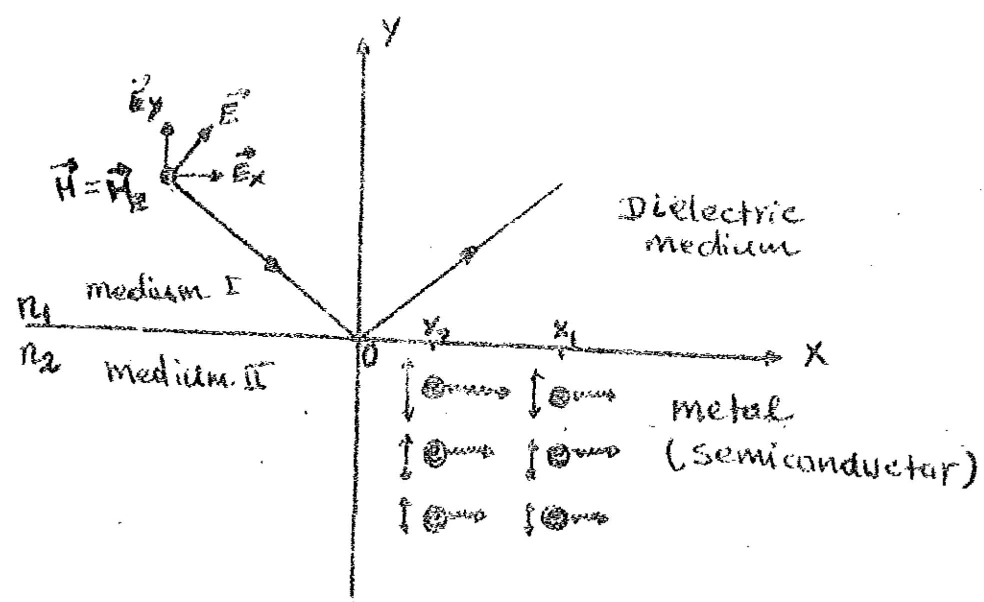

Fig.(1.1) General view of a boundary between semi-infinite dielectric medium and semi-infinite metal or semiconductor.

$$\vec{H} = \langle 0,0,H_z \rangle \text{ ------------- } \quad (1.1)$$

Maxwell's Curl equations and equation (1.1) yield in

$$\vec{E} = \vec{E}_x + \vec{E}_y \text{ --------------- } \quad (1.2)$$

where E_x is parallel to the interface, and E_y is perpendicular to the interface. It is known from the electromagnetic theory that an acclerating charge radiates a secondary electromagnetic wave in the direction perpendicular to the direction of the charges motion. This implies that the E_x component of the incident primary radiation sets up the oscillation of an electron at metal or semiconductor surface

$X = X_o$ in the OX direction. The secondary radiation is in the OY direction. The radiation in the y>0 direction adds up to the radiation reflected from the n_1/n_2 interface. The radiation in the Y<0 direction is absorbed by the IInd medium.

The EY component of the electric field produces oscillation of the electron perpendicular to the surface. The secondary radiation from the electron propagates along the surface. Part of the secondary radiation in OX direction contributes to the radiation reflected from the n_1/n_2 interface and another part of it sets up oscillations of electrons in neighbouring position $X = X_1$ and the metal or semi-conductor surface. The same is true for electrons which are situated below the metal or semiconductor surface at distances of the range of skin depth. See Fig. (1.1)

Transmittance of the OY oscillations in the OX direction via secondary radiation represent a new mode of excitation called surface plasmon polariton (SPP).

Now, let us see the electric and magnetic fields of the guided SPP.

Suppose the H_Z in medium II can be described as:

$$H^P_{Z2} = A_{2e}^{-iK_{2y}Y} e^{i(K_x X - \omega t)} \text{ --------- } (1.3)$$

where $K_{2y} = K'_{2y} + iK''_{2y}$; $K_x = K_x + iK''_x$ (the wave vectors) are describing propagation along OY direction and OX direction (along the surface) respectively.

But from the boundary condition, $H_{2t} - H_{1t} = \hat{J}$ (where H_{it}, (i=1,2) is the tangential component of the magnetic field, and J is linear density of the current flowing parallel to the inteface), if there is no external source, $\hat{J} = 0$ then

then $H_{2t} = H_{1t}$ ---------------- (4a)

equation (4a) implies that there must be some distribution of magnetic field in medium I. Supposing that, magnetic field distribution in medium I is of the same nature as in medium II,

$$H^P_{Z1} = A_1 \, e^{ik_{1Y}Y} \, e^{i(K_X X - wt)} \text{ ------} \qquad (4b)$$

where $K_{1y} = K'_{1y} + iK''_{1y}$ is wave vector that describes propagation along OY direction in medium I. The value of K_x must be universal for both medium, since the electric and magnetic fields in medium I and in medium II are to be matched at Y = 0, at any arbitrary value of X. From the boundary condition

$$H^P_{Z2} \ (Y=0) = H^P_{Z1} \ (Y = 0)$$

which results $A_2 = A_1 = A$, where A is the amplitude. Now let us consider the boundary condition for tangential components of the electric field, E_x component in this case

$$E_{x2} = E_{x1} \quad \text{at } Y = 0.$$

From Maxwell's curl equation we can express E_x through H_Z, that is

$$\nabla \times \vec{H}_Z = \epsilon \frac{\partial \vec{E}}{\partial t} + \hat{J} \text{, but } \hat{J} = 0$$

or
$$\begin{vmatrix} i & j & k \\ \frac{\partial}{\partial x} & \frac{\partial}{\partial y} & 0 \\ 0 & 0 & H_Z \end{vmatrix} = -iw\epsilon(\vec{E}_x + \vec{E}_y)$$

$$H^P_{Z2} = A \, e^{-ik_{2y}Y} \, e^{i(k_x X - wt)}$$

$$H^P_{Z1} = A \, e^{i k_{1y} Y} e^{i(k_x X - wt)}$$

$$\frac{\partial H_Z}{\partial y} = -i w E_x \; ; \; E_x = \frac{i}{w\varepsilon} \frac{\partial H_Z}{\partial y}$$

$$\frac{\partial H_Z}{\partial x} = i w E y \; ; \; E_y = -\frac{i}{w\varepsilon} \frac{\partial H_Z}{\partial x}$$

then it follows

$$E_{x1} = -\frac{K_{1y}}{w\varepsilon_1} H^P_{Z1}$$

$$E_{X2} = +\frac{K_2^Y}{W\varepsilon_2} H^P_{Z2}$$

At $Y = 0$; $-\frac{K_{1y}}{\varepsilon_1} = +\frac{K_{2y}}{\varepsilon_2}$

Or $\frac{K_{1y}}{k_{2y}} = -\frac{\varepsilon_1}{\varepsilon_2}$ or $\frac{K_{1y}}{k_{2y}} = -\frac{\varepsilon r_1}{\varepsilon_{r2}}$ -------- (16)

where εr_1 and $\varepsilon r_2 = \varepsilon r_2' + i\varepsilon r_2''$ are relative dielectric permittivities of medium I and medium II respectively. From now on we shall operate with relative dielectric permittivities only. Therefore, for short writtening representation we shall denote again εr_1 as ε_1, and εr_2 as ε_2.

Now let us find the relationship between K_{1y} and K_1 using the wave equation.

$$\nabla^2 H_Z = \frac{\varepsilon 1}{C^2} \frac{\partial^2 HZ}{\partial t^2} \quad \text{-------------} \quad (17)$$

Since we assume that $H^P_{Z1} \sim e^{i(\vec{k}_1 \cdot \vec{r} - wt)} = e^{i(k_x x + k_{1y} Y - wt)}$ equation (17) can be written as

$$\vec{K}_1 \cdot \vec{K}_1 = K_o^2 \varepsilon_1 \text{ ---------- } \quad (1.8)$$

$$K_1'^2 - K_1''^2 + 2iK_1' K'' \cos (K_1 \wedge K_1'') = K_o^2 \varepsilon_1 \text{ ------ } \quad (1.8a)$$

Resolving equation (1.8) into real and imaginary parts, we get:

$$K_1'^2 - K_1''^2 = K_o^2 \varepsilon_1 \text{ ---------- } \quad (1.9)$$

$$2K_1' K_1''^2 \cos (K_1 \wedge K_1'') = \text{ ---------- } \quad (1.10)$$

equation (1.10) indicates that in dielectric medium I $\vec{K}_1 \perp \vec{K}_1''$

Next let us resolve K' and K" into components

$$\vec{K}_1' = \vec{K}_{1x} + \vec{K}_{1y}' = \vec{K}_x' + \vec{K}_{1y}' \text{ ---------- } \quad (1.11)$$

$$\vec{K}_1'' = \vec{K}_{1x}'' + \vec{K}_{1y}'' = \vec{K}_x'' + \vec{K}_{1y}'' \text{ ---------- } \quad (1.12)$$

On the other hand let us consider

$$K_x^2 + K_{1y}^2 = (K_x' + iK_x'')^2 + (K_{1y}' + iK_{1y}'')^2$$

$$= K_x'^2 - K_x''^2 + K_{1y}''^2 + 2i[K_x' K_x'' + K_{1y}' K_{1y}''] + K_{1y}'^2$$

$$= K_x'^2 + K_{1y}'^2 - K_x''^2 - K_{1y}''^2 + 2iK_L' K_1'' \cos (K_1' \; K_1'')$$

$$= K_1'^2 - K_1''^2 + 2iK_1' K_1'' \cos (\vec{K}_1 \; \vec{K}_1'') \text{ ---- } (1.13)$$

Comparison of equation (1.13) with equation (1.8a) gives results

$$\vec{K}_1 \cdot \vec{K}_1 = K_x^2 + K_{1y}^2 = K_o^2 \varepsilon_1 \text{ ------ } \quad (1.14)$$

Hence

$$K_{1y} = \sqrt{K_o^2 \varepsilon_1 - K_x^2} \quad \text{------} \quad (1.15)$$

Similar consideration for the conducting medium II, with

$$H_{Z2} \sim e^{i(\vec{K}_2 \cdot \vec{r} - wt)} = e^{i(K_x x - K_{2y} y - wt)}$$

gives

$$\vec{K}_2 \cdot \vec{K}_2 = K_o^2 \varepsilon_2 \quad \text{------} \quad (1.16)$$

Or

$$K_2'^2 - K_2''^2 + 2iK_2' K_2'' \cos(\vec{K}_2' \wedge \vec{K}_2'') = K_o^2 \varepsilon_2' + iK_o^2 \varepsilon_2'' \text{ ----}$$

Resolving equation (1.17) into real and imaginary parts we get

$$K_2'^2 - K_2''^2 = K_o^2 \varepsilon_2' \quad \text{------} \quad (1.18)$$

$$2K_2' K_2'' \cos(\vec{K}_2' \wedge \vec{K}_2'') = K_o^2 \varepsilon_2'' \quad \text{------} \quad (1.19)$$

Equation (1.19) indicates that the angle between $\vec{K}_2'$ and $\vec{K}_2''$ is less than $\pi/2$, since $\varepsilon_2'' > 0$.

On the other hand, let us consider the following

$$K_x^2 + K_{2y}^2 = (K_x' + iK_x'')^2 + (K_{2y}' + iK_{2y}'')^2$$

$$= K_x'^2 - K_x''^2 + K_{2y}'^2 - K_{2y}''^2 + 2i[K_x' K_x'' + K_{2y}' K_{2y}'']$$

$$= K_2'^2 - K_2''^2 + 2iK_2' K_2'' \cos(\vec{K}_2' \wedge \vec{K}_2'') \quad \text{------} \quad (1.20)$$

Comparison of equation (1.20) with equations (1.18) and (1.19) results

$$\vec{K}_2 \cdot \vec{K}_2 = K_x^2 + K_{2y}^2 = K_o^2 \varepsilon_2 \quad \text{------} \quad (1.21)$$

Hence

$$K_{2y} = \sqrt{K_o^2 \varepsilon_2 - K_x^2} \quad \text{------} \quad (1.22)$$

The graphical representation for the components of $\vec{K}_1$ and $\vec{K}_2$ is shown at fig. (1.2) below.

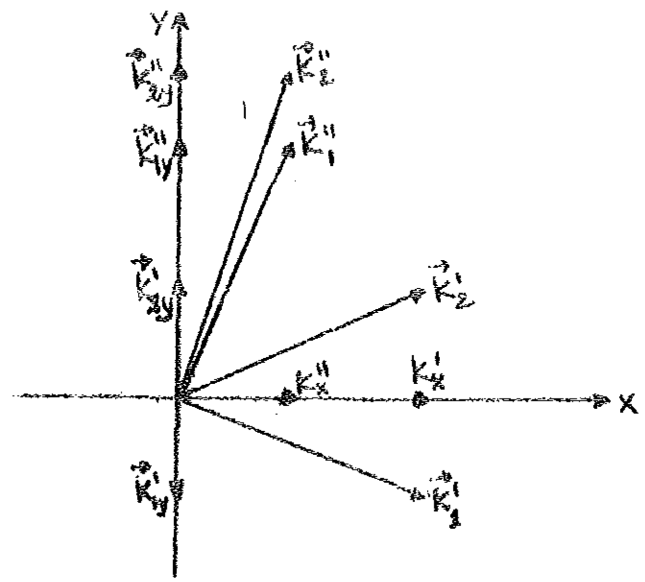

Fig.(1.2) The graph of $\vec{K}_1$ and $\vec{K}_2$ and their components in cartesian representation.

Substitution of equations (1.15) and (1.22) into equation (1.6) results

$$\frac{\sqrt{K_o^2\,\varepsilon_1 - K_x^2}}{\sqrt{K_o^2\,\varepsilon_2 - K_x^2}} = -\frac{\varepsilon_1}{\varepsilon_2} \qquad (1.23)$$

Resolving equation (1.23) for K_x we receive

$$K_x = K_o \sqrt{\frac{\varepsilon_1\,\varepsilon_2}{\varepsilon_1+\varepsilon_2}} \qquad (1.24a)$$

Equation (1.24a) describes the dispersion equation of SPIP

where $K_o = \frac{W}{C}$ is the wave vector in vacuum

$C =$ speed of light in vacuum

$W =$ angular frequency of the source

For metals the dielectric permittivity function of a free electron model is given by (1.24b) [1]. A medium with a positive dielectric function is oftern termed a 'passive medium', and commonly used examples of such media include air, vacuum, glass, etc. A medium with a negative dielectric function is called an 'active medium', and include metals and semiconductors at frequencies below the plasma frequency W_p [1].

$$\varepsilon_2(W) = 1 - \frac{W_p^2}{W(W + i\tau^{-1})} = \varepsilon_2' + i\varepsilon_2'' \qquad \text{------} \qquad (1.24b)$$

$$= 1 - \frac{W_p^2}{(W^2+\tau^{-2})} + i\,\frac{W_p^2}{W\tau} \cdot \frac{1}{(W^2+\tau^{-2})}$$

which results

$$\varepsilon_2'(W) = 1 - \frac{W_p^2}{(W^2+\tau^{-2})} \quad ; \quad \varepsilon_2''(W) = \frac{W_p^2}{W\tau} \cdot \frac{1}{(W^2+\tau^{-2})}$$

$$W_p^2 = \frac{N_e 2}{\varepsilon_o m^*}$$

Where N is the free electron density, e is the electronic charge ε_o is permittivity of free space, m* is the effective 'mass' and τ is the relaxation time describes electron photon collision.

The dependence of ε_2' and ε_2'' on the angular frequency W is seen at figure (1.7).

1.2 The Analysis of the Dispersion Equation

The simplest case in the analysis of the dispersion equation is, the case in which the absorbing part in the expression of ε_2 is zero tha is $\varepsilon_2'' = 0$. Under this case the whole range of frequencies could be separated into three sub ranges.

In the first subrange; $0 < W < \frac{W_p}{\sqrt{\varepsilon_1+1}}$ from equation (1.24a) we have;

$$\varepsilon_2' < 0, \quad \varepsilon_1+\varepsilon_2' < 0 \text{ and } K_x' > 0; \; K_x'' = 0 \quad \text{------------} \quad (1.25)$$

From equation (1.15) and equation (1.22)

$$\left.\begin{array}{ll} K_{1y}' = 0 \; ; & K_{1y}'' > 0 \\ K_{2y}' = 0 \; ; & K_{2y}'' > 0 \end{array}\right. \quad \text{------------} \quad (1.26)$$

which means that a non radiative plasmon exists.

Let us support this conclusion from the general consideration of the energy flow.

Time average poynting vector component along OX direction is given in air at X=0 and Y=0 by

$$S_x^I = \tfrac{1}{2} R_e \, E_{oy}^I \; H_{oZ}^{I*} = \frac{K_x'}{2W\varepsilon_o \; \varepsilon_1} \quad \text{------} \quad (1.27)$$

in metal at X=0, and y=0

$$S_x^{II} = \tfrac{1}{2} R_e E_{oy}^{II} . H_{oZ}^{II*} = \tfrac{1}{2} \; \frac{[\varepsilon_2' K_x' + \varepsilon_2'' K_x'']}{W\varepsilon_o [\varepsilon_2'^2 + \varepsilon_2''^2]} \quad \text{---} \quad (1.28)$$

Time average Poynting vector component along OY direction is given by, in air, at X=0, and y=0 by

$$S_y^I = -\tfrac{1}{2} R_e \; E_{ox}^I \; H_{oZ}^{I*} = \frac{K_{1y}'}{2W\varepsilon_o \varepsilon_1} \quad \text{--------} \quad (1.29)$$

Similarly in metal at X=0, and Y=0

$$S_y^{II} = -\tfrac{1}{2} R_e \, E_{ox}^{II} \, H_{oZ}^{II*} = -\tfrac{1}{2} \frac{[\varepsilon_2' K_{2y}' + \varepsilon_2'' K_{2y}'']}{W\varepsilon_o [\varepsilon_2'^2 + \varepsilon_2''^2]} \quad \text{------} \quad (1.30)$$

The non absorbing case $\varepsilon_2'' = 0$ will be demonstrated as a limiting case of derived general formulas.

Suppose that

$$\varepsilon_2'' < |\varepsilon_2'| \;, \quad \varepsilon_2'' < |(\varepsilon_1 + \varepsilon_2)|$$

Under these assumptions for $0 < W < \dfrac{W_p}{\sqrt{\varepsilon_1 + 1}}$

From equation (1.24a)

$$K_x' = K_o \sqrt{\frac{\varepsilon_1 \varepsilon_2'}{\varepsilon_1 + \varepsilon_2'}} > 0 \quad \text{----------} \quad (1.31)$$

$$K_x'' = K_o \sqrt{\frac{\varepsilon_1 \varepsilon_2'}{\varepsilon_1 + \varepsilon_2}} \cdot \frac{\varepsilon_1 \varepsilon_2''}{2\varepsilon_2' (\varepsilon_1 + \varepsilon_2')} > 0 \quad \text{------} \quad (1.32)$$

See Fig.(13a) and Fig. (14a).

(Note that letter "a" corresponds to $\tau = 10^{1.25}$ sec)

From equation (1.15)

$$K_{1y}' = -\frac{K_x' K_x''}{K_{1y}''} = -\frac{K_o \, \varepsilon_1 \, \varepsilon_2'' \sqrt{-(\varepsilon_1 + \varepsilon_2')}}{2(\varepsilon_1 + \varepsilon_2')^2} < 0 \quad \text{-----} \quad (1.33)$$

$$K_{1y}'' = \sqrt{K_x'^2 - K_o^2 \varepsilon_1} = K_o \frac{\varepsilon_1}{\sqrt{-(\varepsilon_1 + \varepsilon_2')}} > 0 \quad \text{-----} \quad (1.34)$$

From equation (1.22)

$$K_{2y} = \frac{K_o^2 \varepsilon_2'' - 2K_x' K_x''}{2K_{2y}''} = -K_o \frac{\varepsilon_2'' (2\varepsilon_1 + \varepsilon_2')}{2(\varepsilon_1 + \varepsilon_2')^2} \sqrt{-(\varepsilon_1 + \varepsilon_2')} \quad \text{----} \quad (1.35)$$

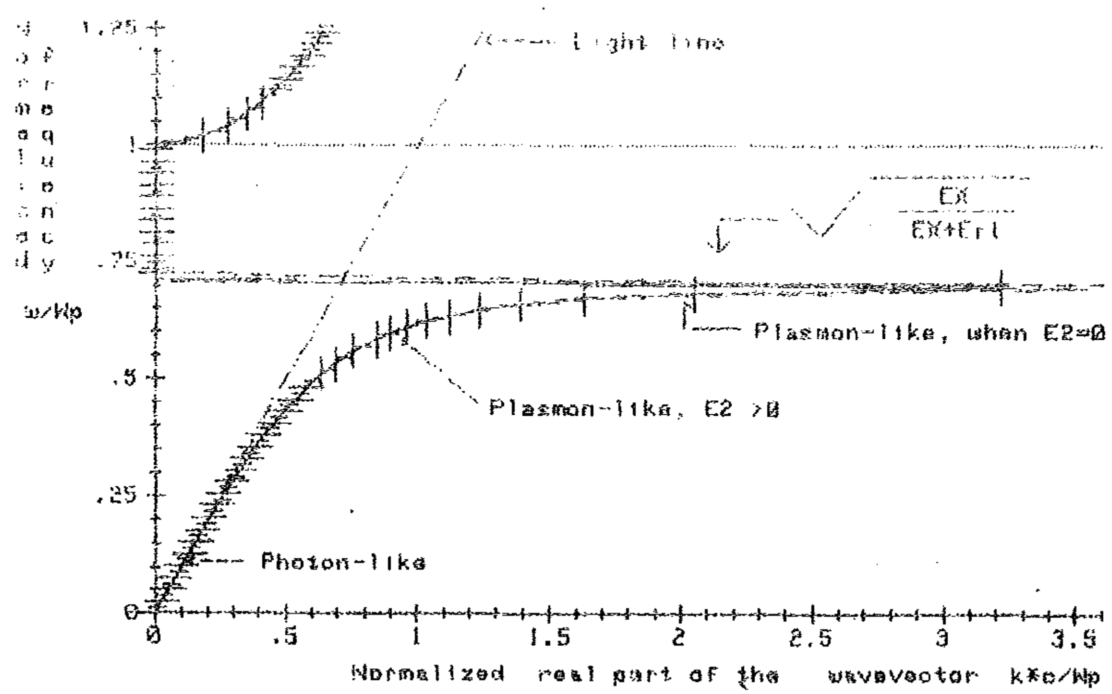

Fig(3a) Surface plasmon-polariton dispersion curve for a free electron metal plotted for: (a) real k, real ω - (solid curve); (b) real ω, real part of complex k - (broken line). The curves are plotted in dimensionless units. Wp = 1.E+15 rad/s ; Tau = 1.E+125 s

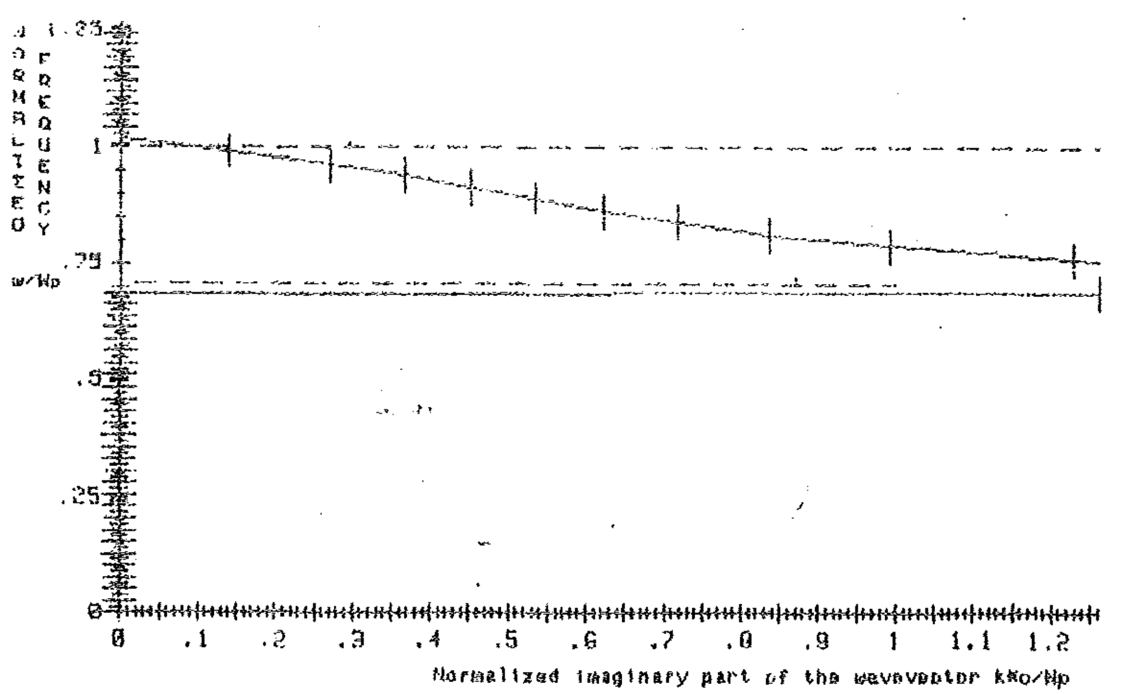

Fig(4a) Surface plasmon-polariton dispersion curve for imaginary part of complex k versus real ω: (a) exact numerical solution (||||| - line); (b) approximate analytical solution - (IIIII line). Wp = 1.E+15 rad/s ; Tau = 1.E+125 s

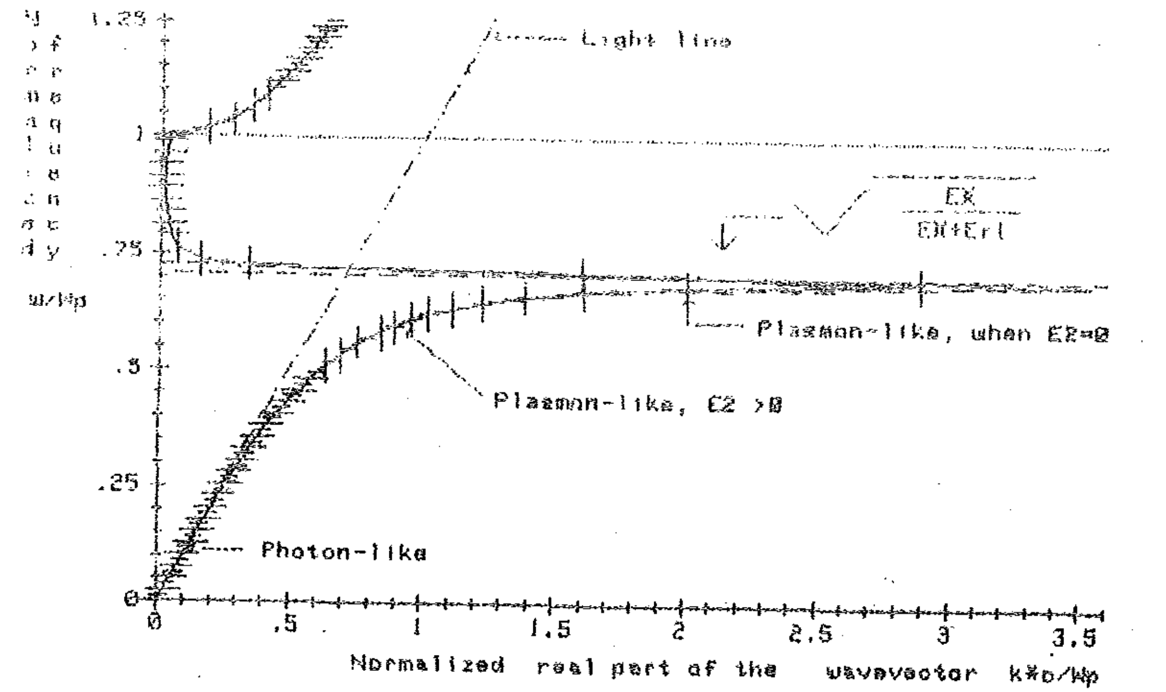

Fig(1-3b) Surface plasmon-polariton dispersion curve for a free electron metal plotted for: (a) real k, real w - (solid curve); (b) real w, real part of complex k - (broken line). The curves are plotted in dimensionless units. Wp = 1.E+15 rad/s ; Tau = 1.E-13 s

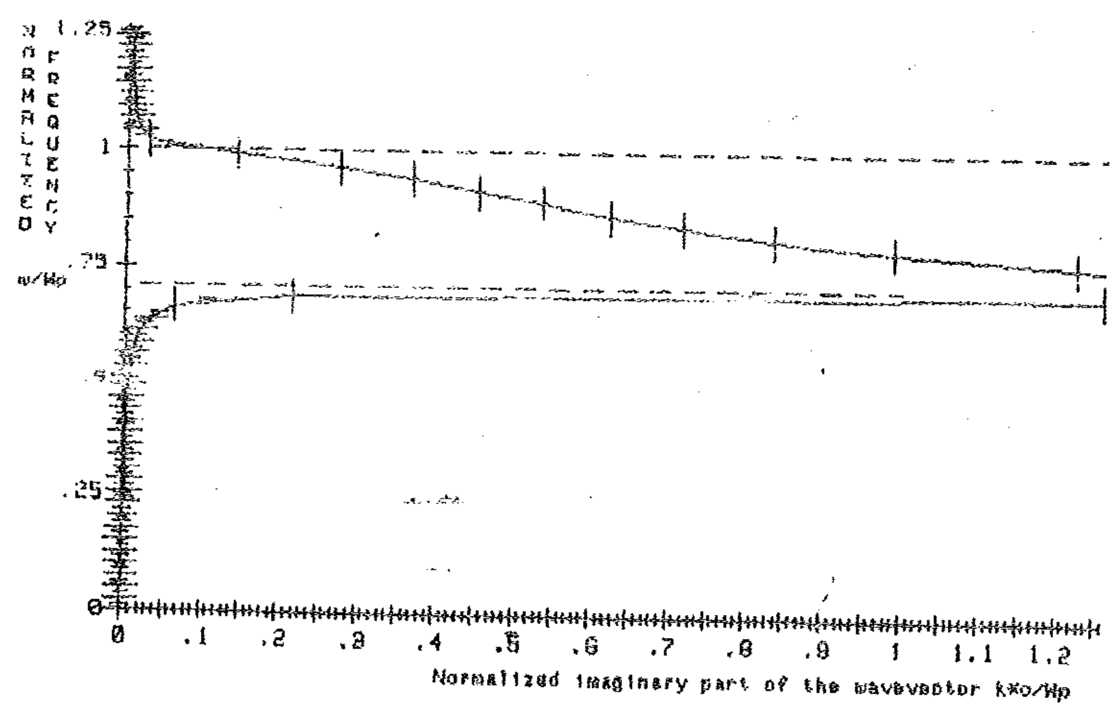

Fig.(1-4b) Surface plasmon-polariton dispersion curve for imaginary part of complex k versus real w: (a) exact numerical solution (||||| - line); (b) approximate analytical solution - (IIIII line). Wp = 1.E+15 rad/s ; Tau = 1.E-13 s

$$K_{2y}'' = K_o \frac{\mathcal{E}_2'}{\sqrt{-(\mathcal{E}_1+\mathcal{E}_2')}} > 0 \text{ ---------- } (1.36)$$

See Fig. (1.5a) and Fig. (1.6a)

From equations (1.27) to (1.30) and using equations (1.31) to (1.36)

$$S_x^{\ I} = \frac{K_o}{2W\varepsilon_o} \quad \frac{1}{\varepsilon_1} \sqrt{\frac{\varepsilon_1 \ \varepsilon_2'}{\varepsilon_1+\varepsilon_2'}} > 0 \text{ ---- } (1.37)$$

$$S_x^{II} = \frac{1}{2W\varepsilon_o} \quad \frac{K_x'}{\varepsilon_2'} = \frac{K_o}{2W\varepsilon_o\varepsilon_2'} \sqrt{\frac{\varepsilon_1\varepsilon_2'}{\varepsilon_1+\varepsilon_2'}} < 0 \text{ ---- } (1.38)$$

$$S_y^{\ I} = -\frac{K_o}{2W\varepsilon_o} \left(\frac{\varepsilon_2'' \sqrt{-(\varepsilon_1+\varepsilon_2')}}{2(\varepsilon_1+\varepsilon_2')2} \right) < 0 \text{ -------- } (1.39)$$

$$S_y^{II} = -\frac{K_o}{2W\varepsilon_o} \left(\frac{\varepsilon_2'' \sqrt{-(\varepsilon_1+\varepsilon_2')}}{2(\varepsilon_1+\varepsilon_2')^2} \right) < 0 \text{ ------- } (1.40)$$

Let us normalize the power flows in equations (1.37) to (1.40) to the total power flow in both media. Since $S_x'' < 0$, we shall take it as follows:

$$S_{tot} = \sqrt{(S_x^{\ I} + |\ S_x^{\ II}|)^2 + S_y^{\ 2}} \text{ ------- } (1.41)$$

where $S_y = S_y^{\ I} = S_y^{\ II}$

For frequencies $0 < w < \frac{W_p}{\sqrt{\varepsilon_1+1}}$, $S_y^{\ 2} << (S_x^{\ I} + |S_x^{\ II}|)^2$

therefore,

$$S_{tot} = S_x^{\ I} + \left|S_x^{\ II}\right|$$

$$\frac{K_o \sqrt{\frac{\varepsilon_1\varepsilon_2'}{\varepsilon_1+\varepsilon_2'}}}{2W\varepsilon_o} \left[\frac{\varepsilon_1+|\varepsilon_2'|}{\varepsilon_1\cdot|\varepsilon_2'|} \right] \text{ ------- } (1.42)$$

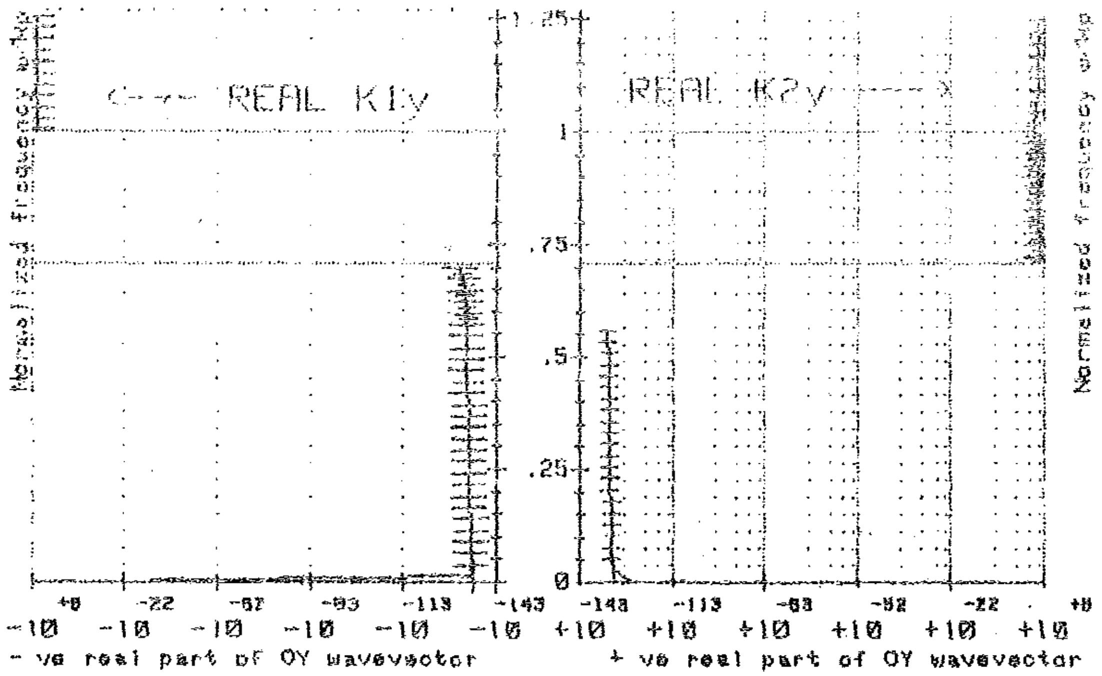

Fig(05a) REAL parts of the Ky wave vector: (a) in dielectric
medium I - (|||| - line); (b) in metal - (IIIII - line)
Wp= 1.E+15 rad/s; Tau= 1.E+125 s *

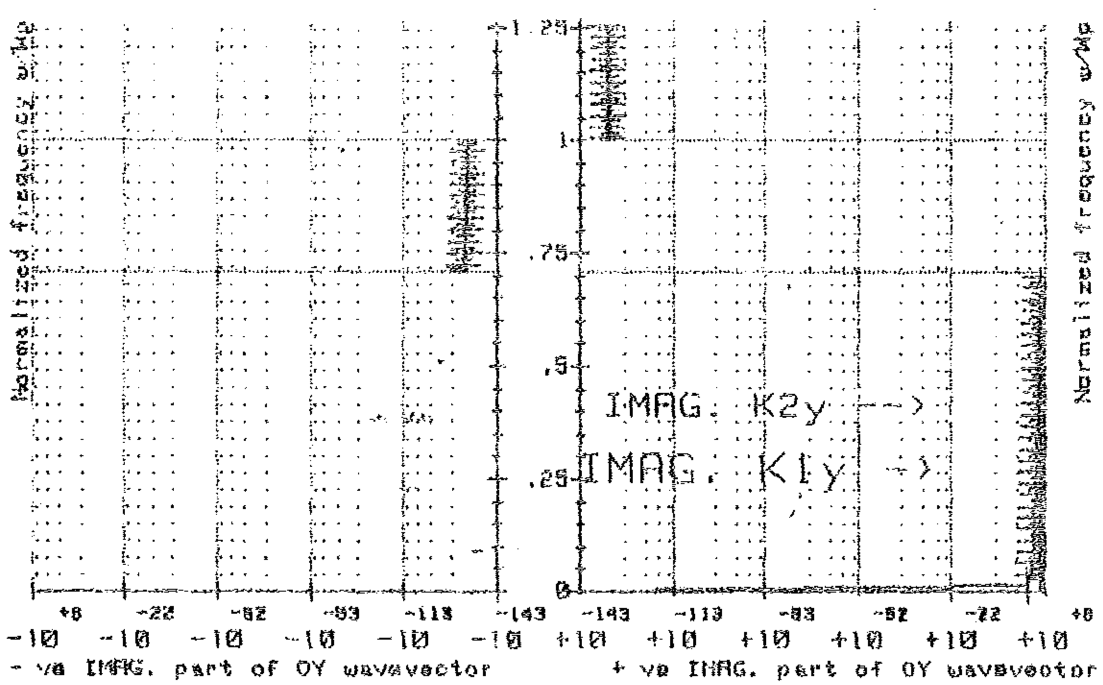

Fig(06a) Imaginary parts of the Ky wave vector: (a) in dielectric
medium I - (|||| - line); (b) in metal - (IIIII - line)
Wp= 1.E+15 rad/s; Tau= 1.E+125 s *

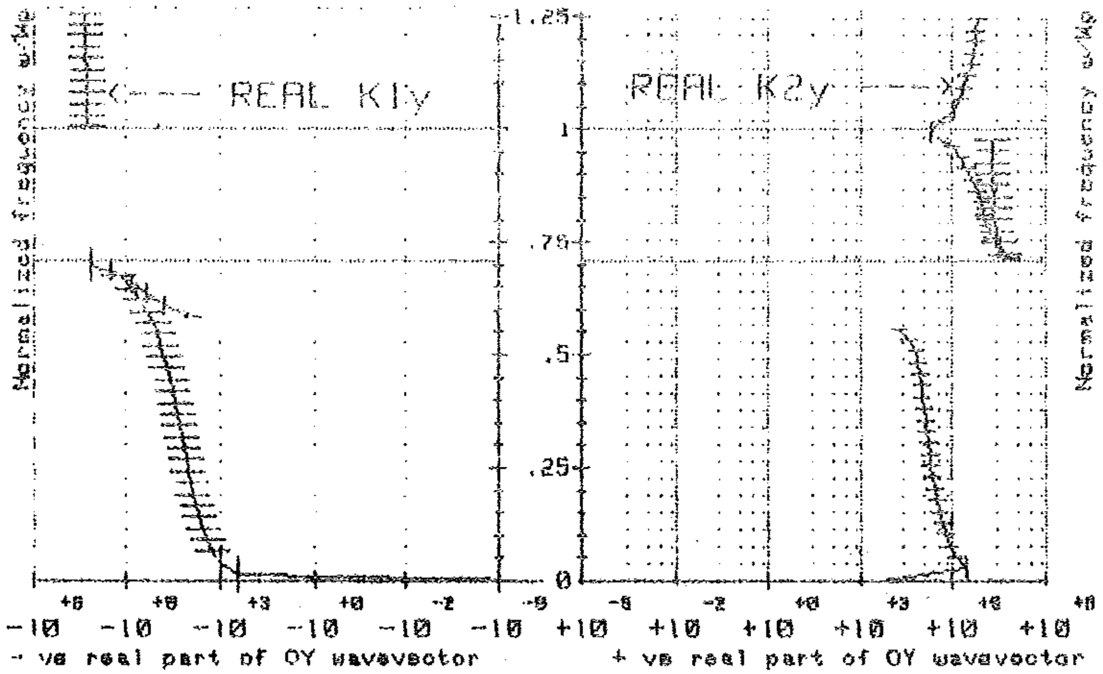

Fig (15b) REAL parts of the Ky wave vector: (a) in dielectric
medium 1 - (|||| - line); (b) in metal - (IIIII - line)
Wp= 1.E+15 rad/s; Tau= 1.E-13 s

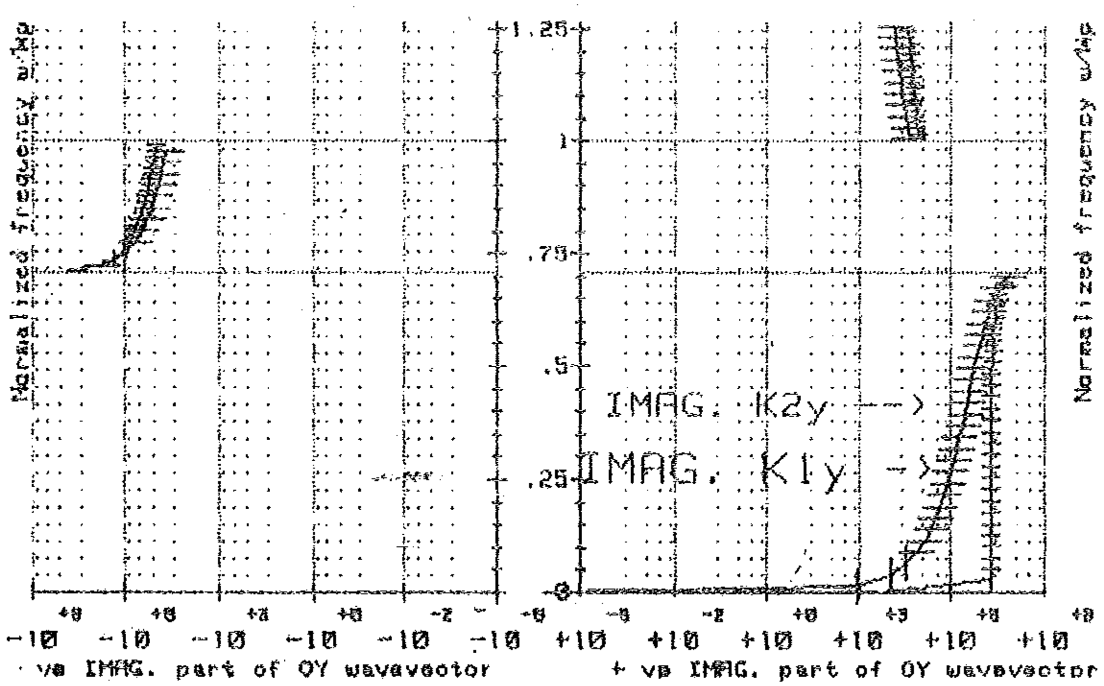

Fig (16b) Imaginary parts of the Ky wave vector: (a) in dielectric
medium 1 - (|||| - line); (b) in metal - (IIIII - line)
Wp= 1.E+15 rad/s; Tau= 1.E-13 s

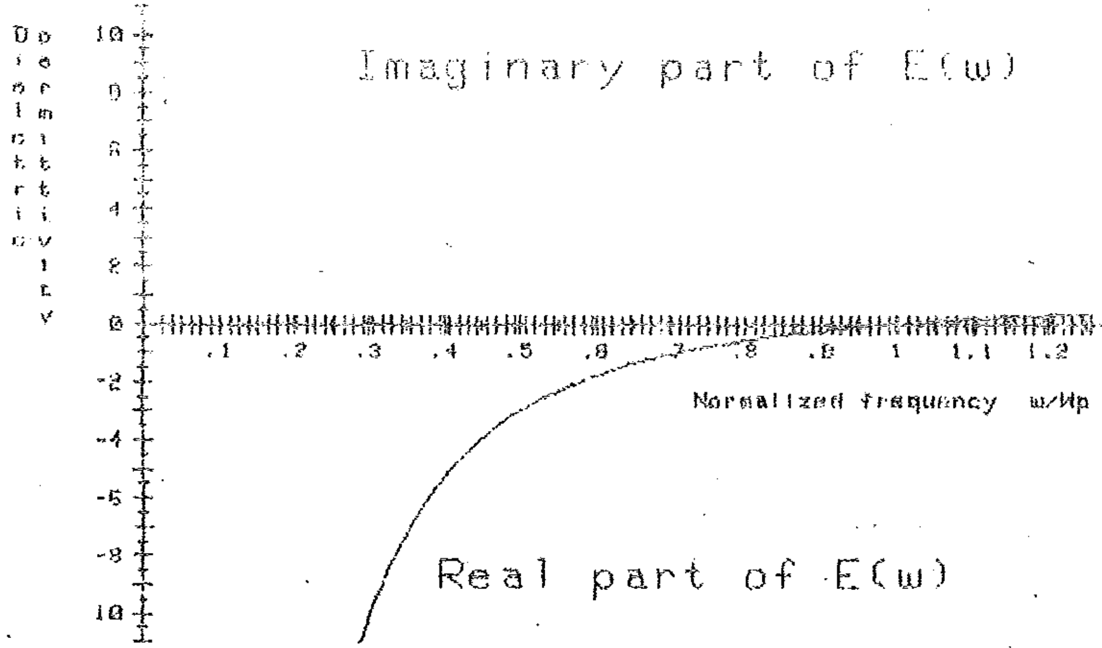

Fig.([illegible]a) Graph of dielectric permittivity versus normalized frequency:
(a) real part of E(w) - (solid line) ; (b) imaginary part
of E(w) - (broken line). Wp = 1.E+15 rad/s ; Tau = 1.E+12[illegible]s

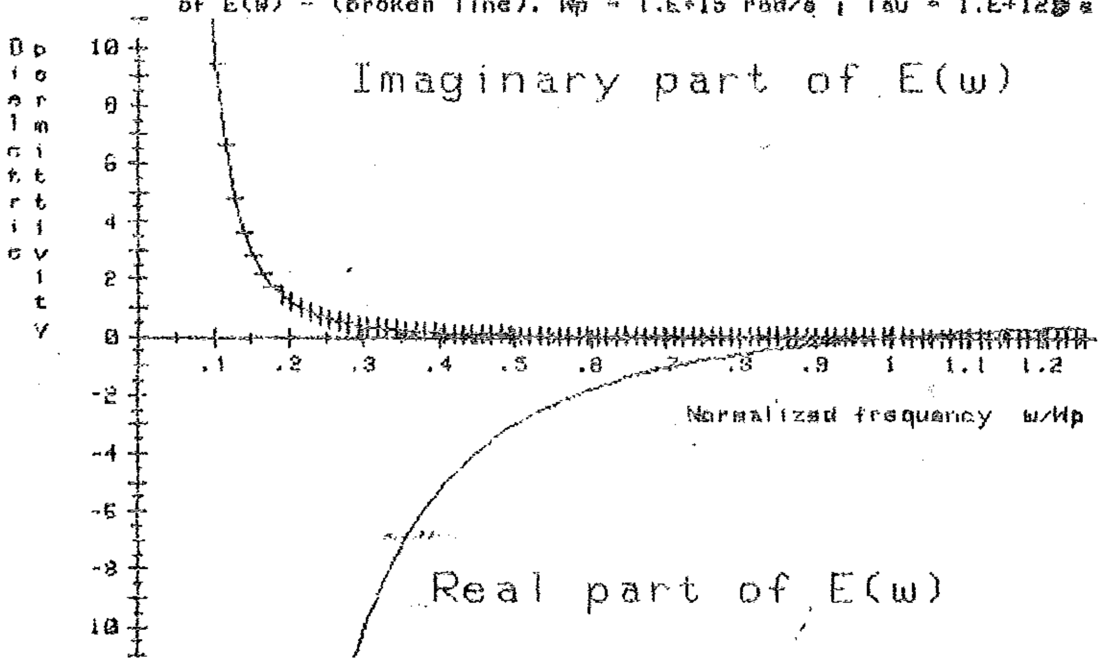

Fig.([illegible]b) Graph of dielectric permittivity versus normalized frequency:
(a) real part of E(w) - (solid line) ; (b) imaginary part
of E(w) - (broken line). Wp = 1.E+15 rad/s ; Tau = 1.E-13*s

The normalized power flow can be expressed as:

$$S_{xn}^{I} = \frac{S_x^{I}}{S_{tot}} = \frac{|\varepsilon_2'|}{\varepsilon_1 + |\varepsilon_2'|} \quad (1.43)$$

$$S_{xn}^{II} = \frac{S_x^{II}}{S_{tot}} = -\frac{\varepsilon_1}{\varepsilon_1 + |\varepsilon_2'|} \quad (1.44)$$

In the limiting cases.

S_{xn}^{I} $(W = 0) = 1$ and S_{xn}^{II} $(W = 0) = 0$

which means that the whole energy is transmitted through dielectric medium I.

$S_{xn}^{I}\left(W = \frac{W_p}{\sqrt{\varepsilon_1 + 1}}\right) = \frac{1}{2}$, and $S_{xn}^{II}\left(W = \frac{W_p}{\sqrt{\varepsilon_1 + 1}}\right) = -\frac{1}{2}$

which means that the net transmitted energy is zero.

(See Fig. (1-8a))

$$S_{yn} = \frac{\varepsilon_2'' \sqrt{\varepsilon_1(-\varepsilon_2')}}{2(\varepsilon_1^2 - \varepsilon_2^{2\prime})} \quad (1.45)$$

In the limiting case (for $\tau \to \infty$)

S_{yn} $(W = 0) = \frac{1}{2W_p\tau}$

The case $W = \frac{W_p}{\sqrt{\varepsilon_1 + 1}}$ can't be considered since

$\varepsilon_2'' \ll (\varepsilon_1 + \varepsilon_2')$ condition becomes violated.

The general behavior of S_{yn} can be seen from figures (1-9a) and (1-9*a)

The field distribution of the plasmon describe by equations (1.3), (and (1.33) - (1.36) is shown at Fig. (1-10a).

The second subrange is, $\frac{W_p}{\sqrt{\varepsilon_1 + 1}} < W < W_p$. In this subrange $\varepsilon_2' < 0$; and

$\varepsilon_2' + \varepsilon_1 > 0$.

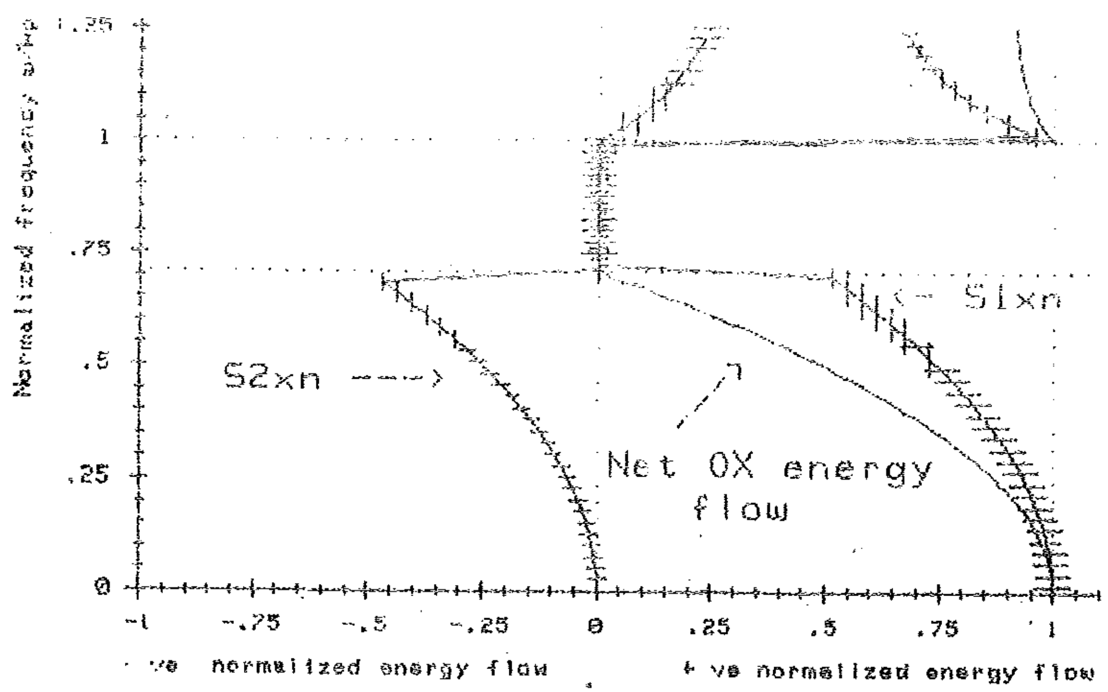

Fig(8a) Graph of normalized energy flow in OX direction as a function of normalized frequency: (a) - for medium 1 (||||| - line), (b) - for medium 2 (IIIII - line), (c)- total energy flow in both media (solid line). Wp = 1.E+15 rad/s ; Tau = 1.E+12 s

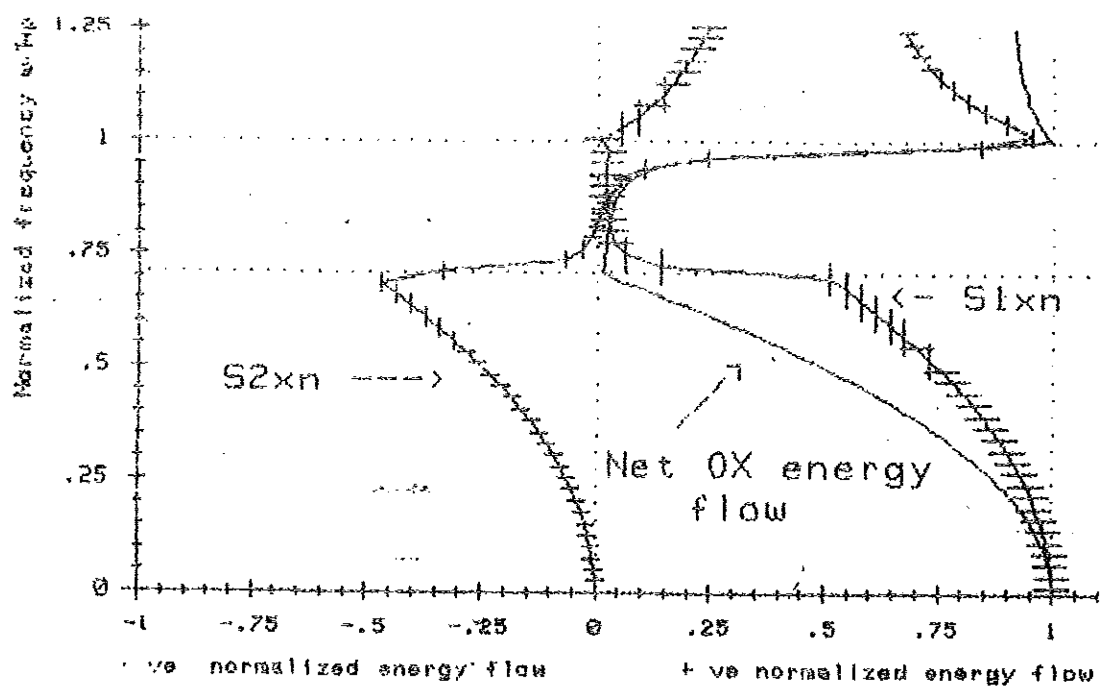

Fig(8b) Graph of normalized energy flow in OX direction as a function of normalized frequency: (a) - for medium 1 (||||| - line), (b) - for medium 2 (IIIII - line), (c)- total energy flow in both media (solid line). Wp = 1.E+15 rad/s ; Tau = 1.E-13 s.

For the ideal case $\varepsilon_2'' = 0$ from equations (1.15), (1.22) and (1.24 a) we get

$$K_x' = 0 \; ; \; K_x'' > 0$$

$$K_{1y}' \gtrless 0; \; K_{1y}'' = 0 \; ; \; K_{2y}' \gtrless 0 \quad K_{2y}'' = 0$$

which means that all incident energy is radiated from the interface either in medium II ($K_{1y} < 0$, $K_{2y}' < 0$), or in medium I ($K_{1y}' > 0$, $K_{2y}' > 0$). The algebraic sign of K_{1y}' and K_{2y}' should be always the same in this subrange since $\varepsilon_2' < 0$ and equation (1.24a) to be written as;

$$\frac{K_{1y}'}{K_{2y}'} = -\frac{\varepsilon_1}{\varepsilon_2'} \quad \text{for} \quad \varepsilon_2''=0 \text{ case.}$$

For the general case ($\varepsilon_2'' \neq 0$) in this subrange from equation (1.24a)

$$K_x' = K_o \sqrt{\frac{\varepsilon_1(-\varepsilon_2')}{\varepsilon_1 + \varepsilon_2'}} \cdot \frac{\varepsilon_1 \varepsilon_2''}{2(-\varepsilon_2')(\varepsilon_1+\varepsilon_2')} > 0 \qquad (1.46)$$

$$K_x'' = K_o \sqrt{\frac{\varepsilon_1(-\varepsilon_2')}{\varepsilon_1 + \varepsilon_2'}} > 0 \; 0 \qquad (1.47)$$

See figures (1.3a) and (1.4a)

From equation (1.15)

$$K_{1y}' = \pm\sqrt{K_o{}^2\varepsilon_1 + K_x''{}^2} = \pm K_o \frac{\varepsilon 1}{\sqrt{\varepsilon_1 + \varepsilon_2'}} \qquad (1.48)$$

$$K_{1y}'' = (\pm) \cdot \frac{-2K_x'K_x''}{2K_{1y}'} = \mp \frac{K_o \varepsilon_1 \varepsilon_2'' \sqrt{\varepsilon_1+\varepsilon_2'}}{2(\varepsilon_1+\varepsilon_2')} \qquad (1.49)$$

From equation (1.22)

$$K_{2y}' = \sqrt{K_o{}^2 \varepsilon_2 - K_x''{}^2} = \pm \frac{K_o(-\varepsilon_2')}{\sqrt{\varepsilon_1+\varepsilon_2'}} \qquad (1.50)$$

$$K_{2y}'' = \frac{K_o 2\varepsilon_2'' - 2K_x K_x''}{2K_{2y}'} = \mp \frac{K_o \varepsilon_2''(2\varepsilon_1+\varepsilon_2')\sqrt{\varepsilon_1+\varepsilon_2'}}{2.(\varepsilon_1+\varepsilon_2')2} \quad \text{------} \quad (1.51)$$

See figures (1.5a) and (1.6a)

From equations (1.27) — (1.30) and using equations (1.46) - (1.51)

$$S_y^I = \frac{+K_{1y}}{2W(\varepsilon_1\varepsilon_o)} = \frac{K_o}{2W\varepsilon_o\sqrt{\varepsilon_1+\varepsilon_2'}} \quad \text{----------} \quad (1.52)$$

$$S_y^{II} = \frac{1}{2W\varepsilon_o}\,\frac{K_{2y}'}{\varepsilon_2'} = \pm\frac{K_o}{2W\varepsilon_o.\sqrt{\varepsilon_1+\varepsilon_2'}} \quad \text{-----} \quad (1.53)$$

$$S_x^I = \frac{K_o}{2W\varepsilon_o}\sqrt{\frac{\varepsilon_1(-\varepsilon_2')}{\varepsilon_1+\varepsilon_2'}}\;.\;\frac{\varepsilon_2''}{2(-\varepsilon_2')(\varepsilon_1+\varepsilon_2')} > 0 \quad \text{-----} \quad (1.54)$$

$$S_x^{II} = \frac{K_o\sqrt{\frac{\varepsilon_1(-\varepsilon_2')}{\varepsilon_1+\varepsilon_2'}}\;\varepsilon_2''(\varepsilon_1+2\varepsilon_2')}{2W\varepsilon_o\,(\varepsilon_2'2+\varepsilon_2''2).2.(\varepsilon_1+\varepsilon_2')} \quad \text{-----------} \quad (1.55)$$

equation (1.55) may assume negative and positive values depending on the value of ε_2' in the given frequency subrange. That is it is negative if $\varepsilon_2' \leqslant -\frac{\varepsilon_1}{2}$ and positive if $\varepsilon_2' > -\frac{\varepsilon_1}{2}$

For $\frac{W_p}{\sqrt{\varepsilon_1+1}} < W < W_p$ the total power flow which is expressed by equation (1.41) can be approximated by

$$S_{tot} \cong S_y$$

Where $S_y = |S_y^I| = |S_y^{II}|$, since the power flows in OY direction always have opposite senses as it may be seen from equations (1.52) and (1.53). The approximation is true because the power flow in OX direction becomes proportional to ε_2'' which is small. Hence

$$S_{tot} = \frac{K_o}{2W\varepsilon_o\sqrt{\varepsilon_1+\varepsilon_2'}} \qquad (1.56)$$

Therefore the normalized power flow can be expressed as:

$$S_{yn}^{I} = S_{yn}^{II} = \pm 1 \qquad (1.57)$$

$$S_{xn}^{I} = \frac{\varepsilon_2'' \cdot \sqrt{\varepsilon_1 \cdot (-\varepsilon_2')}}{4 \cdot (-\varepsilon_2') \cdot (\varepsilon_1+\varepsilon_2')} > 0 \qquad (1.58)$$

(S_{xn}^{I} is the order of 10^{-3} in the middle of the subrange)

$$S_{xn}^{II} = \frac{\varepsilon_2'' \sqrt{\varepsilon_1 (-\varepsilon_2')} \cdot (\varepsilon_1+2\varepsilon_2')}{4(\varepsilon_2')^2 (\varepsilon_1+\varepsilon_2')} = S_{xn}^{I} \cdot \frac{(\varepsilon_1+2\varepsilon_2')}{(-\varepsilon_2')} \qquad (1.59)$$

The sign of S_{xn}^{II} depends upon the sign of $(\varepsilon_1+2\varepsilon_2')$ term. For $\frac{W_p}{\sqrt{\varepsilon_1+1}} < W < W_p \cdot \sqrt{\frac{2}{\varepsilon_1+1}}$ it is negative, elsewhere it is positive.

The results discussed in equations (1.57) - (1.59) are shown at figures (18a), (19a) and (19*a).

The field distribution of the excitation that exists in the second subrange is shown at figures 11a and 11*a. They correspond to the same frequency $\frac{W}{W_p} = 0.70732$ but different in scale in the direction normal to the surface.

Third subrange is $W > W_p$ in this subrange $\varepsilon_2' > 0$ and $\varepsilon_1+\varepsilon_2' > 0$.

For ideal case $\varepsilon_2'' = 0$ from equations (1.15), (1.22) and (1.24a) we get

$K_x' > 0$; $K_x'' = 0$

$K_{1y}' < 0$; $K_{1y}'' = 0$

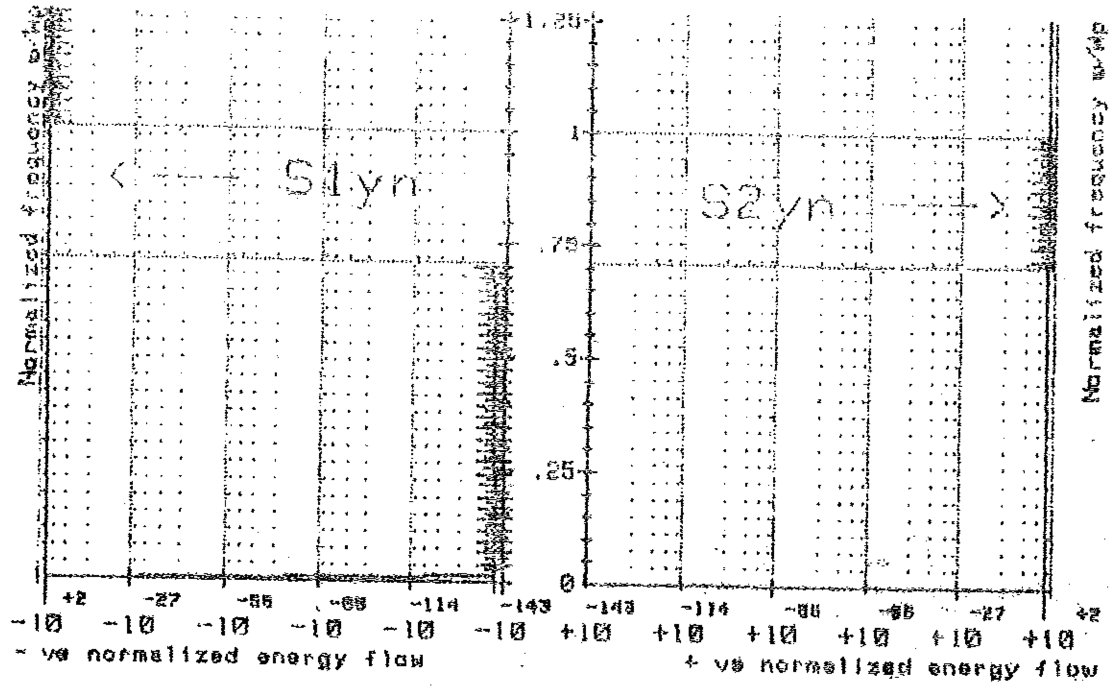

Fig.(10a) Graph of normalized energy flow along OY direction as a function of normalized frequency: (a) - for medium 1, (||||| - line), (b) - for medium 2 (IIIII - line). Wp = 1.E+15 rad/s ;Tau = 1.E+125 s.

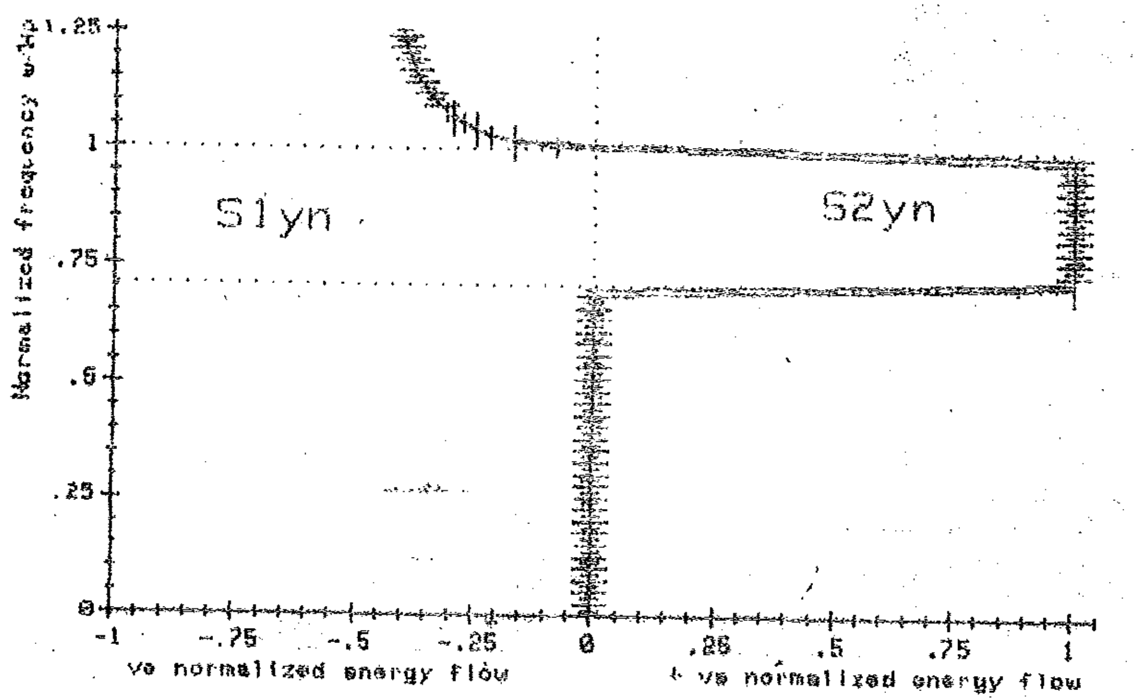

Fig(10*a) Graph of normalized energy flow along OY direction as a function of normalized frequency: (a) - for medium 1 (||||| - line), (b) - for medium 2 (IIIII - line). Wp = 1.E+15 rad/s ;Tau = 1.E+125 s.

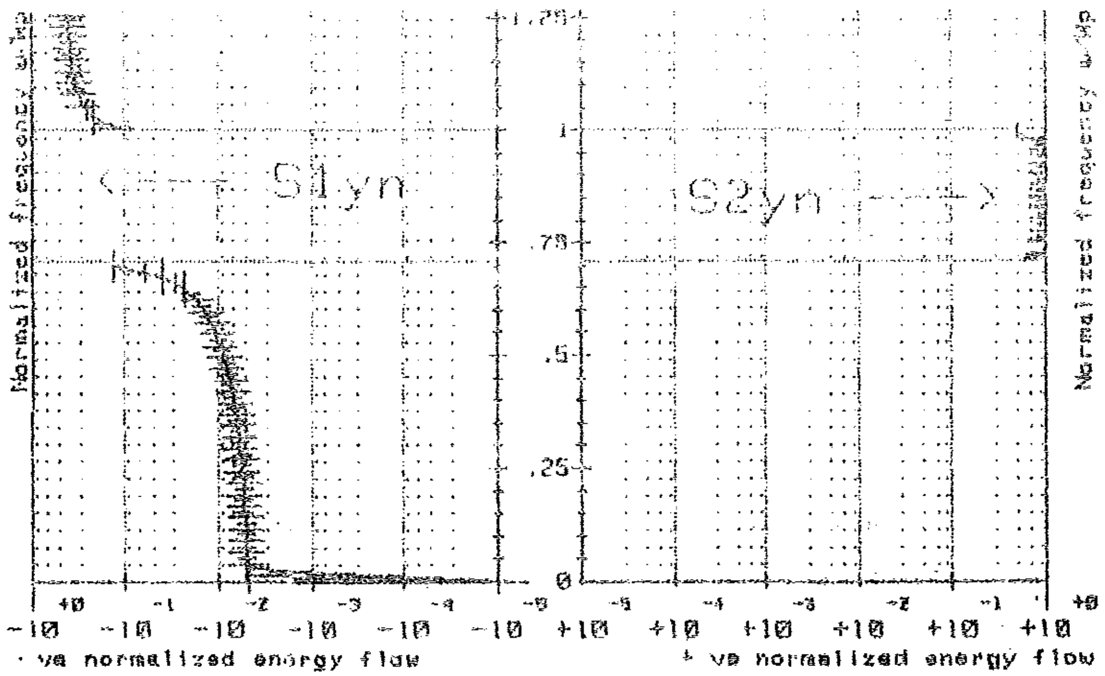

Fig.(9b) Graph of normalized energy flow along OY direction as a functi
of normalized fraquency: (a) - for medium 1 (||||| - line),
(b) - for medium 2 (IIIII - line).
Wp = 1.E+15 rad/s ;Tau = 1.E-13 s.

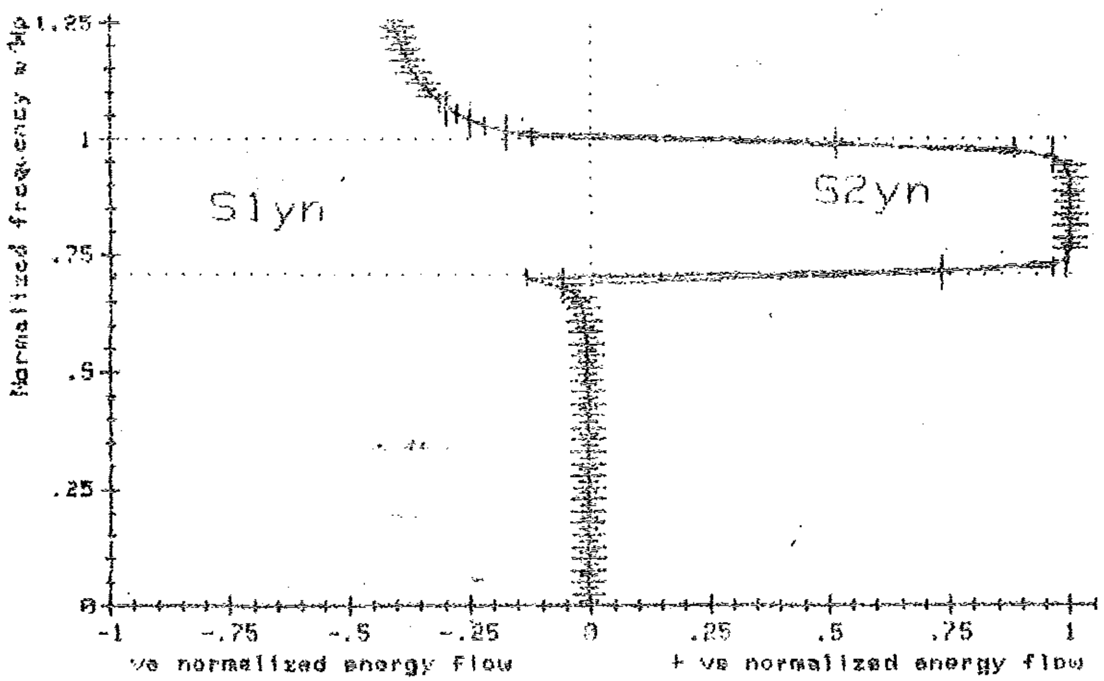

Fig.(9*b) Graph of normalized energy flow along OY direction as a funct
of normalized fraquency: (a) - for medium 1 (||||| - line),
(b) - for medium 2 (IIIII - line).
Wp = 1.E+15 rad/s ;Tau = 1.E-13 s.

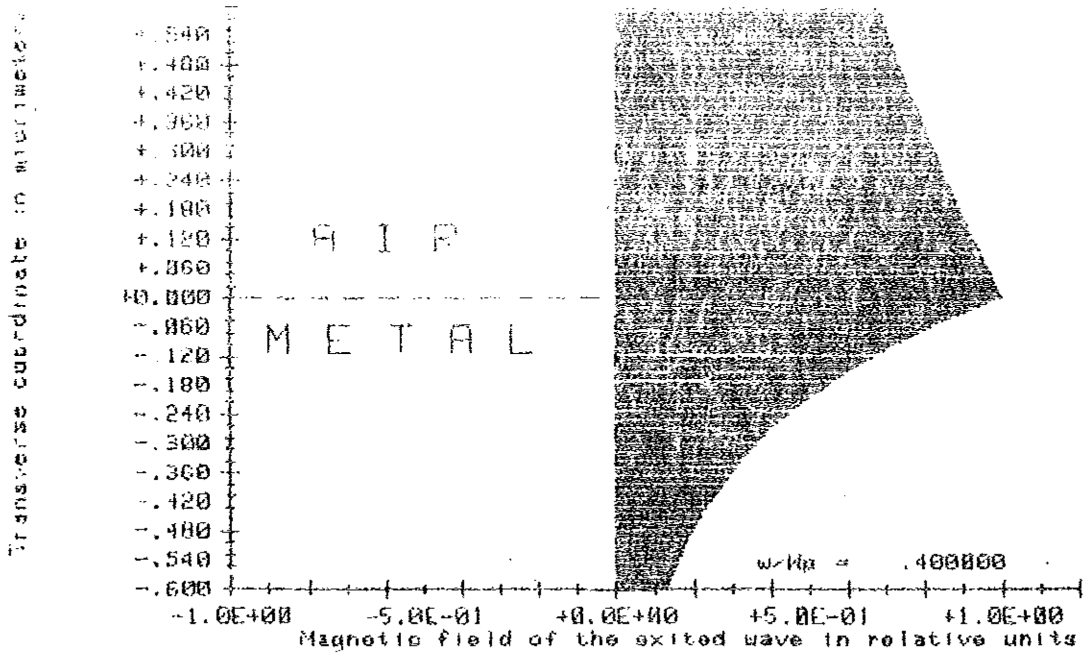

Fig(10a). Magnetic field (Z - component) distribution of the excited wave near the metal surface with respect to transeverse Y - coordinate, (small frequency range).
Wp = 1.E+15 rad/s; Tau = 1.E+125 s *

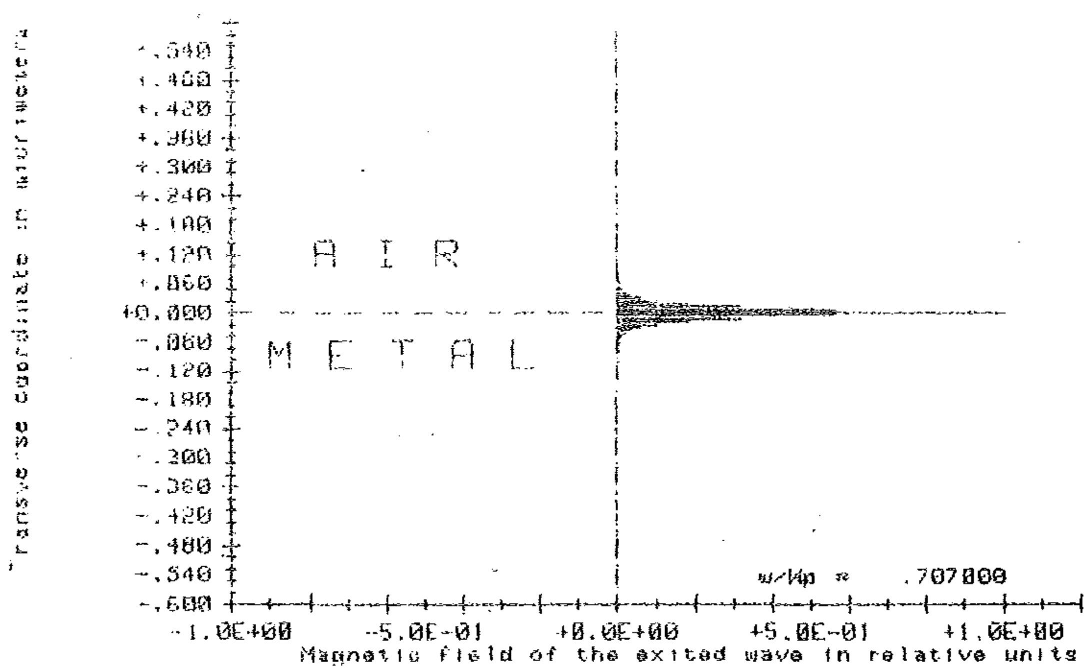

Fig(10b). Magnetic field (Z - component) distribution of the excited wave near the metal surface with respect to transeverse Y - coordinate, (small frequency range).
Wp = 1.E+15 rad/s; Tau = 1.E+125 s *

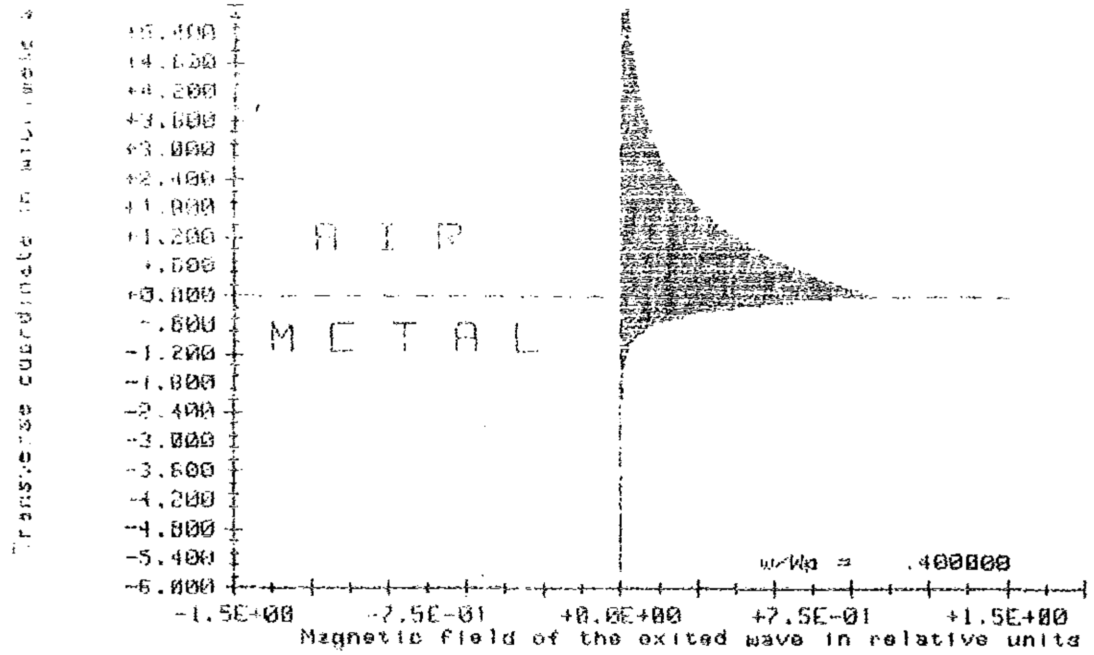

Fig(140b) . Magnetic field (Z - component) distribution of the excited wave near the metal surface with respect to transeverse Y - coordinate, (small frequency range). Wp = 1.E+15 rad/s; Tau = 1.E-13 s *

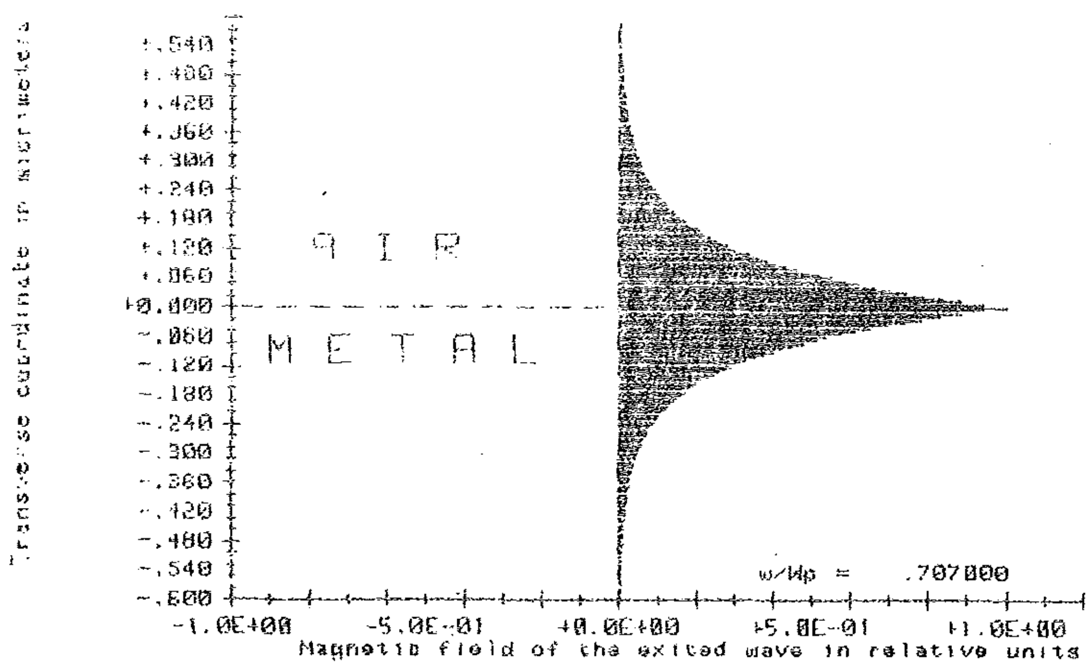

Fig(140b) . Magnetic field (Z - component) distribution of the excited wave near the metal surface with respect to transeverse Y - coordinate, (small frequency range). Wp = 1.E+15 rad/s; Tau = 1.E-13 s *

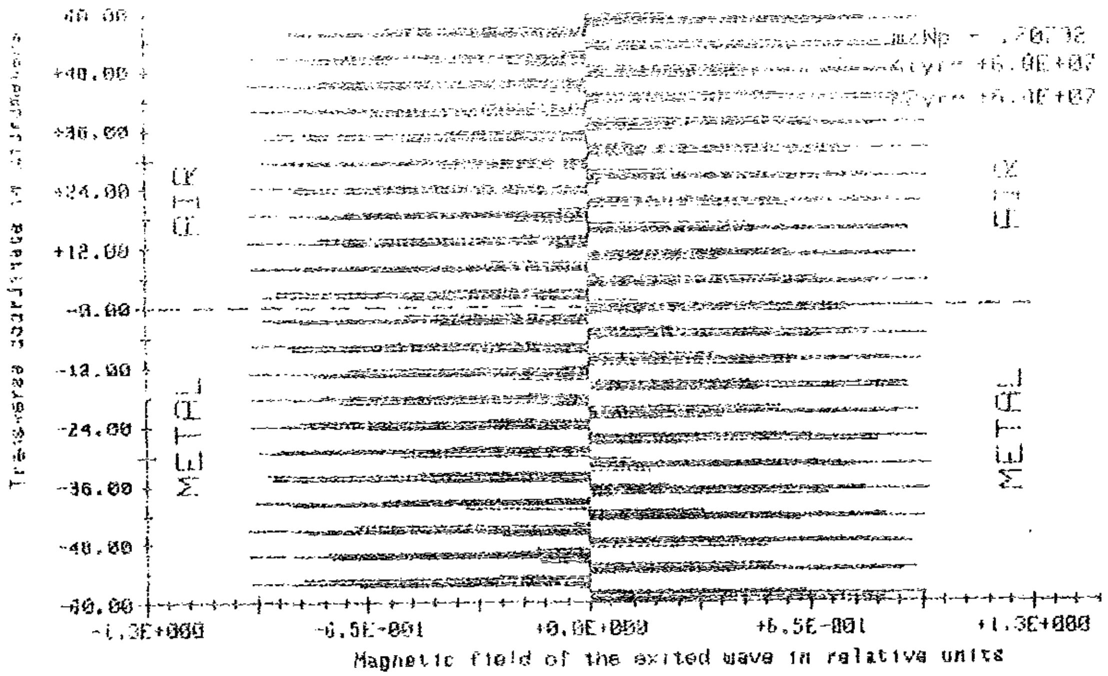

Fig(4.1a) Magnetic field (Z-component) distribution of the excited wave near the metal surface with respect to Y - coordinate (Medium frequency range) . Wp = 1.E+15 rad/s ; Tau = 1.E+125 s

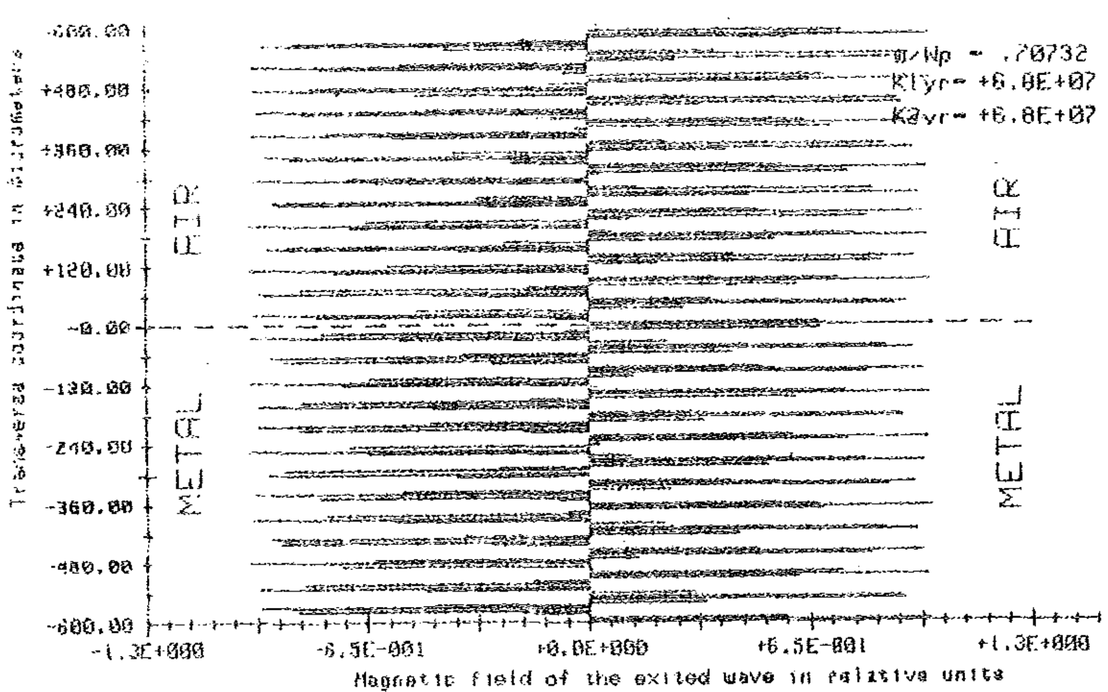

Fig(4.1a) Magnetic field (Z-component) distribution of the excited wave near the metal surface with respect to Y - coordinate (Medium frequency range) . Wp = 1.E+15 rad/s ; Tau = 1.E+125 s

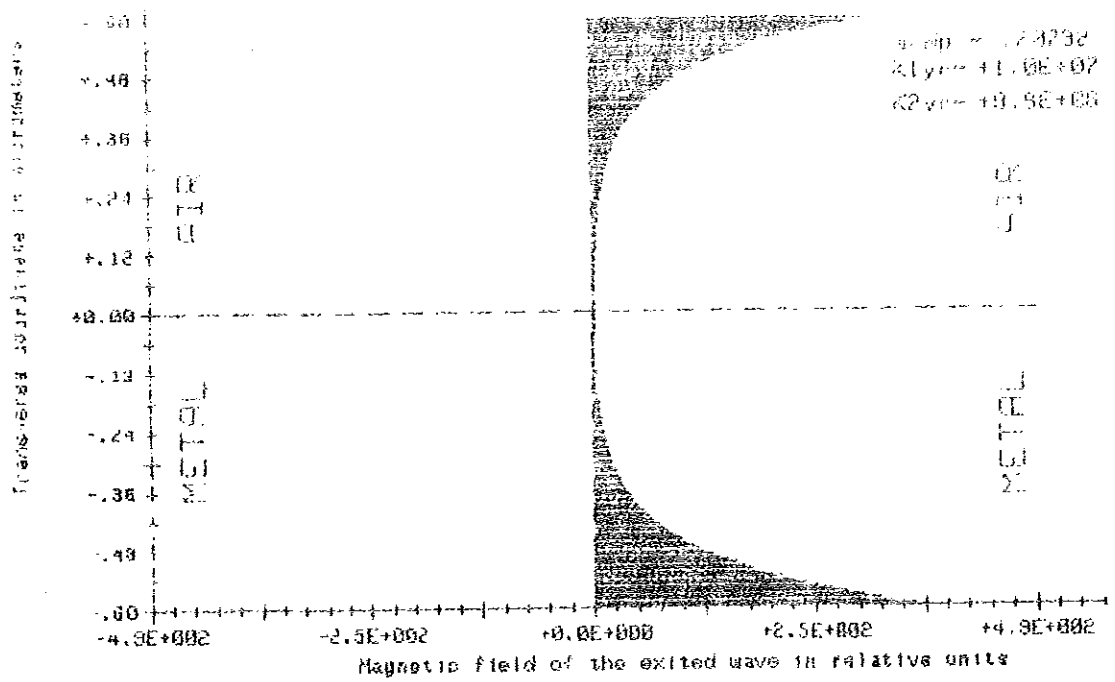

Fig(M1b) Magnetic field (Z-component) distribution of the excited wave near the metal surface with respect to Y - coordinate (Medium frequency range) . Wp = 1.E+15 rad/s ; Tau = 1.E-13*s

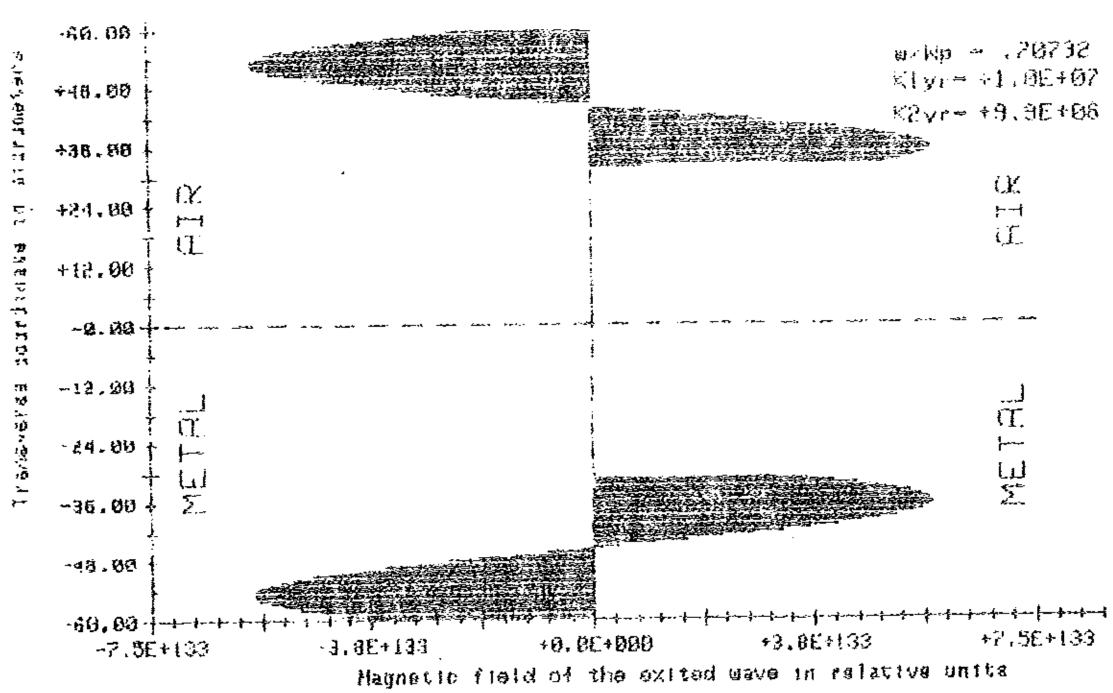

Fig(M1b) Magnetic field (Z-component) distribution of the excited wave near the metal surface with respect to Y - coordinate (Medium frequency range) . Wp = 1.E+15 rad/s ; Tau = 1.E-13*s

$$K_{2y}' > 0 \; ; \quad K_{2y}'' = 0$$

which means that all the incident energy is radiated out through the second medium, since $K_{1y} < 0$ and $K_{2y}' > o$.

In the case $\varepsilon_2'' \neq 0$, but $\varepsilon_2'' < \varepsilon_2'$, $\varepsilon_2'' < \varepsilon_1 + \varepsilon_2'$

From equation (1.24a)

$$K_x' = K_o \sqrt{\frac{\varepsilon_1 \varepsilon_2'}{\varepsilon_1 + \varepsilon_2'}} > 0 \quad \text{-------------} \qquad (1.60)$$

$$K_x'' = K_o \sqrt{\frac{\varepsilon_1 \cdot \varepsilon_2'}{\varepsilon_1 + \varepsilon_2'}} \cdot \frac{\varepsilon_1 \, \varepsilon_2''}{2\varepsilon_2'(\varepsilon_1 + \varepsilon_2')} > 0 \quad \text{-------} \qquad (1.61)$$

See figures (13a) and (14a)

From equation (1.15)

$$K_{1y}' = \sqrt{K_o^2 \varepsilon_1 - K_x'^2} = - K_o \frac{\varepsilon_1}{\sqrt{\varepsilon_1 + \varepsilon_2'}} < 0 \quad \text{------} \qquad (1.62)$$

$$K_{1y}'' = - \frac{K_x' K_x''}{K_{1y}'} = + K_o \frac{\varepsilon_1 \varepsilon_2'' \sqrt{\varepsilon_1 + \varepsilon_2'}}{2(\varepsilon_1 + \varepsilon_2')2} > 0 \quad \text{-------} \qquad (1.63)$$

From equation (22)

$$K_{2y}' = \sqrt{K_o^2 \varepsilon_2' - K_x'^2} = + K_o \frac{\varepsilon_2'}{\sqrt{\varepsilon_1 + \varepsilon_2'}} > 0 \text{ --} \quad (1.64)$$

$$K_y^{2''} = \frac{K_o \varepsilon_2'' - 2K_x' K_x''}{2K_{2y}'} = + \frac{K_o \varepsilon_2''[2\varepsilon_1 + \varepsilon_2'] . \sqrt{\varepsilon_1 + \varepsilon_2'}}{2.(\varepsilon_1 + \varepsilon_2)^2} > 0 \text{ ---} \quad (1.65)$$

See figures (15a) and (16a)

From equations (1.27) to (1.30) and using equations (1.60) to (1.65)

$$S_y I = -\frac{1}{2W\varepsilon_o} \cdot \frac{K_o}{\sqrt{\varepsilon_1+\varepsilon_2'}} < 0 \qquad (1.66)$$

$$S_y II = -\frac{1}{2W\varepsilon_o} \cdot \frac{K_o}{\sqrt{\varepsilon_1+\varepsilon_2'}} < 0 \qquad (1.67)$$

$$S_x I = \frac{1}{2W\varepsilon_o} \cdot \frac{K_o\sqrt{\varepsilon_1 . \varepsilon_2'}}{\varepsilon_2' \cdot \sqrt{\varepsilon_1+\varepsilon_2'}} > 0 \qquad (1.68)$$

$$S_x II = \frac{1}{2W\varepsilon_o} \cdot \frac{K_o\sqrt{\varepsilon_1 \cdot \varepsilon_2'}}{\varepsilon_2' \sqrt{\varepsilon_1+\varepsilon_2'}} > 0 \qquad (1.69)$$

For this subrange $S_x I$, $S_x II$ and $|S_y| = |S_y I| = |S_y II|$ have close order of magnitude. Thus

$$S_{tot} = \sqrt{(S_x I + S_x II)2 + S_y^2} = \frac{K_o}{2W\varepsilon_o} \cdot \sqrt{\frac{(\varepsilon_1+\varepsilon_2')^2 + \varepsilon_1\varepsilon_2'}{\varepsilon_1 \cdot \varepsilon_2' \cdot (\varepsilon_1+\varepsilon_2')}} \qquad (1.70)$$

The normalized power flows can be expressed as

$$S_{xn} I = \frac{S_y^I}{S_{tot}} = \frac{\varepsilon_2}{\sqrt{(\varepsilon_1+\varepsilon_2')^2+\varepsilon_1 . \varepsilon_2'}} > 0 \qquad (1.71)$$

$$S_{xn}^{II} = \frac{S_x II}{S_{tot}} = \frac{\varepsilon_1}{\sqrt{(\varepsilon_1+\varepsilon_2')^2+\varepsilon_1 . \varepsilon_2'}} > 0 \qquad (1.72)$$

$$S_{yn} = \frac{S_y I}{S_{tot}} = \frac{S_y II}{S_{tot}} = -\frac{\sqrt{\varepsilon_1 . \varepsilon_2'}}{\sqrt{(\varepsilon_1+\varepsilon_2')^2+\varepsilon_1\varepsilon_2'}}$$

In the limiting cases: with $\varepsilon_1 = 1$

$W = W_p$; $S_{xn}^{I} = 0$; $S_{xn}^{II} = 1$; $S_{yn} = 0$

$W = \infty$ $S_{xn}^{I} = \frac{1}{\sqrt{5}}$; $S_{xn}^{II} = \frac{1}{\sqrt{5}}$; $S_{yn} = -\frac{1}{\sqrt{5}}$

$$(S_{xn}^{I} + S_{xn}^{II}) + S_{yn}^{2} = \left(\frac{1}{\sqrt{5}} + \frac{1}{\sqrt{5}}\right)^2 + \left(-\frac{1}{\sqrt{5}}\right)^2 = 1$$

The same results follow from figures (6a), (9a), and (9*a). The field distribution for the excitation in the third subrange is shown at fig. 12.

1.3 Dispersion Equation for Strong Absorption Case

The results of calculations according to exact equations (1.24a), (1.15), (1.22) and equations (1.27) to (1.30), equations (13), and (14b) are represented at figures (13b) to (18)(b) (letter "b" refers to $\tau = 10^{-13}$ sec)

Among the particularities of these results it is necessary to point out the following.

1. Growth of Real parts of K_y wave vector in the first subrange, see figure (15b).
2. As a result of point 1, we note the growth of energy flow in OY direction in the first subrange, see figure (19b).
3. However, it does not bring vital changes in the field distribution of plasmon in the first subrange (see fig. (10b)) in the sense that the plasmon type of field distribution remains. On it becomes clear that in strong absorption case it is not possible to compress the field so close to the interface beyond $0.3\lambda o$ at $1/e$ level. Where λo is the wave length of the exciting light in vacuum.
4. Growth of imaginary parts of K_y wave vector in the third subrange see figure (16b).

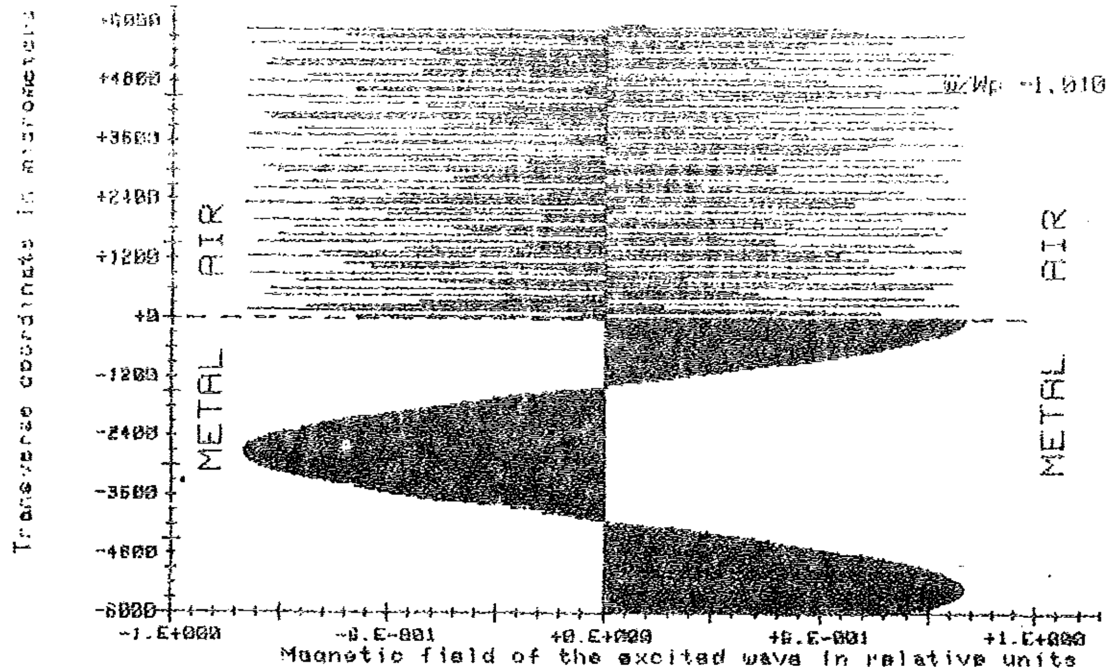

Fig(12 a) Magnetic field (Z-component) of the excited wave near the metal surface with respect to transeverse Y - coordinate, (Big Frequency range) , Wp = 1.E+15 rad/s ; Tau = 1.E+12* s

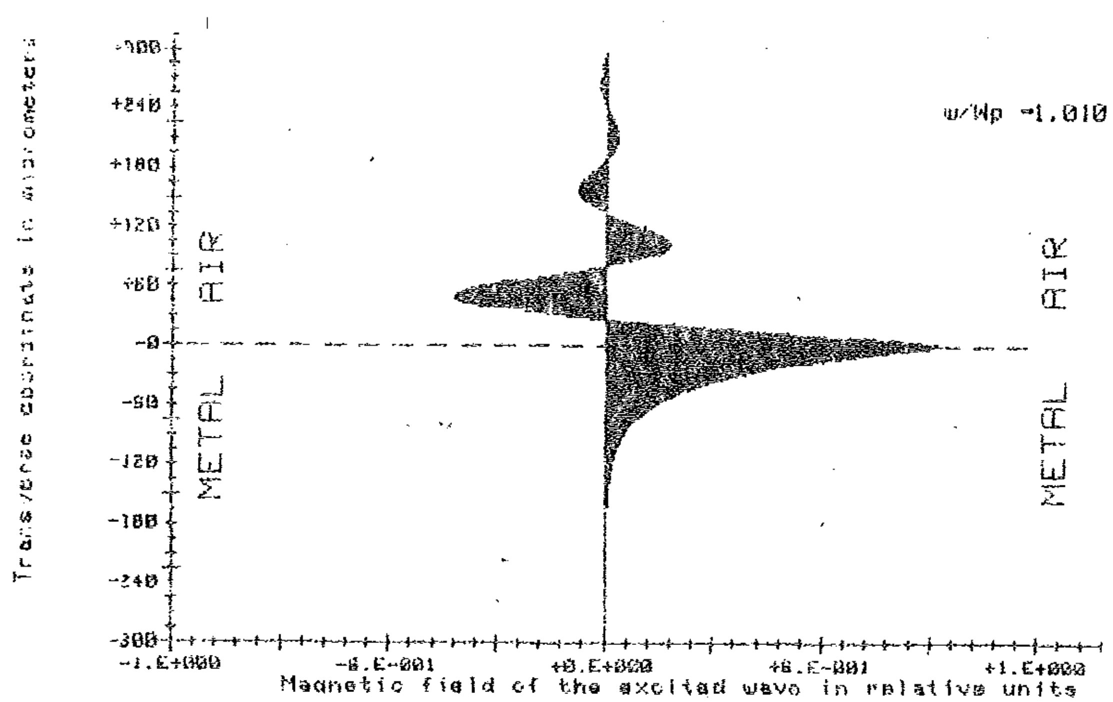

Fig(12 b) Magnetic field (Z-component) of the excited wave near the metal surface with respect to transeverse Y - coordinate, (Big Frequency range) . Wp = 1.E+15 rad/s ; Tau = 1.E-13*s

5. As a result of point 4, we note that a decrease of energy flow in OY direction in the third subrange.
6. As a results of points 4 and 5 we get a plasmon type field distribution at fig.(1.12(b) in the third subrange. Comparing it with fig.(1.12 a) we note that the field distribution became considerably less radiative. However, the field is extended at 10^3 time larger distances from the interface than in the case of plasmon in the first subrange.

Chapter 2

2.1 Derivation of SPIP equation for dielectric medium I - metal film dielectric medium 3.

Consider a thin metallic film with ε_2 and thickness h boundarying with dielectric medium 1 with ε_1 and dielectric medium 3 with ε_3. Suppose $\varepsilon_3 \geq \varepsilon_1$

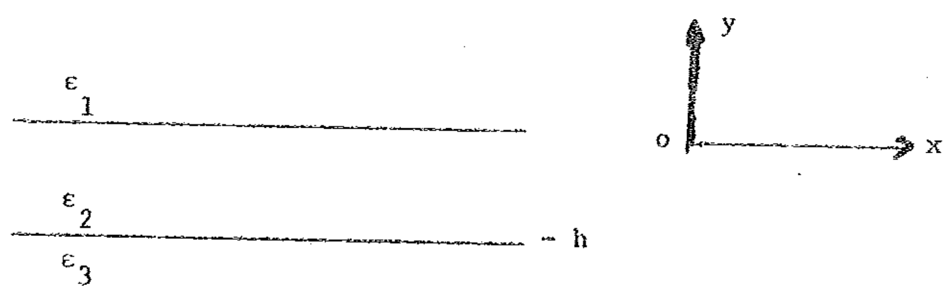

Fig. (2.1) Schematic diagram of thin metallic film (ε_2) boundarying dielectric medium 1 (ε_1), and dielectric medium 3 (ε_3).

Considering T.M polarization, the magnetic field H_Z can be given respectively in the three media;

$$H_{Z1} = A_1 \, e^{+iK_{1y}} \, e^{i(K_x X - Wt)}$$

$$H_{Z2} = \left(A_2 \, e^{+iK_{2y} y} + B_2 e^{-iK_{2y} y} \right) e^{i(K_x X - Wt)} \qquad \text{------ (2.1)}$$

$$H_{Z3} = A_3 \, e^{-iK_{3y} y} \, e^{i(K_x X - Wt)}$$

The expression for H_{Z2} contains two terms because there might be two waves travelling in the film due to reflections at $\varepsilon_1/\varepsilon_2$ interface and at $\varepsilon_3/\varepsilon_2$ interface. Their superposition describes a standing wave in OY direction with in the film.

From Maxwell's curl equation the corresponding E_x (tangential) components of the electric field in the three media respectively are;

$$E_{x1} = -A_1\frac{K_{1y}}{W\varepsilon_1} e^{+iK_{1y}Y} e^{i(K_xX-Wt)}$$

$$E_{x2} = \left[-A_2\frac{K_{2y}}{W\varepsilon_2} e^{iK_{2y}Y} + B_2\frac{K_{2y}}{W\varepsilon_2}\right] e^{i(K_xX-Wt)} \text{ --- } (2.2)$$

$$E_{x3} = A_3\frac{K_{3y}}{W\varepsilon_3} e^{-iK_{3y}Y} e^{i(K_xX-wt)}$$

Let's apply boundary conditions for H_Z and E_x at y=0, for any arbitrar:

$$H_{Z1}\ (y = 0) = H_{Z2}\ (y = 0)$$

$$A_1 = A_2 + B_2 \text{ ---------- } (2.3)$$

$$E_{x1}\ (y = 0) = E_{x2}\ (y = 0)$$

$$-A_1\frac{K_{1y}}{\varepsilon_1} = -A_2\frac{K_{2y}}{\varepsilon_2} + B_2\frac{K_{2y}}{\varepsilon_2} \text{ -------- } (2.4)$$

again applying boundary condition at y = -h for any arbitrary x:

$$H_{Z2}\ (y=-h) = H_{Z3}\ (y=-h)$$

$$A_2e^{-iK_{2y}h} + B_2e^{+iK_{2y}h} = A_3e^{+iK_{3y}h} \text{ ------- } (2.5)$$

$$E_{x2}\ (y=-h) = E_{x3}\ (y=-h)$$

$$-A_2\frac{K_{2y}}{\varepsilon_2} e^{-iK_{2y}h} + B_2\frac{K_{2y}}{\varepsilon_2} e^{+iK_{2y}h} = A_3\frac{K_{3y}}{\varepsilon_3} e^{iK_{3y}h} \text{ ---- } (2.6)$$

Suppose A_1 is given, in this case equations (2.3) → (2.6) form a syste: of four equations with A_2, B_2, A_3, and K_x unknown noting that K_{1y}, and K_{2y} can be expressed through K_x, and the expression for K_{3y} can be derived from the wave equation for medium 3 similarly as it was done for medium. 1. Therefore;

$$K_{3y} = \sqrt{K_o^2\varepsilon_3 - K_2^2} \qquad (2.7)$$

In order to derive the dispersion equation ($K_x = f(w)$) we shall exclude all amplitude factors from equations (2.4) $\rightarrow$ (2.6)

From equations (2.3) and (2.4)

$$-(A_2+B_2)\frac{K_{1y}}{\varepsilon_1} = -(A_2-B_2)\frac{K_{2y}}{\varepsilon_2} \qquad (2.8)$$

or

$$-B_2\left[\frac{K_{1y}}{\varepsilon_1} + \frac{K_{2y}}{\varepsilon_2}\right] = A_2\left[\frac{K_{1y}}{\varepsilon_1} - \frac{K_{2y}}{\varepsilon_2}\right]$$

Multiplying equation (2.5) by a factor $\frac{K_{3y}}{W\varepsilon_3}$ and subtracting from the result equation (2.6)

$$(A_2e^{-iK_{2y}h} + B_2e^{+iK_{2y}h})\frac{K_{3y}}{W\varepsilon_3} - (-A_2\frac{K_{2y}}{W\varepsilon_2}e^{-iK_{2y}h} + B_2\frac{K_{2y}}{W\varepsilon_2}e^{+iK_{2y}h}) = 0$$

$$A_2e^{-iK^2{}_yh}\left[\frac{K_{3y}}{\varepsilon_3} + \frac{K_{2y}}{\varepsilon_2}\right] + B_2e^{+iK_{2y}h}\left[\frac{K_{3y}}{\varepsilon_3} - \frac{K_{2y}}{\varepsilon_2}\right] = 0$$

$$A_2 + B_2e^{2iK_{2y}h}\frac{\left[\frac{K_{3y}}{\varepsilon_3} - \frac{K_{2y}}{\varepsilon_2}\right]}{\left[\frac{K_{3y}}{\varepsilon_3} + \frac{K_{2y}}{\varepsilon_2}\right]} = 0$$

$$A_2 - B_2r_{23}\,e^{2iK_{2y}h} = 0$$

$$A_2 = B_2r_{23}e^{2iK_{2y}h} \qquad (2.9)$$

Substitution of equation (2.9) into equation (2.8) gives

$$B_2 = B_2r_{12}.r_{23}e^{2iK_{2y}h}$$

$$-1 = r_{12}r_{23}e^{2iK_{2y}h}$$

$$r_{21}r_{23}e^{2iK_{2y}h} = 1 \qquad (2.10)$$

where
$$r_{21} = \frac{\frac{K_{2y}}{\varepsilon_2} - \frac{K_{1y}}{\varepsilon_1}}{\frac{K_{2y}}{\varepsilon_2} + \frac{K_{1y}}{\varepsilon_1}} \qquad (2.11)$$

$$r_{23} = \frac{\frac{K_{2y}}{\varepsilon_2} - \frac{K_{3y}}{\varepsilon_3}}{\frac{K_{2y}}{\varepsilon_2} + \frac{K_{3y}}{\varepsilon_3}} \qquad (2.12)$$

Equation(2.10) represents together with equations (2.11), (2.12), (1.15), (1.22), and (2.7) an exact dispersion equation for a thin metallic film [2].

2.2 Approximate solution for the dispersion equation.

Let's suppose that thickness h of the metallic film is big enough, so that the influence of medium 3 on the dispersion properties is small. In this case we can build an approximate solution using the solution expressed in equation (1.24a) for the semi-infinite case as the basis. Thus we'll express:

$$K_x = K_{xo} + K_{x1} \qquad (2.13)$$

where K_{xo} is given by equation (1-24a)

K_{x1} is a small quantity describing the influence of medium 3.

For this purpose let's denote the reciprocal of the left side of equation (2.10) as a function of K_x

$$f(K_x) = \left(r_{21} r_{23} e^{2iK_{2y}h}\right)^{-1} = \frac{1}{r_{21}} \cdot \frac{1}{r_{23}} e^{-2iK_{2y}h} \qquad (2.14)$$

Let's expand $f(K_x)$ in Taylor's series near the point $K_x = K_{xo}$, where K_{xo} is given by equation(1.24a) for the semi-infinite case

$$f(K_x) = f(K_{xo}) + \left.\frac{\partial f}{\partial K_x}\right|_{K_{xo}} K_{x1} + \text{------} \qquad (2.15)$$

In appendix A it is shown that

$$f(K_{xo}) = 0 \qquad \text{------------------} \qquad (2.16)$$

$$\left.\frac{\partial f}{\partial K_x}\right|_{K_{xo}} = \frac{\epsilon_2-\epsilon_1}{2K_o}\left(\frac{\epsilon_1-\epsilon_2}{\epsilon_1.\epsilon_3}\right)^{3/2}\cdot\frac{1}{r^o_{23}}\; e^{-i2K^o_{2y}h} \qquad \text{----} \qquad (2.17)$$

$$r^o_{23} = \frac{\epsilon_3 - \sqrt{\epsilon_1\epsilon_3 + \epsilon_2(\epsilon_3-\epsilon_1)}}{\epsilon_3 + \sqrt{\epsilon_1\epsilon_3 + \epsilon_2(\epsilon_3-\epsilon_1)}} \qquad \text{-------------} \qquad (2.18)$$

$$K^o_{2}y = iK_o\frac{(-\epsilon_2)}{\sqrt{-(\epsilon_1+\epsilon_2)}} \qquad \text{------------} \qquad (2.19)$$

Since $f(K_x) = 1$ (see equations (2.10) and (2.14)) substitution of equation (2.16) to (2.19) into equation (2.15) gives

$$K_{x1} = K_o\frac{2}{(\epsilon_2-\epsilon_1)}\cdot\left(\frac{\epsilon_1.\epsilon_2}{\epsilon_1+\epsilon_2}\right)^{3/2}\cdot r^o_{23}e^{+2iK^o_{2y}h} \qquad \text{---} \qquad (2.20)$$

Let's analyze equation (2.20) for the case when $\epsilon_2''=0$. First from equation (2.18) we get:

$$r^o_{23} = \frac{\epsilon_3 - \sqrt{\epsilon_1\epsilon_3 + \epsilon_2'(\epsilon_3-\epsilon_1)}}{\epsilon_3 + \sqrt{\epsilon_1\epsilon_3 + \epsilon_2'(\epsilon_3-\epsilon_1)}} \qquad \text{----------} \qquad (2.21)$$

The expression under the square root is negative in the range of frequencies $0 \le W \le W^*$. Where W^* is determined from the condition;

$$\epsilon_1\epsilon_3 + \left(1 - \frac{W_p^2}{W^{*2}}\right)(\epsilon_3 - \epsilon_1) = 0$$

$$W^* = W_p \cdot \sqrt{\frac{\epsilon_3 - \epsilon_1}{\epsilon_1\epsilon_3 + \epsilon_3 - \epsilon_1}} \qquad \text{--------------} \qquad (2.22)$$

The frequency W^* corresponds also to the intersection point of graphs $K_{xo}'(W)$ and $K_3(W)$.

$$K_o\sqrt{\frac{\epsilon_1\epsilon_2'(W^*)}{\epsilon_1+\epsilon_2'(W^*)}} = K_o\sqrt{\epsilon_3} \qquad (2.23)$$

It means W^* is the maximum frequency for a SPIP to be excited by the light incident from medium 3 on the ϵ_1/ϵ_2 interface.

To avoid imaginarity under the square root let's rewirte equation (2.21) as

$$r^o_{23} = \frac{\epsilon_3 - i\sqrt{-[\epsilon_1\epsilon_3+\epsilon_2'(\epsilon_3-\epsilon_1)]}}{\epsilon_3+i\sqrt{-[\epsilon_1\epsilon_3+\epsilon_2'(\epsilon_3-\epsilon_1)]}} =$$

$$= \frac{\epsilon_3^2+[\epsilon_1\epsilon_3+\epsilon_2'(\epsilon_3-\epsilon_1)]}{\epsilon_3^2-[\epsilon_1\epsilon_3+\epsilon_2'(\epsilon_3-\epsilon_1)]} + i\,\frac{2\epsilon_3\sqrt{-[\epsilon_1\epsilon_3+\epsilon_2'(\epsilon_3-\epsilon_1)]}}{\epsilon_3^2-[\epsilon_1\epsilon_3+\epsilon_2'(\epsilon_3-\epsilon_1)]} \qquad (2.24)$$

Finally the real and imaginary components of K_x can be written as (it fol from equations (2.13), (2.20), (2.24);

$$K_x' = K_o\sqrt{\frac{\epsilon_1\epsilon_2'}{\epsilon_1+\epsilon_2'}} + K_o\,\frac{2}{\epsilon_2-\epsilon_1}\left(\frac{\epsilon_1\epsilon_2'}{\epsilon_1+\epsilon_2}\right)^{3/2}\frac{\epsilon_3^2+[\epsilon_1\epsilon_3+\epsilon_2'(\epsilon_3-\epsilon_1)]}{\epsilon_3^2-[\epsilon_1\epsilon_3+\epsilon_2(\epsilon_3-\epsilon_1)]}\,\cdot$$

$$\cdot\,\mathrm{EXP}\left[2K_{oh}+\frac{\epsilon_2'}{\sqrt{-(\epsilon_1+\epsilon_2')}}\right] \qquad (2.25)$$

$$K_x'' = -K_o\,\frac{2}{\epsilon_2'-\epsilon_1}\cdot\left(\frac{\epsilon_1\epsilon_2}{\epsilon_1+\epsilon_2}\right)^{3/2}\frac{2\epsilon_3\sqrt{-[\epsilon_1\epsilon_3+\epsilon_2(\epsilon_3-\epsilon_1)]}}{\epsilon_3^2-[\epsilon_1\epsilon_3+\epsilon_2(\epsilon_3-\epsilon_1)]}\,\mathrm{EXP}\left[2K_{oh}\frac{\epsilon_2'}{\epsilon_1+\epsilon_2'}\right] \qquad (2.26)$$

For the frequency range $W^* < W \leq \frac{W_p}{\sqrt{\epsilon_1+1}}$, r^o_{23} becomes a purely real quantity, making $K_x'' = 0$. Thus, in this range of frequency, the real part of K_x can be expressed as;

$$K'_x = K_0 \sqrt{\frac{\varepsilon_1 \varepsilon'_2}{\varepsilon_1 + \varepsilon'_2}} + K_0 \frac{2}{\varepsilon'_2 - \varepsilon_1} \left(\frac{\varepsilon_1 \varepsilon'_2}{\varepsilon_1 + \varepsilon'_2} \right)^{3/2} \left\{ \frac{\varepsilon_3 - \sqrt{\varepsilon_1 \varepsilon_3 + \varepsilon'_2 (\varepsilon_3 - \varepsilon_1)}}{\varepsilon_3 + \sqrt{\varepsilon_1 \varepsilon_3 + \varepsilon'_2 (\varepsilon_3 - \varepsilon_1)}} \right\} \times$$

$$\times \; E_{xp} \left[2K_o h \frac{\varepsilon'_2}{\sqrt{-(\varepsilon_1 + \varepsilon'_2)}} \right] \qquad (2.27)$$

The graph for K'_x as a function of W for different value of thickness h of the metallic film is shown at figures (2.2a) and (2.2b) by a continuous (solid) line. The broken line at these figures represent the dispersion graph for K'_{xo} (semi infinite case). The comparison of the two types of lines at each figure shows that the approximation introduced by equations (2.13) and (2.20) is valid in the whole range of frequencies $0 < \frac{W}{W_p} < \frac{1}{\sqrt{\varepsilon_1 + 1}}$ only if the thickness of the film is greater than the order of 0.3 ~ 0.4μm.

On the other hand for a narrow frequency range $0 < W \le W^{**}$ the coincidence of the two types of lines is good for metallic films, of infinite simally small thickness.

The value of W** is determined from the condition $R_e(r^0_{23}(W^{**}) = 0$. Which means from equation (2.24).

$$\varepsilon_3^2 + \varepsilon_1 \varepsilon_3 + \varepsilon'_2 (\varepsilon_3 - \varepsilon_1) = 0$$

$$\varepsilon'_2 = -\frac{(\varepsilon_3^2 + \varepsilon_1 \varepsilon_3)}{(\varepsilon_3 - \varepsilon_1)}$$

$$1 - \frac{W_p^2}{W^{**2}} = -\frac{(\varepsilon_3^2 + \varepsilon_1 \varepsilon_3)}{(\varepsilon_3 - \varepsilon_1)}$$

$$1 + \frac{\varepsilon_3^2 + \varepsilon_1 \varepsilon_3}{\varepsilon_3 - \varepsilon_1} = \frac{W_p^2}{W^{**2}}$$

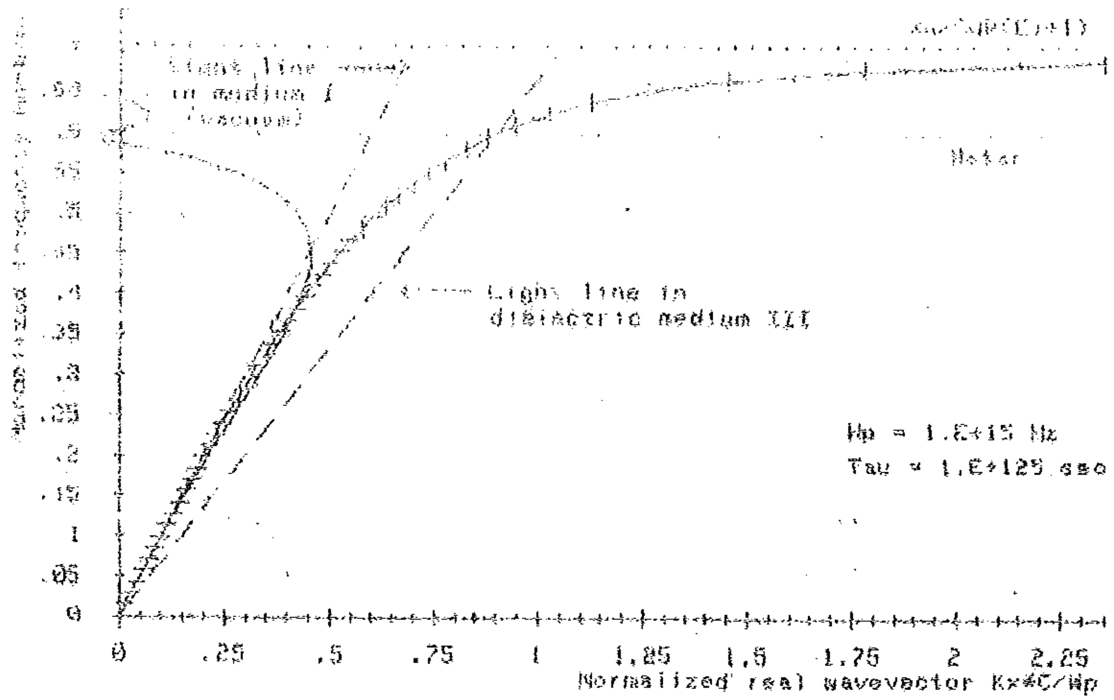

Fig.(2.2a) SPIP dispersion curve of REAL Kx as a function of frequency : (a) - for thin metalic film of thickness H boundering dielectric media (E1 and E3) - continious line, (b) - for infinite media METAL/DIELECTRIC interface (broken line). H = .04 micrometers

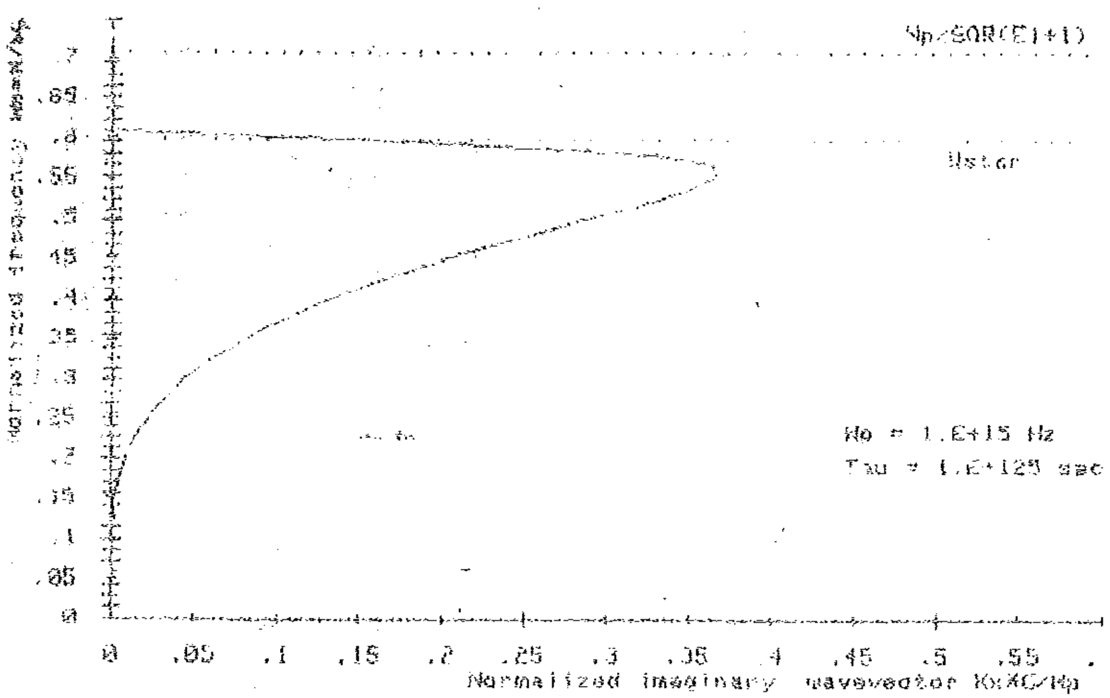

Fig.(2.3a) SPIP dispersion graph of IMAGINARY Kx as a function of frequency: (a) - for thin metalic film of thickness H boundering dielectric media (E1 and E3) - continuous line ; (b) - for infinite media METAL/AIR interface (broken line). H = .01 micrometers

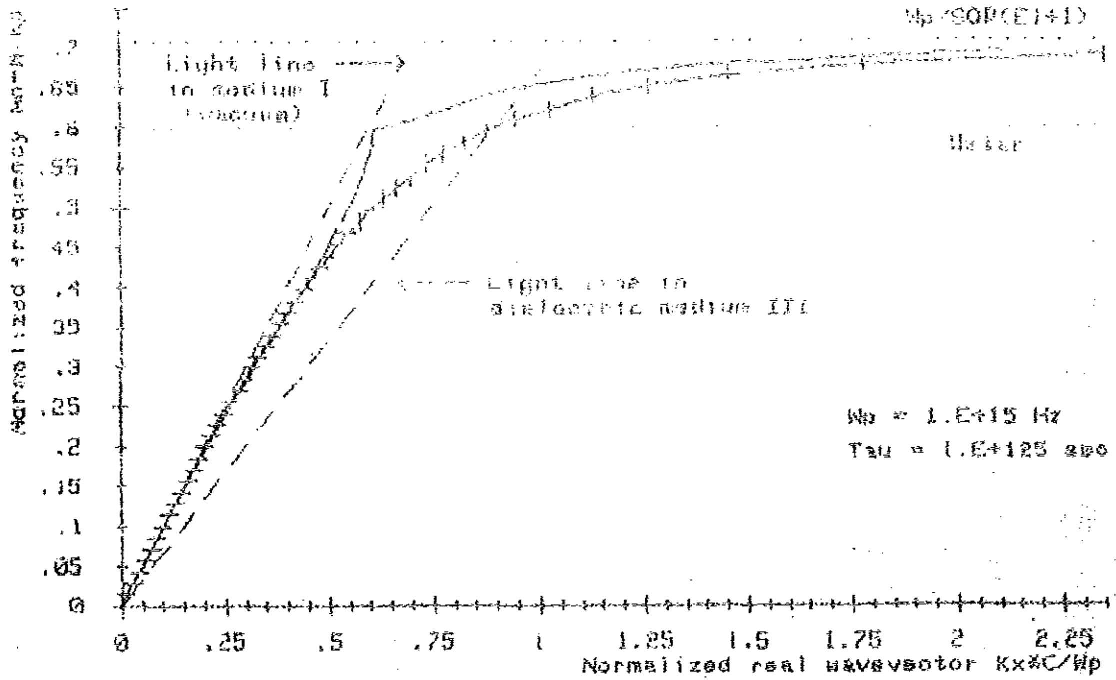

Fig.(2.2b) SPIP dipersion curve of REAL Kx as a function of frequency : (a) -for thin metalic film of thickness H boundering dielectric media (E1 and E3)- continious line, (b) - for infinite media METAL/DIELECTRIC interface (broken line), H = .2 micrometers"

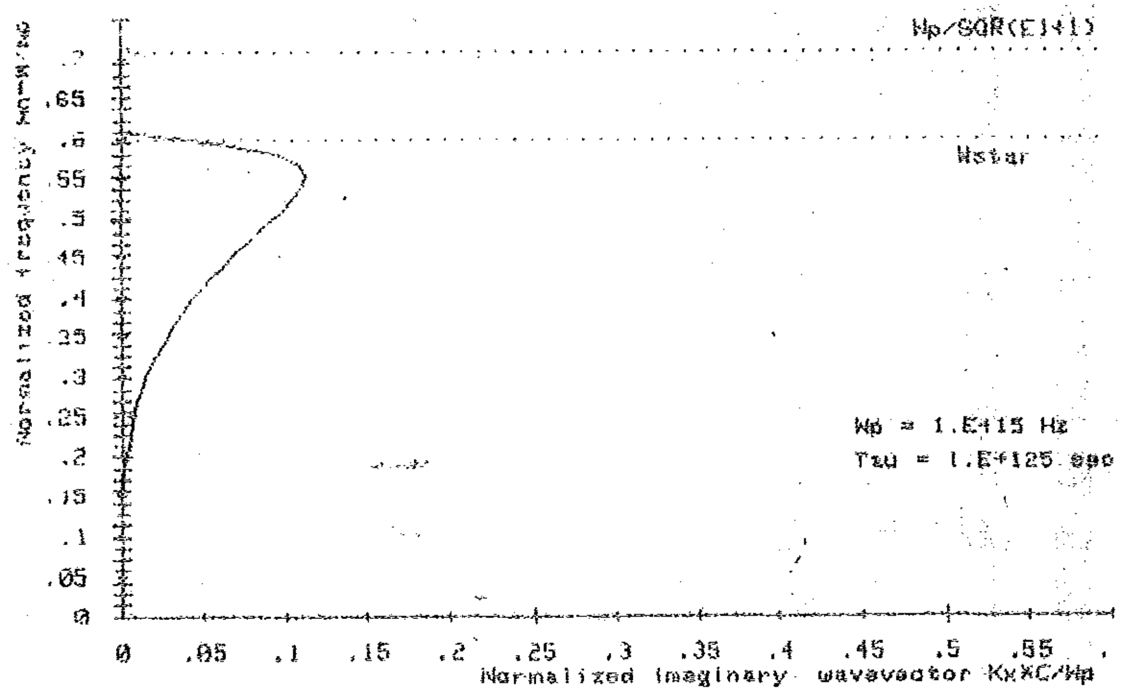

Fig.(2.3b) SPIP dispersion graph of IMAGINARY Kx as a function of frequen (a)- for thin metalic film of thickness H boundering dielectric media (E1 and E3) -continuous line ;(b)- for infinite media METAL/AIR interface (broken line). H = .2 micrometers

$$W^{**} = W_p \sqrt{\frac{\varepsilon_3 - \varepsilon_1}{\varepsilon_3 - \varepsilon_1 + \varepsilon_3^2 + \varepsilon_1 \varepsilon_3}} \qquad (2.28)$$

The definition of W** represents a new fact. Earlier Authors [3,4] introducing equations (2.13) and (2.20) claimed they are applicable in the whole range of frequencies $0<W<\frac{W_p}{\sqrt{\varepsilon_1+1}}$.

Equation (2.27) together with figures (2.3a) (2.4a) and (2.4c) at which K_x'' is shown as a function of W for various thickness of metallic film show that, even if ε_2'' approaches zero (according $\tau \approx 10^{125}$ sec) the value of K_x'' does not tend to zero for $0 \leq W < W^*$, and it tends to zero for $W^* \leq W < \frac{W_p}{\sqrt{\varepsilon_1+1}}$. This means that in the first subrange we have naturally a leakage of energy from SP1P into medium 3 (leaky plasmons), On the other hand exactly this particularity allows to excite SP1P by external light source located in medium 3. In the second subrange there is no leakage of energy from SP1P (non-radiative SP1P), Such SP1P cannot be excited in the way discussed above.

Figures (2.2d), (2.3d), and (2.4d) describe the same type of dependences, but for strong absorption case when $\tau \approx 10^{-13}$ sec. Both K_{xo} and K_{x1} are increasing and have nearly the same order. In general the graph drawn at Fig. (2.4) in logarithmic scale is, inorder to show how much the SP1P energy is affected due to the existance of the metallic film

2.3 Excitation of SP1P by Attenuated Total Reflection Technique

Several techniques are available in the experimental study of SP1P, and their use is dictated by the frequency and the wave number range in whic the excitation is being examined. For example at short wave lengths

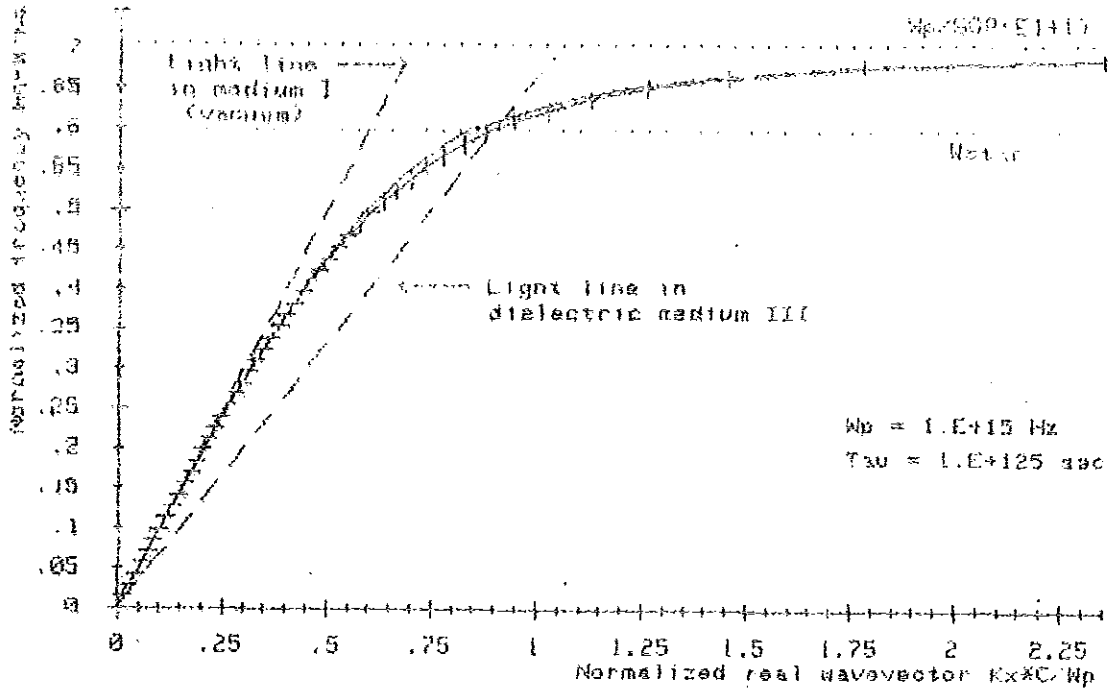

Fig.(2.2c) SPIP dispersion curve of REAL Kx as a function of frequency : (a) -for thin metalic film of thickness H boundering dielectric media (E1 and E3)- continious line, (b) - for infinite media METAL/DIELECTRIC interface (broken line). H = .4 micrometers*

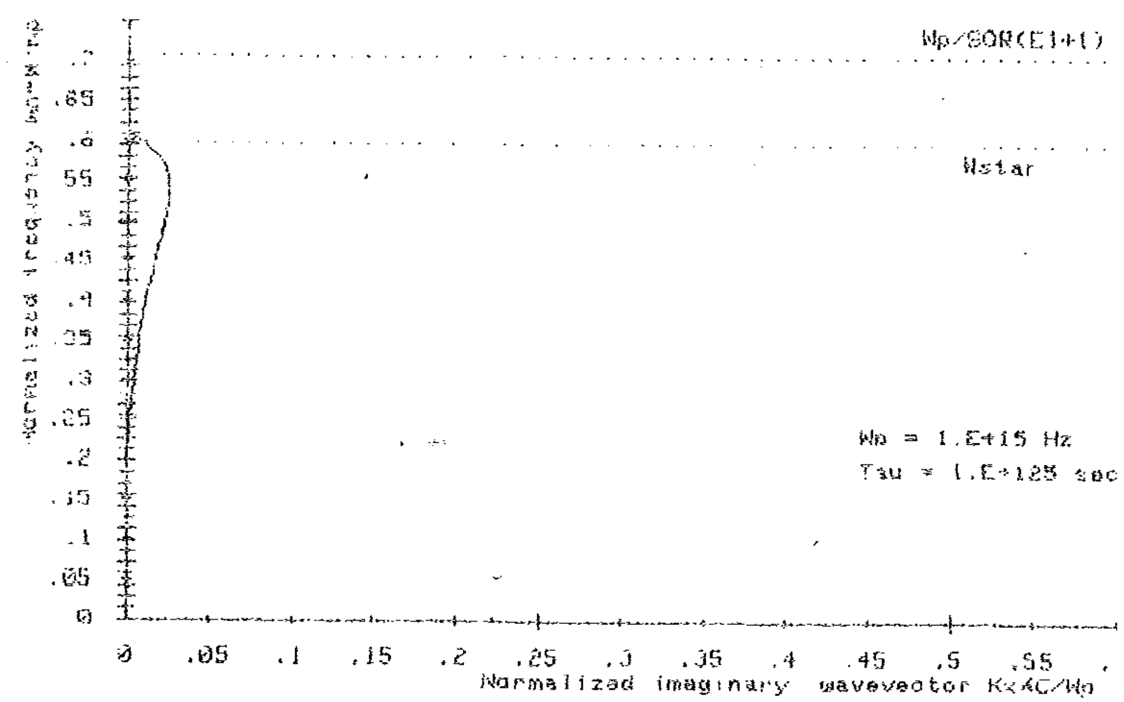

Fig.(2.3C) SPIP dispersion graph of IMAGINARY Kx as a function of frequency: (a)- for thin metalic film of thickness H boundaring dielectric media (E1 and E3) continuous line ;(b)- for infinite media METAL/AIR interface (broken line). H = .4 micrometers *

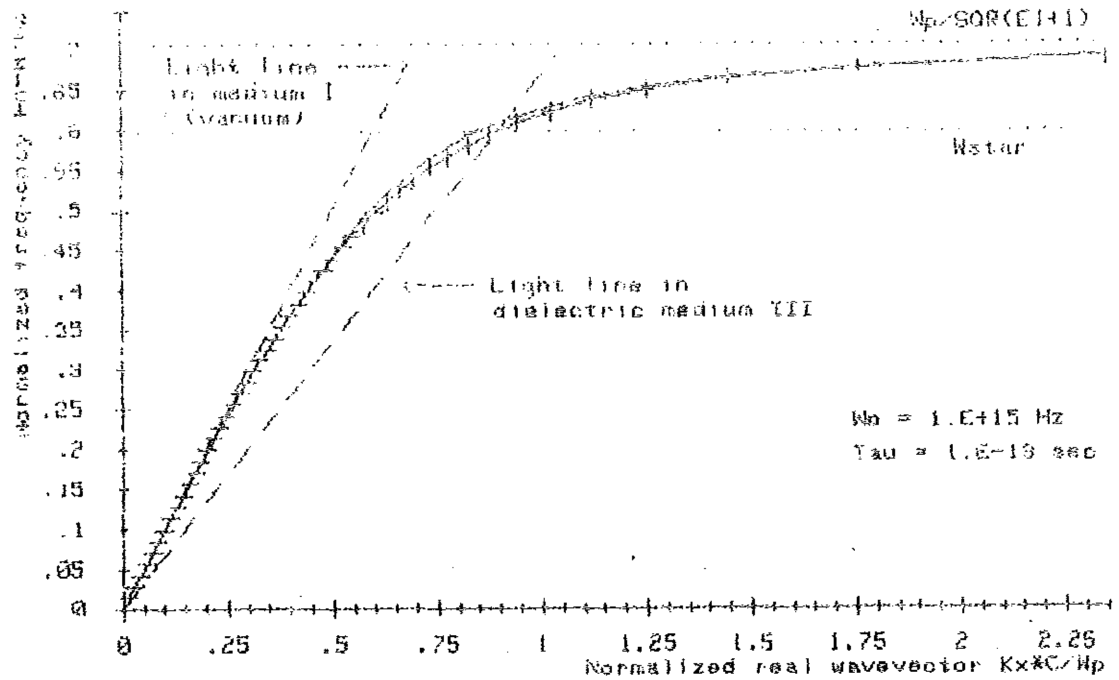

Fig.(2.2d) SPIP dipersion curve of REAL Kx as a function of frequency : (a) -for thin metalic film of thickness H baundering dielectric media (E1 and E3)- continious line, (b) - for infinite media METAL/DIELECTRIC interface (broken line). H = .4 micrometers*

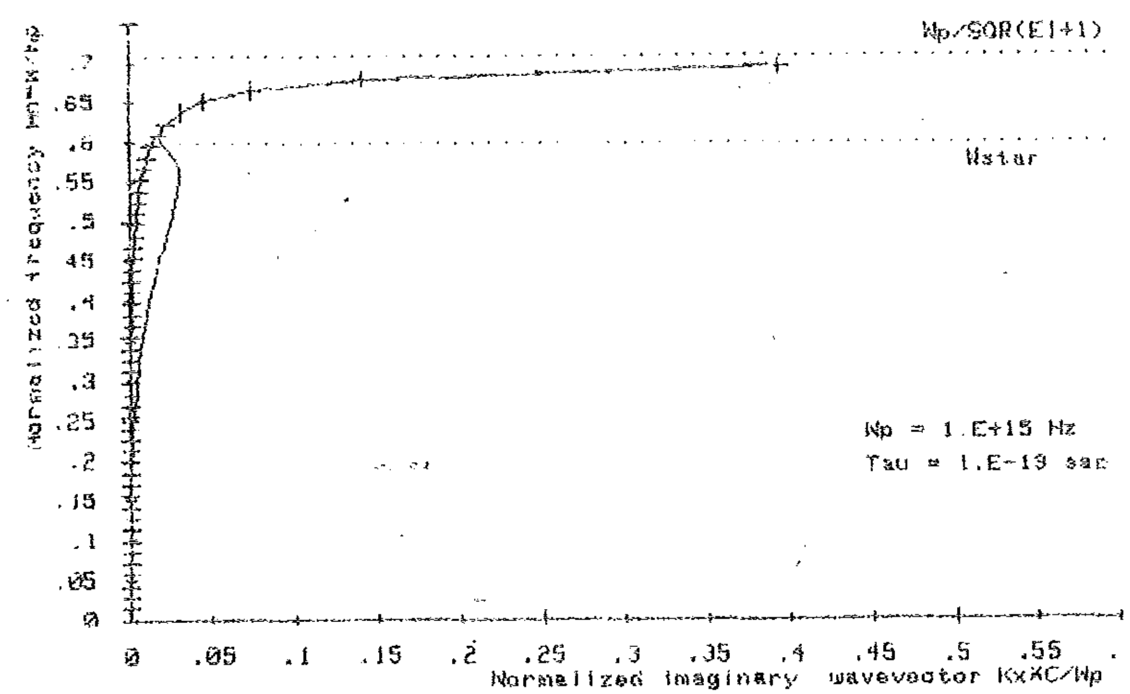

Fig.(2.3d) SPIP dispersion graph of IMAGINARY Kx as a function of frequency: (a)- for thin metalic film of thicknass H boundaring dielectric media (E1 and E3) -continuous line ;(b)- for infinite media METAL/AIR interface (broken line). H = .4 micrometers *

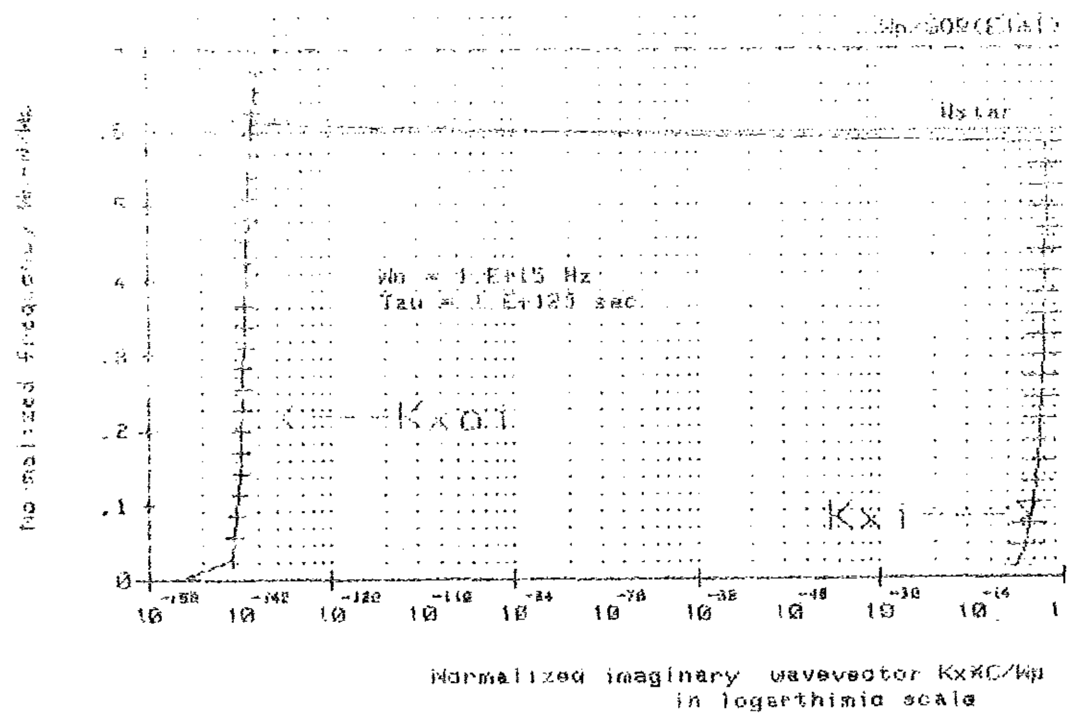

Fig.(2.4a) SPIP dispersion graph of imaginary Kx as a function of frequency:
(a)- for thin metalic film of thickness H boundaring dielectric media (E) and E3) |-|-|-| line; (b)- for infinite media METAL/AIR interface (I-I-I-I line).H = .04 micrometers

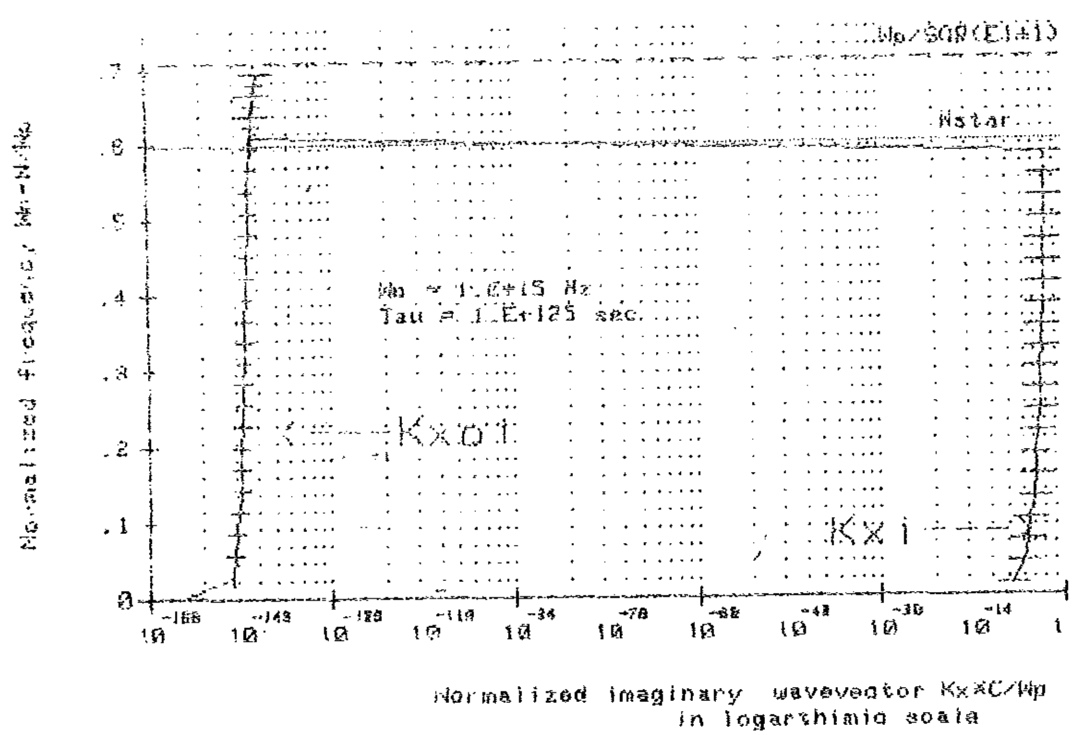

Fig.(2.4b) SPIP dispersion graph of imaginary Kx as a function of frequency:
(a)- for thin metalic film of thickness H boundaring dielectric media (E) and E3) |-|-|-| line; (b)- for infinite media METAL/AIR interface (I-I-I-I line).H = .2 micrometers

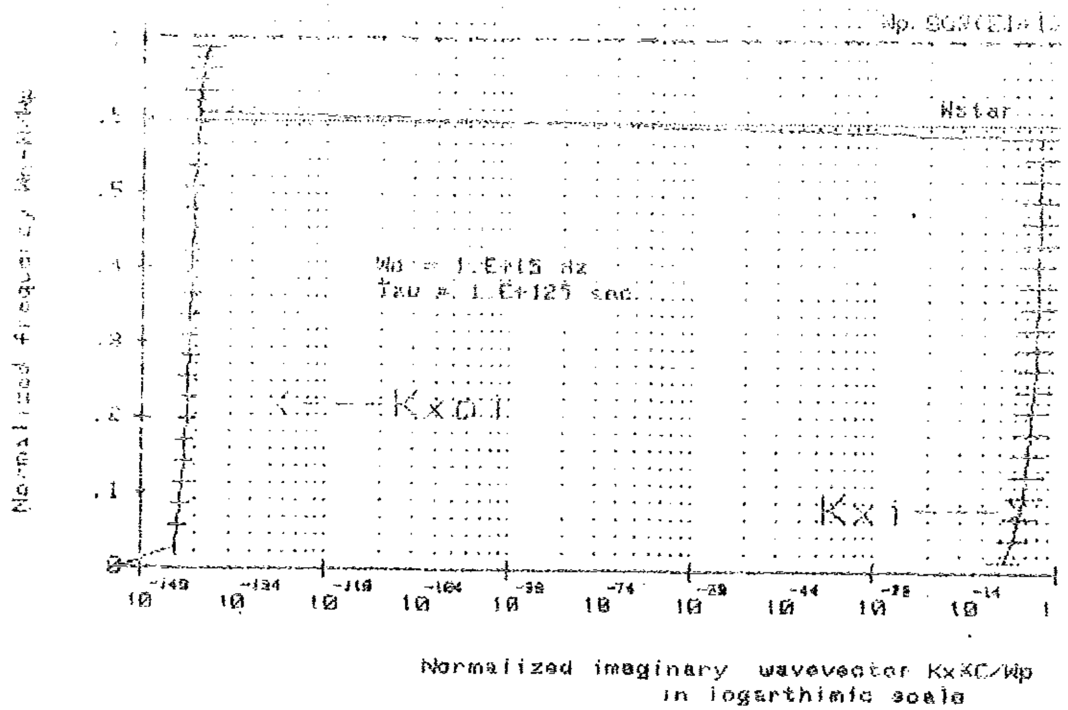

Fig.(2.4c) SPIP dispersion graph of imaginary Kx as a function of frequency: (a)- for thin metalic film of thickness H boundering dielectric media (E1 and E3) |-|-|-| line; (b)- for infinite media METAL/AIR interface (I-I-I-I line).H = .4 micrometers *

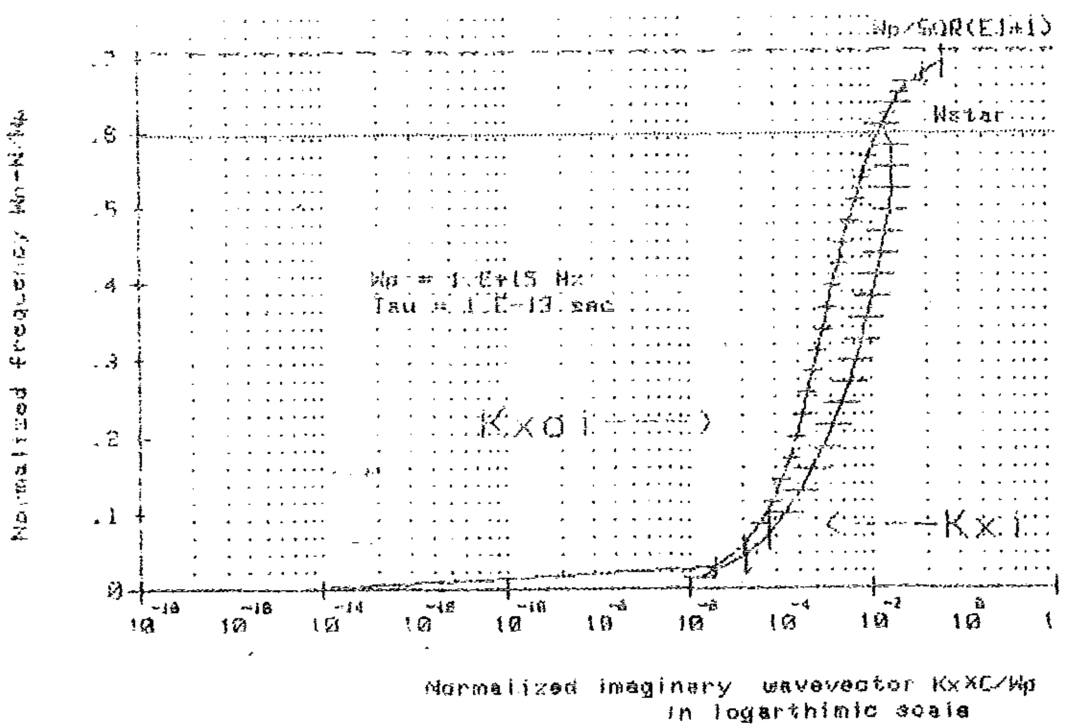

Fig.(2.4d) SPIP dispersion graph of imaginary Kx as a function of frequency: (a)- for thin metalic film of thickness H boundering dielectric media (E1 and E3) |-|-|-| line; (b)- for infinite media METAL/AIR interface (I-I-I-I line).H = .4 micrometers * (that is large wave number values) where the SP1P is most "Plasmon like" (see fig.2.1) the most suitable probe of the dispersion equation is an experiment involving electrons, such as thin film electron diffraction [5]. Conversely, at larger wave lengths (that is small wave number values) where the SP1P is most "photon-like" (see fig.2.2) the most suitable probe is an experiment involving light of the appropriate frequency, and it is one such technique that is discussed here, which is known as attenuated total reflection (ATR) [1].

ATR involves the use of the evanescent wave that is set up at a conducting medium/air interface when light in a high refractive index dielectric medium such as glass, suffers total internal reflection [6]. It is the reduction of the reflected wave due to absorption that is called ATR. If the weakening occurs by some other means it is usually called frustrated total internal reflection (FTIR). It is remarkable that FTIR can be traced back to Newton [7] and the knowledge and use of ATR has been wide spread only since the early 1960s due to pioneering work by Fahrenfort and Harrik [8,9]. Inspite of all this work, however, the fundamental idea of using ATR to generate SP1P was first published by Otto [10] as late as 1968.

An inspection of the dispersion curves (see fig. 1.3) reveals that in the photon like region, where it might be thought that SP1P could be stimulated by incident electromagnetic waves, the dispersion curve, in the first subrange $0 < W < \frac{W_p}{\sqrt{\varepsilon_1 + 1}}$ lies below the light line. Unfortunately, for a plane electromagnetic wave incident on the interface between $\varepsilon_1 = 1$ ε_2 at some angle θ_1, the relationship between the component of wave number parallel to the surface and θ_1 is given by:

$$K'_x = \frac{\omega}{c} n_1 \sin\theta_1 \quad \text{------------} \quad (2.29)$$

This corresponds to a line steeper than the light line on Fig.(2.2) and hence, to the region above the light line, therefore SPIP can't be generated. This awkawrd difficuly can be overcome in an ATR system as first proposed by Otto [10] and subsquently by Kretschmann [11], fig. (2.5).

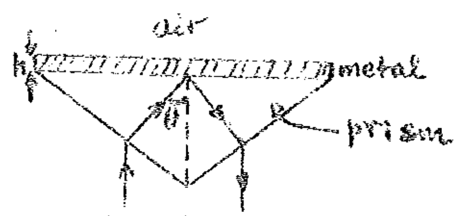

Fig. (2.5) Kretschmann Prism-metal-Air ATR Configuration with an active film of thickness h deposited on the base of the prism.

In this thesis we'll stick to Kretschmann's Scheme, which proved to be more convenient for practical use. Light incident, through the prism on to the prism-metal film interface at angles greater than the critical angle θ_{3crit} is normally totally reflected back out through the prism:

$$\theta_{3crit} = \arc \sin \frac{n'_2}{n_3} \quad \text{------------} \quad (2.30)$$

However, under total internal reflection conditions there will always be an exponentially decaying evanescent field extending into the metallic film. The totally reflected wave has a component of wave number parallel to the surface now is given by equation:

$$K'_x = \frac{W}{C} \sqrt{\varepsilon_3} \, \sin\theta_3 \quad \text{------------} \quad (2.31)$$

The corresponding dispersion curve (see fig. 2.2) in the small K region lies only below the light line. The evanescent wave, created by total reflection in the prism, actually exists in the range $\theta_{3crit} < \theta_3 \leq 90^0$. Hence the range of SP1P real wave number (in OX direction) associated with the evanescent wave is

$$\frac{W}{C} < K_x' < \frac{W}{C}\sqrt{\varepsilon_3} \qquad (2.32)$$

and corresponds to a region above the prism light line, but below the air or vacuum light line (see fig. 1.3).

From a practical point of view it is evident that, provided the thickness of the metallic film is sufficiently small, then the evanescent field from the prism can reach the air/metal film interface and SP1P can be excited. Energy from the incident wave is then used to stimulate a surface wave resulting in a weakening of the reflected intensity returned by the prism.

2.4 ATR Model

Let us consider a T-M polarization incident from dielectric medium 3 (prism) at an angle θ_3 to the normal of the medium 3/metal film interface (see fig. 2.6). The magnetic field in each medium may be expressed in the form

$$H_{Z1} = A_1 e^{+iK_{2y}Y} e^{i(K_xX - Wt)}$$

$$H_{Z2} = (A_2 e^{+iK_{2y}Y} + B_2 e^{-iK_{2y}Y}) e^{i(K_xX - Wt)} \qquad (2.33)$$

$$H_{Z3} = (A_3 e^{+iK_{3y}Y} + B_3 e^{-iK_{3y}Y}) e^{i(K_xX - Wt)}$$

Using the Maxwell's Curl equation with J = 0, that is $\nabla X \vec{H} = \varepsilon \frac{\partial \vec{E}}{\partial t}$ the corresponding tangential component electric field distributions are given respectively for the three media by

$$E_{x1} = \frac{A_1K_{1y}}{W\varepsilon_1} e^{iK_{1y}Y} e^{i(K_xX - Wt)}$$

$$E_{x2} = -\frac{A_2K_{2y}}{W\varepsilon_2} e^{iK_{2y}Y} + \frac{B_2K_{2y}}{W\varepsilon_2} e^{iK_{2y}Y} \quad e^{i(K_xX - Wt)} \quad \text{------} \quad (2.34)$$

$$E_{x3} = -\frac{A_3K_{3y}}{W\varepsilon_3} e^{iK_{3y}Y} + \frac{B_3K_{3y}}{W\varepsilon_3} e^{-iK_{3y}Y} \quad e^{i(K_xX - Wt)}$$

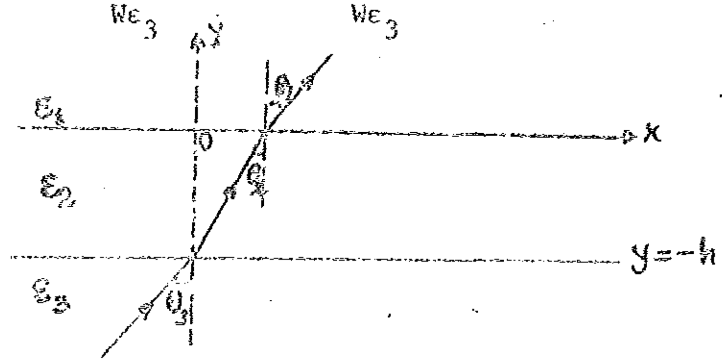

Fig. (2.6) illustration of the two interface model for an ATR system for Prism-Metal-Air (PMA) configuration.

Applying boundary conditions at Y = 0 and Y = -h;

$$A_1 = A_2 + B_2 \quad \text{---------} \quad (2.35)$$

$$-\frac{A_1K_{1y}}{\varepsilon_1} = -\frac{A_2K_{2y}}{\varepsilon_2} + \frac{B_2K_{2y}}{\varepsilon_2} \quad \text{------} \quad (2.36)$$

$$A_2e^{-iK_{2y}h} + B_2e^{iK_{2y}h} = A_3e^{-K_{3y}h} + B_3e^{+iK_{3y}h} \quad \text{---} \quad (2.37)$$

$$-\frac{A_2K_{2y}}{\varepsilon_2} e^{-iK_{2y}h} + \frac{B_2K_{2y}}{\varepsilon_2} = -\frac{A_3K_{3y}}{\varepsilon_3} e^{-iK_{3y}h} + \frac{B_3K_{3y}}{\varepsilon_3} \quad \text{---} \quad (2.38)$$

From equation (2.35) and (2.36)

$$-(A_2+B_2)\frac{K_{1y}}{\varepsilon_1} = -\frac{A_2K_{2y}}{\varepsilon_2} + \frac{B_2K_{2y}}{\varepsilon_2}$$

$$A_2\left(\frac{K_{2y}}{\varepsilon_1} - \frac{K_{1y}}{\varepsilon_1}\right) = B_2\left(\frac{K_{2y}}{\varepsilon_2} + \frac{K_{1y}}{\varepsilon_1}\right)$$

$$\frac{B_2}{A_2} = \frac{\left[\frac{K_{2y}}{\varepsilon_2} - \frac{K_{1y}}{\varepsilon_1}\right]}{\left[\frac{K_{2y}}{\varepsilon_2} + \frac{K_{1y}}{\varepsilon_1}\right]} = r_{21} \quad \text{------} \quad (2.39)$$

r_{21} is reflection coefficient at the interface of medium 2/medium 1.

Multiplying equation (2.37) by a factor $\frac{K_{3y}}{\varepsilon_3}$ and adding the result with equation (2.38) we get

$$A_2\left[\frac{K_{3y}}{\varepsilon_3} - \frac{K_{2y}}{\varepsilon_2}\right] e^{-iK_{2y}h} + B_2\left[\frac{K_{3y}}{\varepsilon_3} + \frac{K_{2y}}{\varepsilon_2}\right] e^{iK_{2y}h} = 2B_3\frac{K_{3y}}{\varepsilon_3} e^{iK_{3y}h} \quad \text{--} \quad (2.$$

Again multiplying equation (2.37) by a factor $\frac{K_{3y}}{\varepsilon_3}$ and from the result subtracting equation (2.38) we get

$$A_2\left[\frac{K_{3y}}{\varepsilon_3} + \frac{K_{2y}}{\varepsilon_2}\right] e^{-iK_{2y}h} + B_2\left[\frac{K_{3y}}{\varepsilon_3} - \frac{K_{2y}}{\varepsilon_2}\right] e^{iK_{2y}h} = 2A_3\frac{K_{3y}}{\varepsilon_3} e^{-iK_{3y}h} \quad \text{---} \quad (2.41)$$

Dividing equation (2.40) by equation (2.41) results;

$$\frac{A_2\left[\frac{K_{3y}}{\varepsilon_3} - \frac{K_{2y}}{\varepsilon_2}\right] e^{-iK_{2y}h} + B_2\left[\frac{K_{3y}}{\varepsilon_3} + \frac{K_{2y}}{\varepsilon_2}\right] e^{iK_{2y}h}}{A_2\left[\frac{K_{3y}}{\varepsilon_3} + \frac{K_{2y}}{\varepsilon_2}\right] e^{-iK_{2y}h} + B_2\left[\frac{K_{3y}}{\varepsilon_3} - \frac{K_{2y}}{\varepsilon_2}\right] e^{iK_{2y}h}} = \frac{B_3}{A_3} e^{2iK_{3y}h} \quad \text{---} \quad (2.42)$$

Using equation (2.39), equation (2.42) can be arranged to give

$$\frac{A_2 r_{32} + A_2 r_{21} e^{2iK_{2y}h}}{A_2 + A_2 r_{32} r_{21} e^{2iK_{2y}h}} = \frac{B_3}{A_3} e^{2iK_{3y}h} \quad \text{------} \quad (2.43)$$

or

$$\frac{r_{32} + r_{21} e^{2iK_{2y}h}}{1 + r_{32} r_{21} e^{2iK_{2y}h}} = \frac{B_3}{A_3} e^{2iK_{3y}h} = r \quad \text{------} \quad (2.44)$$

where $$r_{32} = \frac{\left[\frac{K_{3y}}{\varepsilon_3} - \frac{K_{2y}}{\varepsilon_2}\right]}{\left[\frac{K_{3y}}{\varepsilon_3} + \frac{K_{2y}}{\varepsilon_2}\right]} \quad \text{------------} \quad (2.45)$$

is the coefficient of reflection at the interface of medium 3/medium 2.

r is coefficient of reflection for medium 3.

Quantities r_{21}, r_{32} and r can be expressed in terms of incident angle θ_3.

Using Snell's law

$$K_{1y} = K_1 \cos\theta_1 = K_o \sqrt{\varepsilon_1} \cos\theta_1$$
$$K_{2y} = K_2 \cos\theta_2 = K_o \sqrt{\varepsilon_2} \cos\theta_2 \quad \text{----------} \quad (2.46)$$
$$K_{3y} = K_3 \cos\theta_3 = K_o \sqrt{\varepsilon_3} \cos\theta_3$$

From Snell's law,

$$\sqrt{\varepsilon_3} \sin\theta_3 = \sqrt{\varepsilon_2} \sin\theta_2$$
$$\sqrt{\varepsilon_2} \sin\theta_2 \quad \sqrt{\varepsilon_1} \sin\theta_1$$

$$\cos\theta_1 = \sqrt{1 - \frac{\varepsilon_3}{\varepsilon_1} \sin^2\theta_3} \quad \text{-------} \quad (2.47)$$
$$\cos\theta_2 = \sqrt{1 - \frac{\varepsilon_3}{\varepsilon_2} \sin^2\theta_3}$$

Using equations (2.46) and (2.47)

$$r_{21} = \frac{\sqrt{\varepsilon_1}\sqrt{1 - \frac{\varepsilon_3}{\varepsilon_2}\sin^2\theta_3} - \sqrt{\varepsilon_2}\sqrt{1 - \frac{\varepsilon_3}{\varepsilon_1}\sin^2\theta_3}}{\sqrt{\varepsilon_1}\sqrt{1 - \frac{\varepsilon_3}{\varepsilon_2}\sin^2\theta_3} + \sqrt{\varepsilon_2}\sqrt{1 - \frac{\varepsilon_3}{\varepsilon_1}\sin^2\theta_3}} \quad \text{-----} \quad (2.48)$$

$$r_{32} = \frac{\sqrt{\varepsilon_2}\cos\theta_3 - \sqrt{\varepsilon_3}\sqrt{1 - \frac{\varepsilon_3}{\varepsilon_2}\sin^2\theta_3}}{\sqrt{\varepsilon_2}\cos\theta_3 + \sqrt{\varepsilon_3}\sqrt{1 - \frac{\varepsilon_3}{\varepsilon_2}\sin^2\theta_3}} \qquad (2.49)$$

$$r = \frac{r_{32} + r_{21}e^{\left(2iK_o\sqrt{\varepsilon_2 - \varepsilon_3\sin^2\theta_3}\right)}}{1 + r_{32}r_{21}e^{\left(2iK_o\sqrt{\varepsilon_2 - \varepsilon_3\sin^2\theta_3}\right)}} \qquad (2.50)$$

Note that r_{21}, r_{32} and r are complex quantities, and in experiment it is the reflectance $R = |r|^2$ which is determined.

2.5 <u>Typical Results</u>

As an example of the use of the ATR technique for the SPIP excitation data for sodium (a good free electron metal, which has a complex refractive index $n_2 = 0.044 + i2.42$) was used. The computer simulated experiment was run for a fixed angle scan and a fixed frequency scan Table 1 contains a truncated copy of the data file showing the interesting parts of a fixed angle scan for Prism-Metal film-Air structure using a free electron model with data appropriate to sodium. The graph obtained with this data is shown in Fig. 2.[illegible]. This scan at 60^o shows a deep minimum in the reflected intensity at a frequency $w/w_p \sim 0.57$. This corresponds to a "pole" in R_{21} that is at a slightly lower frequency (see third column in the table I). The difference is due to the perturbation by the prism of the metal/air interface.

As a second example, a truncated set of results is displayed in table 2 for a fixed frequency scan. The graphs obtained from this data is shown at figure 2.8.

It can be seen that the reflected intensity in the fourth column of table 2 exhibits a sharp peak at $\tilde{}42^{0}$ which is the critical angle for a prism air interface. This feature is typical of the PMA configuration and is due to the fact that the final medium in the system is Air with $\varepsilon_1 = 1$. An examination of the third column containing $R_{21} = |r_{21}|^2$ reveals a very large peak near 47^{0} corresponding to the launching of a surface wave associated with the metal/air interface. Note that the reflected intensity shows a minimum very near to this angle, the shift being due again to the fact that perturbation occurs because we realy have a coupled system. The degree to which this perturbation occurs is a function of the film thickness. It is possible to determine the optimum value of h and corresponding w/w_p for which $R \to 0$.

As an example of such opportunity we prepared figures (2.9) and (2.10) in which the frequency curve becomes very sharp and the R min ~ 0

TABLE 1. Fixed angle calculation. Reflectivity of PRISM-METAL FILM-AIR struct as a function of the normalized incident frequency. R32 - is the reflectivity of the PRISM/METAL film interface; R21 - is the reflectivity of METAL/AIR interface. The angle of the ATR scan Teta= 60 degrees
Relative dielectric permittivities: PRISM - E3= 2.25 , METAL film - E21(w), E22(w), AIR - E1 = 1 .
Thickness of the film H = .04 micrometers, plasma frequency Wp= 8.38197252587E+15 Hz , relaxation time Tau = 1.00583208114E-14 sec .

w/Wp	R32	R21	Total reflectance	
1.E-6	.999076341509	1.00037159662	.880473950791	1
.090001	.934010552955	1.55521045039	.869103716413	7
.180001	.940474202187	2.51882248753	.878710779317	13
.270001	.948764893815	4.51441171474	.895891395757	19
.360001	.956985811829	10.0539888904	.908153856989	25
*	*	*	*	*
.435001	.963123778141	29.1701862487	.903651770634	30
.450001	.964254614904	39.5566971917	.898830846811	31
.465001	.965352327785	57.122416416	.891380952001	32
.480001	.966417016022	89.5088067708	.879988161923	33
.495001	.967448947899	160.299144058	.862398996631	34
.510001	.968448530528	365.928884110	.834603369880	35
.525001	.969416283523	1457.05369428	.789382132437	36
.540001	.970352816224	7521.79345258	.714912895797	37
.555001	.971258808138	901.24544344	.602150260562	38
.570001	.972134992231	273.526575910	.495479634049	39
.585001	.972982140764	127.966080293	.52592711851	40
.600001	.973801053353	73.3643921814	.668102837844	41
.615001	.974592546973	47.2773954259	.78701960122	42
.630001	.975357447648	32.8641032323	.858129511243	43
.645001	.976096583589	24.0880097073	.898967450695	44
*	*	*	*	*
.660001	.976810779581	18.3617548936	.92338623537	45
.810001	.982753222042	3.33142988724	.976643432098	55
.960001	.986988381819	1.23591977197	.985164027118	65
1.110001	.990039023208	.598545378843	.989344787862	75
1.260001	.99226452126	.334117933587	.991979549061	85
1.410001	.993909765483	.204019366569	.993791698303	95

TABLE 2. Fixed normalized frequency calculation. Reflectivity of PRISM-METAL FILM-AIR structure as a function of the incident angle. R32 - is the reflectivity of the PRISM/METAL film interface; R21 - is the reflectivity of the METAL/AIR interface. The freq.of the ATR scan w/Wp= .382 rad/sec
Relative dielectric permittivities: PRISM - E3= 2.25 ,METAL film -E21(w)= -5.8462817042 ,E22(w)= .212578670128 ,AIR - E1 = 1 .
Thickness of the film H = .04 micrometers plasma frequency Wp= 8.38197252587E+15 Hz. τ = 100583208114E-14 sec

Teta (deg)	R32	R21	Total reflectance	
4	.967858965634	.974499371602	.677776988447	1
20	.965457243788	.970399395708	.659782534977	5
36	.960997189305	.960297853665	.625991039039	9
*	*	*	*	*
36.05	.960982735032	.960277751031	.626044302114	10
37.15	.960667418691	.960036946689	.628775064618	32
38.25	.960358328985	.960422612618	.636157131225	54
39.35	.960057159185	.962099997981	.652866945083	76
40.45	.959765703781	.968805029038	.691682555938	98
41.55	.959485863685	.982309968519	.810592150038	120
42.65	.959219651436	5.54559165123	.978017995094	142
43.75	.958969196284	17.2892818316	.964375983017	164
44.85	.958736749076	55.9680051784	.914137010827	186
45.95	.95852468682	285.972833139	.800017778117	208
47.05	.958335516777	8778.26024704	.691960572604	230
48.15	.958171879936	465.025457783	.694936453403	252
49.25	.958036553675	142.019214892	.744603867245	274
50.35	.95793245339	74.2787947453	.788761332324	296
51.45	.957862632866	48.35861158	.820765319316	318
*	*	*	*	*
52	.95784156941	40.9121947329	.833142742612	329
66	.961850632179	9.34117226286	.930998930053	336
80	.979321035409	6.79104970606	.970477089832	343

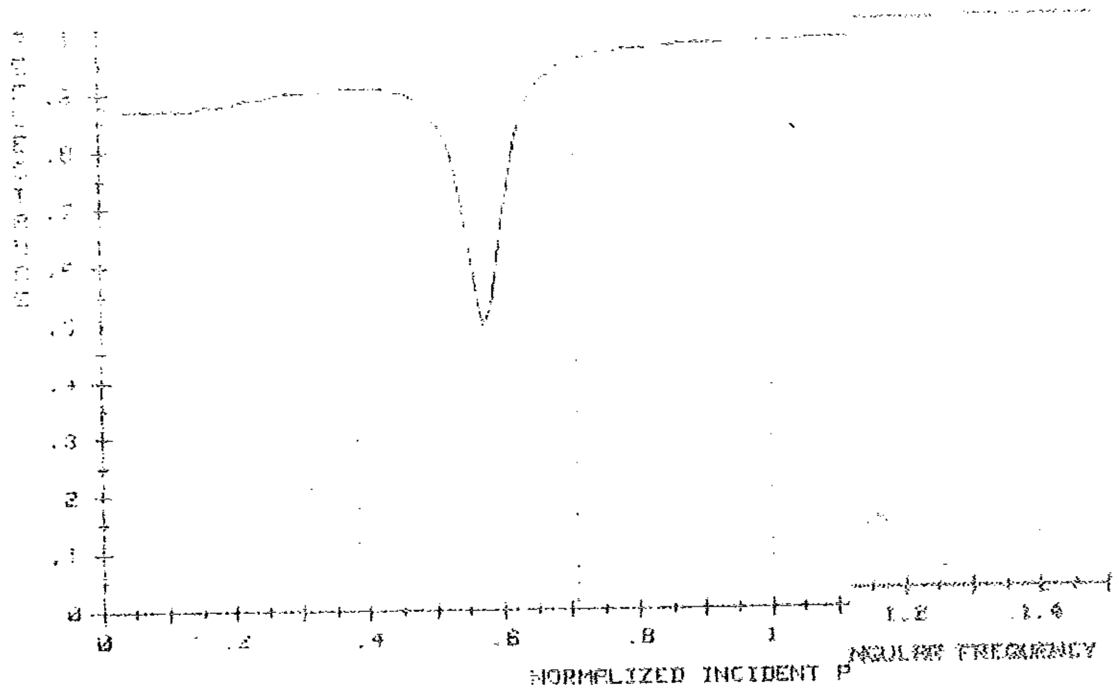

Fig.2.7 Graph of reflectivity R as a function of incident angular frequency w for PMA configuration at angle of beam Teta = 60 degrees. Thickness of the metal film H = .04 micrometers. wp = 8.36E+15rad/sec; Tau = 1.01E-14 sec.

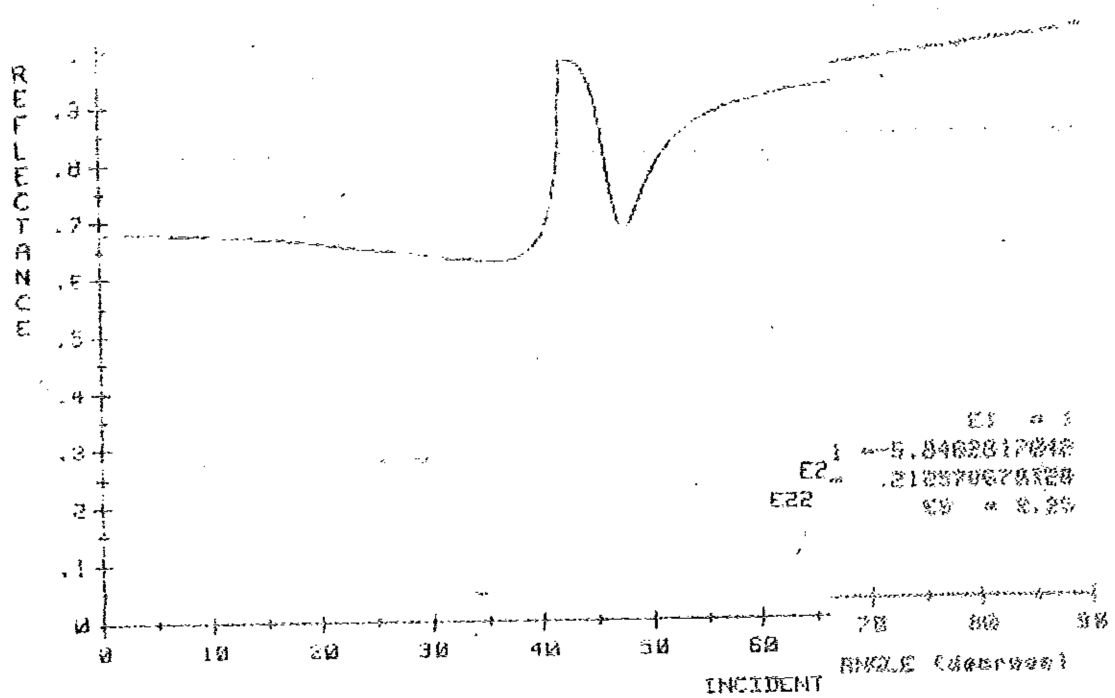

Fig.2.8 Graph of reflectivity R as a function of incident angle Teta for PMA configuration at normalized frequency of beam w/Wp=.382 . Thickness of the metal film H = .04 micrometers. wp = 8.30E+15 rad/sec; Tau = 1.01E-14 sec.

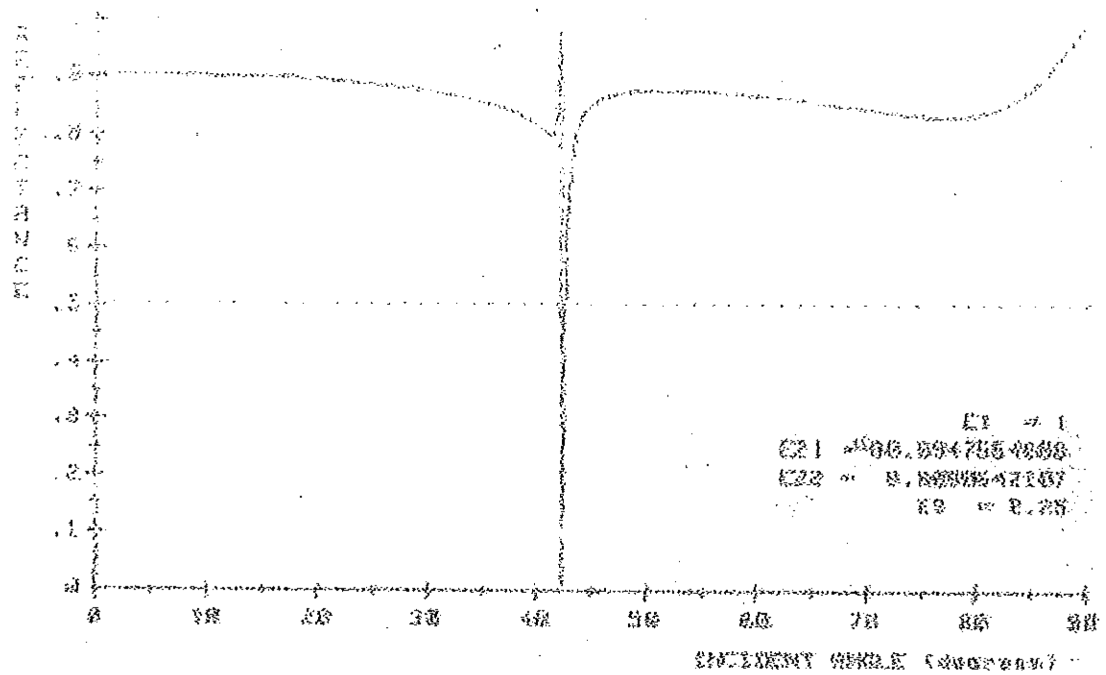

Fig.2.9 Graph of reflectivity R as a function of incident angle Teta for PMR configuration at normalized frequency of beam $w/wp = .110$, Thickness of the metal film $H = .04$ micrometers. $Wp = 8.30E+15$ rad/sec; $Tau = 1.01E-14$ sec.

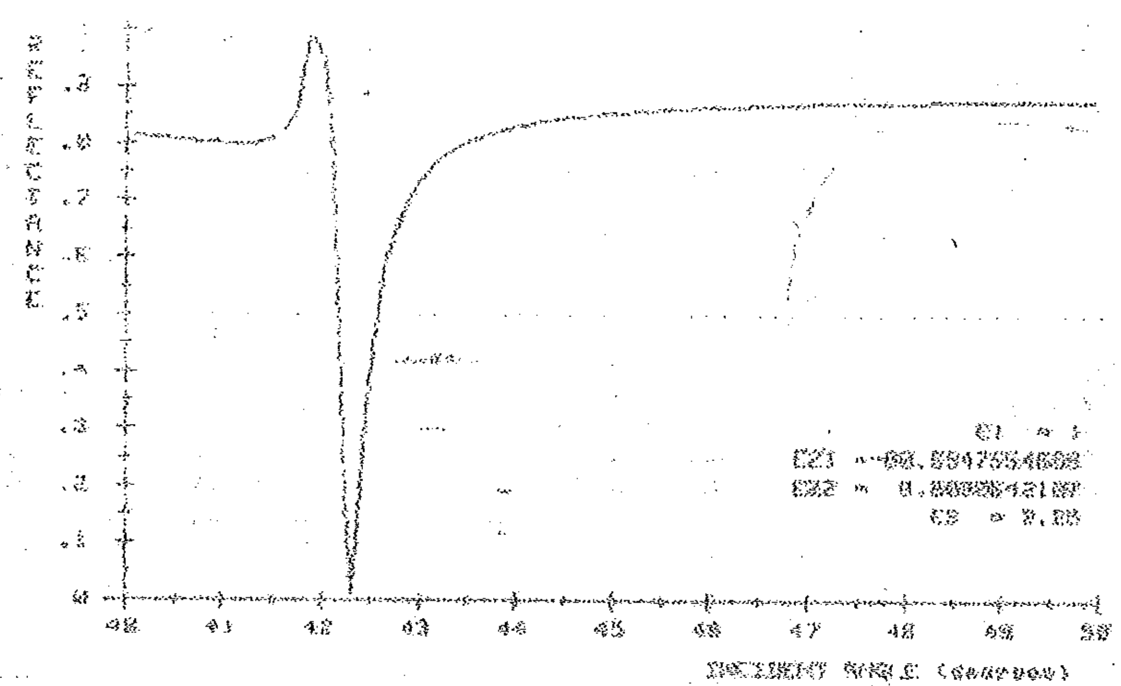

Fig.2.10 Graph of reflectivity R as a function of incident angle Teta for PMR configuration at normalized frequency of beam $w/wp = .110$, Thickness of the metal film $H = .04$ micrometers. $Wp = 8.30E+15$ rad/sec; $Tau = 1.01E-14$ sec.

Chapter 3

3.1 Use of SPIP for determination of the thickness and optical constants of thin metallic films

The optical properties of a metallic film can be characterized by a frequency dependent complex dielectric constant $\varepsilon_2(w) = \varepsilon_2' + i\varepsilon_2''$ (see equ. (1.24b). Among many optical methods [12], [13], the SPIP technique is particularly suited for the study of $\varepsilon_2(w)$ a few hundred angstroms in thickness. In many studies a preset expression for $\varepsilon_2(w)$ is required. That is w_p and τ values are to be known. However, in most cases a preset expression for $\varepsilon_2(w)$ that includes the contributions from the inter band transition is impossible. Therefore a method of determining $\varepsilon_2(w)$ and h at any given frequency without a preset $\varepsilon_2(w)$ expression is needed. Such method is described in the article [3]. The basic formulas and the concept are as follows, the geometry of the method is shown on fig. (2.5). with the angle of incidence of the external monochromatic plane wave θ close to θ_{ATR} (of attenuated total reflection) the minimum reflectance R_{min} can be approximately expressed as a function of θ_ω as [4]

$$R_{min} = 1 - \frac{4\eta}{(1+\eta)^2} \qquad (3.1)$$

$$\text{where } \eta = \frac{I_m(K_{xo})}{I_m(K_{x1})} \qquad (3.2)$$

With K_{xo} given by eqn. (1.31) and eqn. (1.32) and K_{x1} given by eqn. (2.20) and $K_x = K_{xo} + K_{x1}$.

Here K_x is the complex wave vector of the SPIP in the Kretschmann configuration (see fig. (2.5) and K_{xo} is the complex wave vector of the SPIP at the metal - vacuum interface in the absence of the prism (semi infinite case, described in chapter 1). K_{x1} is the perturbation to K_{xo}

in the presence of the prism. $I_m K_{xo}$ describes intrinsic damping in the absence of the prism, represents the Joule - loss, $I_m K_{xr}$ describes the radiative damping in the presence of the prism, represents the leakage loss of SPIP back into the prism.

The reflectance has a Lorentz dip at $\theta = \theta_{ATR}$ with a half width W_θ [where $I_m(K_x) \ll R_e(K_x)$]

$$W_\theta = 2I_m(K_x)\cos(\theta_{ATR})\frac{c}{\sqrt{\varepsilon_3}W} \quad \text{-------} \quad (3.3)$$

with

$$\theta_{ATR} = \arcsin\left(R_e(K_x)\cdot\frac{c}{\sqrt{\varepsilon_3}W}\right) \quad \text{-------} \quad (3.4)$$

with eqns. (3.1) to (3.4) and eqns. (2.20), (1.31), and (1.32) one can determine $\varepsilon_2(W)$ and h of a metal film from the measured R versus θ curve, by best fitting of the data with R given by eqn. (3.1)

A detailed description of the necessary steps is given in section 3.2 where we first suggest a more convenient modification of this method.

3.2 A suggested modification of the method for the determination of $\varepsilon(W)$ and h.

The measured quantities are θ_{ATR}, W_θ and R_{min} under the assumption that $R_eK_x \approx R_eK_{xo} = \frac{W}{c}\cdot\sqrt{\frac{\varepsilon_1\varepsilon_2'}{\varepsilon_1+\varepsilon_2'}}$ see eqn. (1.24b) and using eqn. (3.4), one can arrive to a formula;

$$\varepsilon_2' = \frac{\varepsilon_1\varepsilon_3\sin^2\theta_{ATR}}{\varepsilon_1-\varepsilon_3\sin^2\theta_{ATR}} \quad \text{-------} \quad (3.5)$$

Next eqn. (3.3) can be written as

$$I_mK_x = \frac{W_\theta}{2}\,\frac{1}{\cos\theta_{ATR}}\,\frac{W}{C}\,\sqrt{\varepsilon_3} = I_mK_{xo} + I_mK_{x1} \quad \text{------} \quad (3.6)$$

with

$$I_mK_{xo} = \frac{W}{C}\sqrt{\frac{\varepsilon_1\varepsilon_2'}{\varepsilon_1+\varepsilon_2'}}\;\frac{\varepsilon_1\varepsilon_2''}{2\varepsilon_2'(\varepsilon_1+\varepsilon_2')} \quad \text{------} \quad (3.7)$$

on the other hand, from eqn. (3.1)

$$\eta = \frac{(1+R_{min})\pm 2\sqrt{R_{min}}}{1-R_{min}} = \frac{1\pm\sqrt{R_{min}}}{1\mp\sqrt{R_{min}}} \quad \text{------} \quad (3.8)$$

The choice of algebraic signs in eqn. (3.8) should be based upon the physical sense of which is clear from eqn. (3.2). In the limiting case $h\to\infty$ I_mK_{x1} should vanish, giving $\eta\to\infty$. This result can be achieved from eqn. (3.8) if the upper signs (both in the numerator and the denominator) are used with $R_{min}\to 1$. This case would be denoted as η_+. In the other limiting case $h\to 0$, the perturbation I_mK_{x1} prevails over I_mK_{xo}, therefore $\eta\to 0$. This result follows from eqn. (3.8) if the lower signs are used, with $R_{min}\to 1$. This case would be denoted as η_-.

This consideration of the limiting cases suggest that there must be a switch from the upper case to the lower case as h change from ∞ to 0. This abrupt change occurs at $h = h_{opt}$, when $R_{min}\to 0$. The qualitative graph for $\eta = \eta(h)$ is shown at fig. (3.1a)

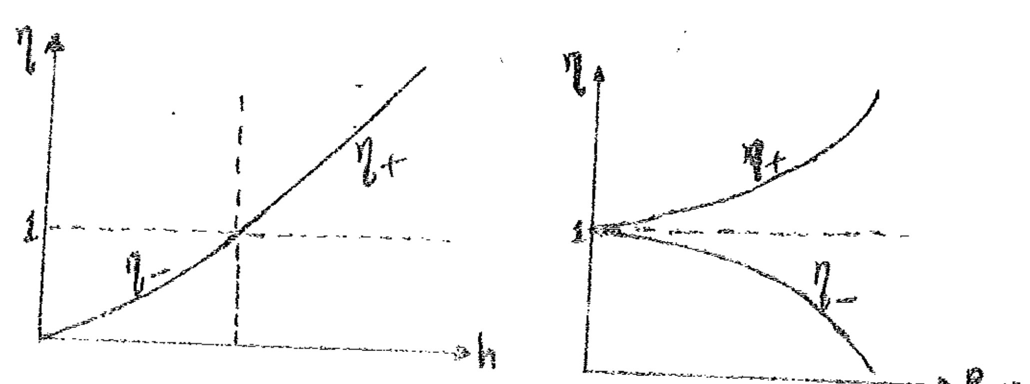

Fig. (3.1a) Illustration to the switch of sign operation.

with the help from eqn. (3.8), (3.2), (3.7), (3.6) and (3.5)

$$I_m K_{x1} = \frac{I_m K_{xo}}{\eta} ;$$

$$I_m K_{x1} = \frac{W_\theta}{2} \frac{1}{\cos\theta_{ATR}} \frac{W}{C} \sqrt{\varepsilon_3} - I_m K_{xo} \quad \text{-----} \quad (3.9)$$

$$I_m K_{xo} \cdot (1+\eta) = \eta \frac{W_0}{2} \frac{1}{\cos\theta_{ATR}} \frac{W}{C} \sqrt{\varepsilon_3}$$

with

$$\varepsilon_2'' = \frac{W_0}{2} \left(1 \pm \sqrt{R_{min}} \right) \frac{\varepsilon_1^2 \varepsilon_3 \tan\theta}{(\varepsilon_1 - \varepsilon_3 \sin^2\theta)^2} \quad \text{------} \quad (3.10)$$

where the upper sin (+) is for $h > h_{opt}$, and the lower sign (−) for $h < h_{opt}$

At $h = h_{opt}$ $R_{min} = 0$.

Now using eqns. (3.10), (3.7) and (3.9) we can derive a formula, which is useful for the final step for determination of h.

$$I_m K_{x1} = \frac{W}{C} \frac{W_\theta \sqrt{\varepsilon_3}}{4\cos\theta_{ATR}} \left(1 \mp \sqrt{R_{min}} \right) \quad \text{----} \quad (3.11)$$

where the convention of algebraic signs is the same as above.

Eqn. (3.11) gives the experimentally measured values of $(I_m K_{x1})_{exp}$.

The theoretical value of $(I_m K_{x1})$theor. as a function of h is given by eqn.(2.20). The numerical solution of the equation:

$$(I_m K_{x1}) (h))_{theor.} = (I_m K_{x1})_{exp} \quad \text{----} \quad (3.12)$$

gives the experimentally determined thickness h of the metallic film.

3.3 The accuracy of the method

Eqn. (3.5) shows that $\varepsilon_2' = \varepsilon_2' (\theta_{ATR})$, therefore

$$|\Delta\varepsilon_2'| = \left[\frac{\partial\varepsilon_2'}{\partial\theta_{ATR}} \right] \Delta\theta_{ATR} \quad \text{-------} \quad (3.13)$$

Where $\Delta\theta_{ATR}$ is the experimental accuracy of the angular measurement of the resonant angle θ_{ATR}. Performing the differentiation of eqn. (3.5) the relative accuracy of ε_2' determination can be expressed

$$\frac{|\Delta\varepsilon_2'|}{|\varepsilon_2'|} = \frac{2\varepsilon_1 \quad \Delta\theta_{ATR}}{(\varepsilon_1-\varepsilon_3\sin^2{}_\theta)\tan_\theta} \quad \text{-----} \quad (3.14)$$

Similarly, eqn. (3.1) indicates $\varepsilon_2'' = \varepsilon_2''\,(\theta_{ATR}, W_\theta, R_{min})$, therefore:

$$|\Delta\varepsilon_2''| = \left|\frac{\partial\varepsilon_2''}{\partial\theta_{ATR}}\right| |\Delta\theta_{ATR}| + \left|\frac{\partial\varepsilon_2''}{\partial W_\theta}\right| |\Delta W_\theta| + \left|\frac{\partial\varepsilon_2''}{\partial R_{min}}\right| \Delta R_{min} \quad \text{--} \quad (3.15)$$

where ΔW_θ, ΔR_{min} are experimental accuracies of measurements for half-width of the resonant curve and minimum of reflectance respectively.

performing partial differentiation of eqn. (3.10) gives

$$\frac{\partial\varepsilon_2''}{\partial\theta} = \frac{W_\theta}{2}\,(1\pm\sqrt{R_{min}})\;\varepsilon_1^{\,2}\varepsilon_3\left[\frac{\sec^2{}_\theta(\varepsilon_1-\varepsilon_3\sin^2{}_\theta)+4\varepsilon_3\sin^2{}_\theta}{(\varepsilon_1-\varepsilon_3\sin^2{}_\theta)^2}\right] \quad (3.16)$$

$$\frac{\partial\varepsilon_2''}{\partial W_\theta} = \frac{1}{2}\,(1\pm\sqrt{R_{min}})\;\frac{\varepsilon_1{}^2\varepsilon_3\tan_\theta}{(\varepsilon_1-\varepsilon_3\sin^2{}_\theta)^2} \quad \text{----} \quad (3.17)$$

$$\frac{\partial\varepsilon_2''}{\partial R_{min}} = \pm\;\frac{W_\theta}{4}\;\frac{\varepsilon_1^{\,2}\varepsilon_3\tan_\theta}{(\varepsilon_1-\varepsilon_3\sin_\theta)2}\cdot\frac{1}{\sqrt{R_{min}}} \quad \text{----} \quad (3.18)$$

where the convention of the algebraic signs is the same as above.

Let's normalize eqns (3.16) to (3.18) with respect to ε_2''

$$\frac{\partial\varepsilon_2''}{\varepsilon_2''\,\partial\theta} = \frac{\varepsilon_1-\varepsilon_3\sin^2{}_\theta+4\varepsilon_3\sin^2{}_\theta\cos^2{}_\theta}{\sin_\theta\cos_\theta\;(\varepsilon_1-\varepsilon_3\sin^2{}_\theta)} \quad \text{-------} \quad (3.19)$$

$$\frac{\partial\varepsilon_2''}{\varepsilon_2''\,\partial W_\theta} = \frac{1}{W_\theta} \quad \text{-----} \quad (3.20)$$

$$\frac{\partial \varepsilon_2''}{\varepsilon_2'' \partial R_{min}} = \pm \frac{1}{2\sqrt{R_{min}}\,(1 \pm \sqrt{R_{min}})} \qquad (3.21)$$

Hence, substituting eqns. (3.19) to (3.21) into eqn. (3.15) the relative accuracy of ε_2'' determination can be expressed as;

$$\left|\frac{\Delta\varepsilon_2''}{\varepsilon_2''}\right| = \left|\frac{\varepsilon_1 - \varepsilon_3 \sin^2\theta + 4\varepsilon_3 \sin^2\theta \cos^2\theta}{\sin\theta\cos\theta(\varepsilon_1 - \varepsilon_3 \sin^2)}\right| \Delta\theta_{ATR} + \frac{\Delta W\theta}{|W\theta|} + \frac{1}{\left|2\sqrt{R_{min}}\,(1 \pm \sqrt{R_{min}})\right|}\Delta R_{min} \qquad (3.22)$$

The relative accuracy of h determination was determined by numerical procedure as the described in the next paragraph.

3.4 The Computer Program

The basic idea of the computer program is represented on Fig. (3.1b) and (3.1d). The program first simulates the values of θ_{ATR}, W_θ and R_{min} as if they were measured in an ideal experiment with out any instrumental error ($\Delta\theta = \Delta W\theta = \Delta R = 0$). These values of θ_{ATR}, W_θ and R_{min} are named as "expected experimental values".

With an expected experimental value of θ_{ATR} from eqn. (3.4) it is possible to find the value of $\varepsilon_2'{}_{exp}$ from eqn. (3.5). Note that, since instrumental error $\Delta\theta$ is neglected, the result might be affected only by the approximation made in the theory. The calculations and comparison with the exact value of $\varepsilon_2'{}_{theor.}$ given by eqn. (1.24b) show that $\Delta\varepsilon_2' = \varepsilon_2'{}_{theor.} - \varepsilon_2'{}_{exp}$ realy depends upon the frequency used. The following results were obtained.

$$\left(\frac{\Delta\varepsilon_2'}{\varepsilon_2'}\right)_{theor} \left(\frac{W}{W_p} = 0.05\right) = 5.7\% \qquad \left(\frac{\Delta\varepsilon_2'}{\varepsilon_2'}\right)_{theor} \left(\frac{W}{W_p} = 0.3\right) = 0.2\%$$

$$\left(\frac{\Delta\varepsilon_2'}{\varepsilon_2'}\right)_{theor} \left(\frac{W}{W_p} = 0.1\right) = 1.4\%$$

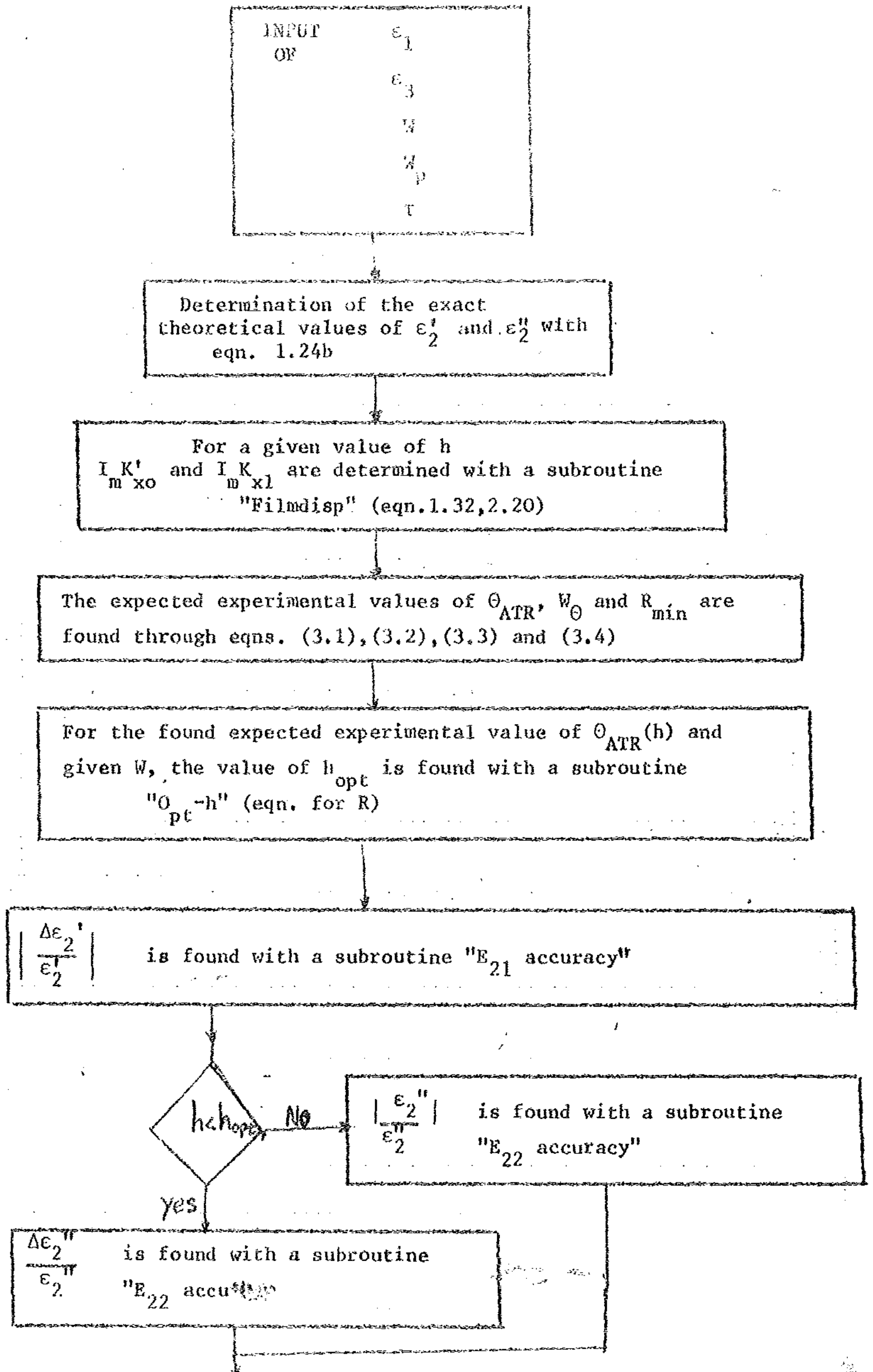

Fig. (3.1b) Block diagram of the computer program (to be continued).

Using eqn. (3.1), (3.3), and (3.4) and the expected experimental values of θ_{ATR} W_0, R_{min}, the experimental value of h is found. The procedure involves a subroutine "Bisect" from the numerical analysis library which finds the root of a function $(I_m K_{x1})_{exp}$, − $(I_m K_{x1})_{theor}$, see eqn. (2.20), (3.11), the subfunction FNF (H), a subroutine "Film disp 2" in which ε_2' and ε_2'' are calculated as experimentally determined (see equn. (3.5), (3.10))

↓

$\frac{h_{exp}}{h_{exp}}$ as a function of $\Delta\theta_{ATR}$, $\Delta W\theta$, ΔR_{min} is numerically calculated and stored in arrays $Dh_0(*)$, $Dh_1(*)$ and $Dh_2(*)$. The total error is stored in an array $D_{ht}(*)$

↓

Next h

↓

PRINTING The graphs of $\frac{\Delta\varepsilon_2'}{\varepsilon_2'}$, $\frac{\Delta\varepsilon_2''}{\varepsilon_2''}$, $\frac{\Delta_{hexp}}{hexp}$ versus h

(The list of the program is found in Appendix B.)

Fig. (3.1c) Block diagram of the computer program.

This frequency dependence becomes clear if we recall that eqn.(2.2) is valid only for $\frac{\varepsilon_2''}{|\varepsilon_2''|} \ll 1$. If we check this ratio at the specified frequencies, we get, $\frac{\varepsilon_2''}{|\varepsilon_2'|}$ $(\frac{W}{W_p} = 0.05) = 0.24$; $\frac{\varepsilon_2''}{|\varepsilon_2'|}$ $(\frac{W}{W_p} = 0.1) = 0.12$; $\frac{\varepsilon_2''}{|\varepsilon_2''|}$ $(\frac{W}{W_p} = 0.3) = 0.04$

Since the value of ε'_{2exp} is used in the subsequent evaluations of $\varepsilon_2''{}_{exp}$ and h_{exp} the first conclusion can be made.

Conclusion 1

The accuracy of the method has a tendency to improve as the frequency grow from 0 upto W** (see eqn. (2.28)). For frequencies greater than W** the accuracy again starts to deteriorate because the perturbation term in eqn. (2.13) becomes comparable to the basic term, making the solution (see eqn. (2.20)) in valid.

The first try of the program without any instrumental error allow to estimate the accuracy of the mathematical soft ware used in the method. The errors made due to a finite accuracy of the soft ware we'll call "software errors". It is clear that the 'software errors' in determination of ε_2', ε_2'', h should be always less than the errors which originate from finite instrumental accuracy. These latter errors we'll call experimental errors. For a practical use the instrumental error can be taken as $\Delta\theta = \Delta W = 5''$, $\Delta R = 0.01$. These values are used in the second, third, forth and fifth tries of the program, when all partial experimental and a total experimental errors are calculated. It is necessary to underline that the 'software error' is always incorporated in the calculation of the experimental errors, and for this reason it must be always checked first.

3.5 Analysis of the Methods Accuracy

As an example of the kind of results obtained from this program, data for sodium

($W_p = 8.38197252587 \times 10^{15}$ Hz, $\tau = 1.00583208114 \times 10^{-14}$ sec) was used. The refractive index of the prism was taken as, $n_3 = 1.5$. The surrounding medium was air with $n_1 = 1$. Typical results are shown at fig. (3.2) (3.3a), (3.3b), (3.3c), (3.4a), (3.4b), and (3.4c).

Fig. (3.2) shows that $\frac{\Delta\varepsilon_2'}{|\varepsilon_2'|_{exp}}$ is independent from h which is understandable since $R_e K_{xo}$ used in eqn. (3.4) does not depend upon h. On the other hand the comparison of the curves at fig. (3.2) with the values of $\frac{\Delta\varepsilon_2'}{|\varepsilon_2'|_{theor.}}$ shows that; the theoretical error is roughly 3 times bigger than the experimental error due to $\Delta\theta \neq 0$.

Conclusion 2

It is reasonable to perform the measurements for the determination of ε_2' only for normalized frequencies not less than $\frac{W}{W_p} = 0.1$. For less frequencies the software error rapidly grows bringing the total experimental error to 8% at $\frac{W}{W_p} = 0.05$.

The most striking result comes from Figs. (3.3a), (3.3b), and (3.3c) at which $\frac{\Delta\varepsilon_2''}{\varepsilon_2''_{exp}}$ as a function of h is shown for different normalized frequencies.

The figures show that a decisive contribution to the total experimental error comes from a partial experimental error due to an instrumental error in measuring R_{min}. In particular at h in the vicinity of h_{opt}, when the value of $R_{min} \to 0$, this partial experimental error exhibits an unlimited growth. This result is

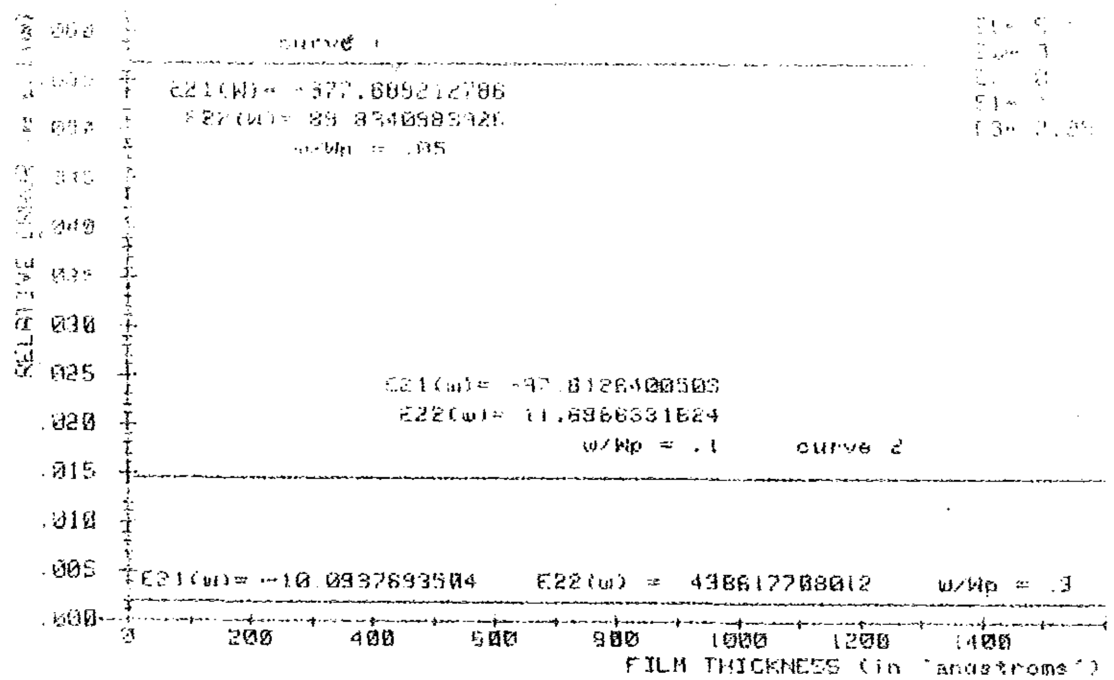

Fig.3.2. Dependence of relative error in determination of E21(ω) on the thickness of metallic film. Absolute errors of measurement : Eθ – for the resonant angle, Eω – for the half-width of the resonant curve, Er – for the minimum reflectivity at resonance .

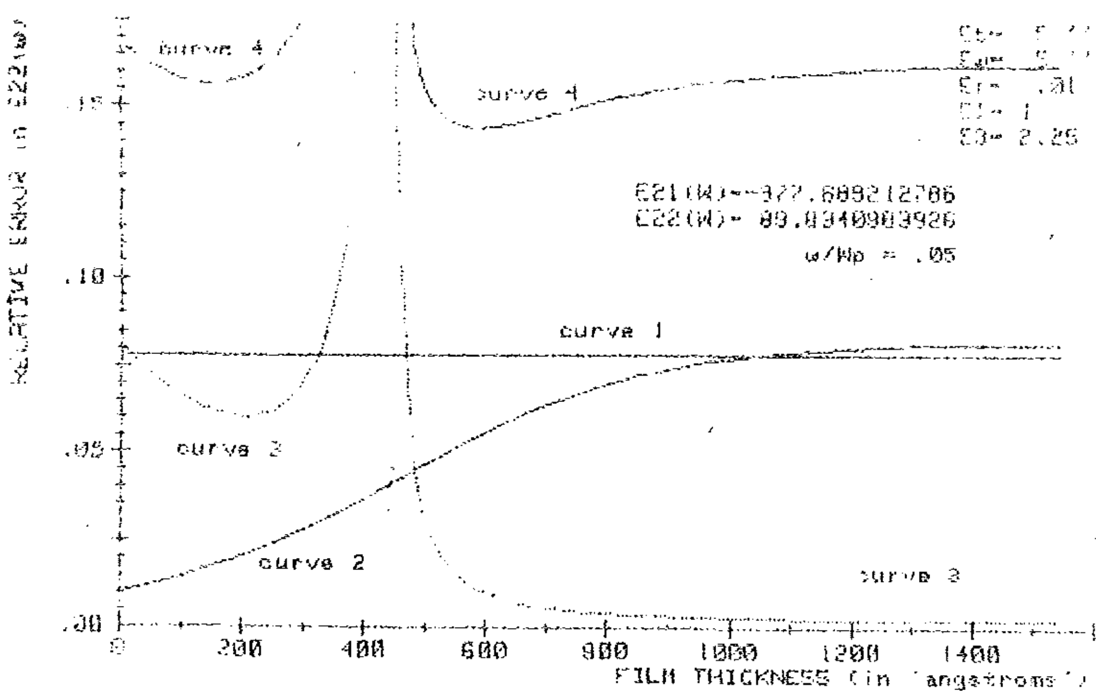

Fig.3.3@ Dependence of relative error in determination of E22(ω) versus thickness of metal film. Curve 1 gives a partial relative error due to finite accuracy in measuring the resonant angle, curve 2 – in half-width, curve 3 – in R min, curve 4 – the total relative error

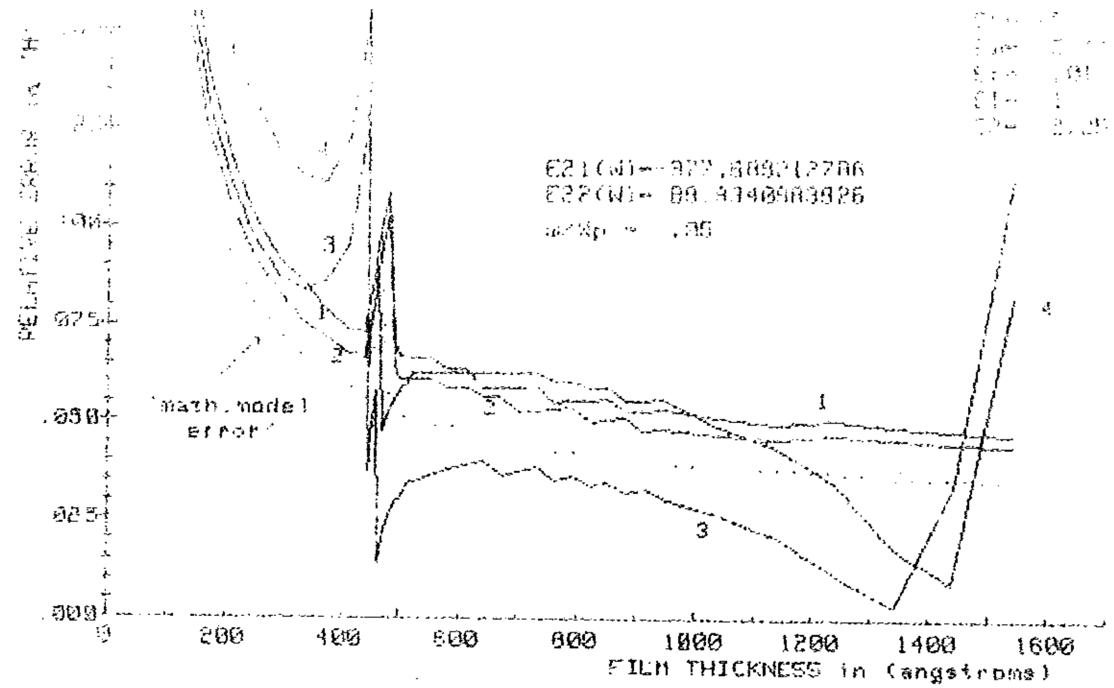

Fig. 3.4a Dependence of relative error in thickness on thickness of the metallic film. Curve 1 gives a partial relative error due to finite accuracy in measuring the resonant angle, curve 2 - in half-width, curve 3 - in Rmin, curve 4 - the total relative error

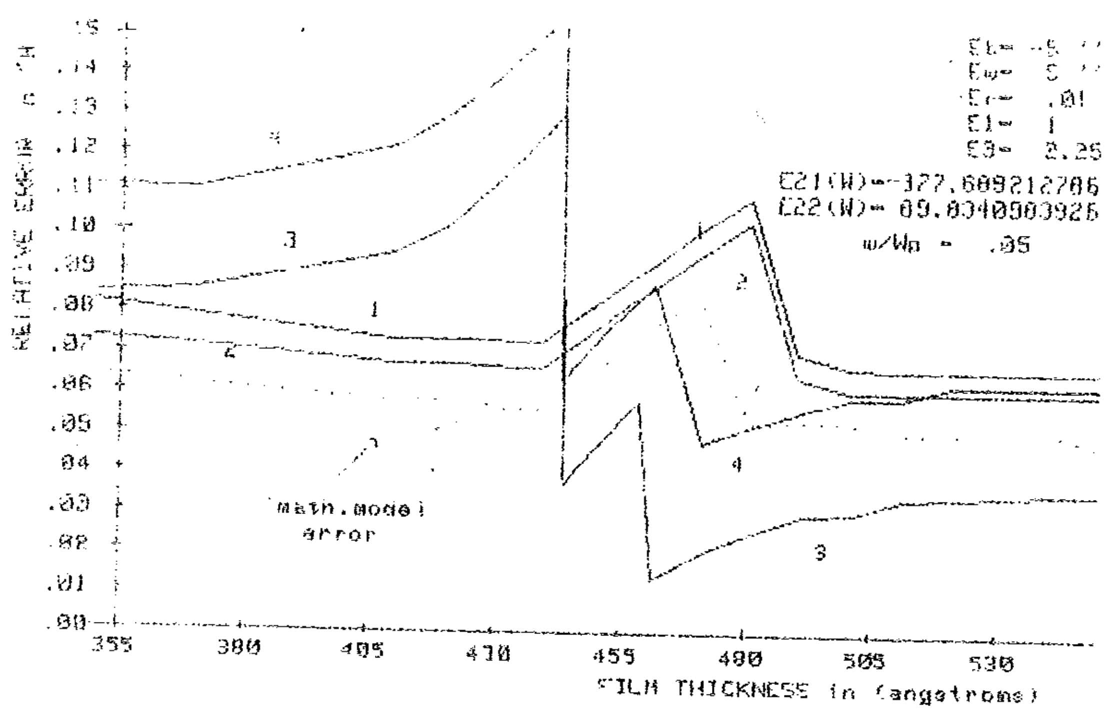

Fig. 3.4b (expanded scale) Dependence of relative error in thickness on the thickness of the metallic film.

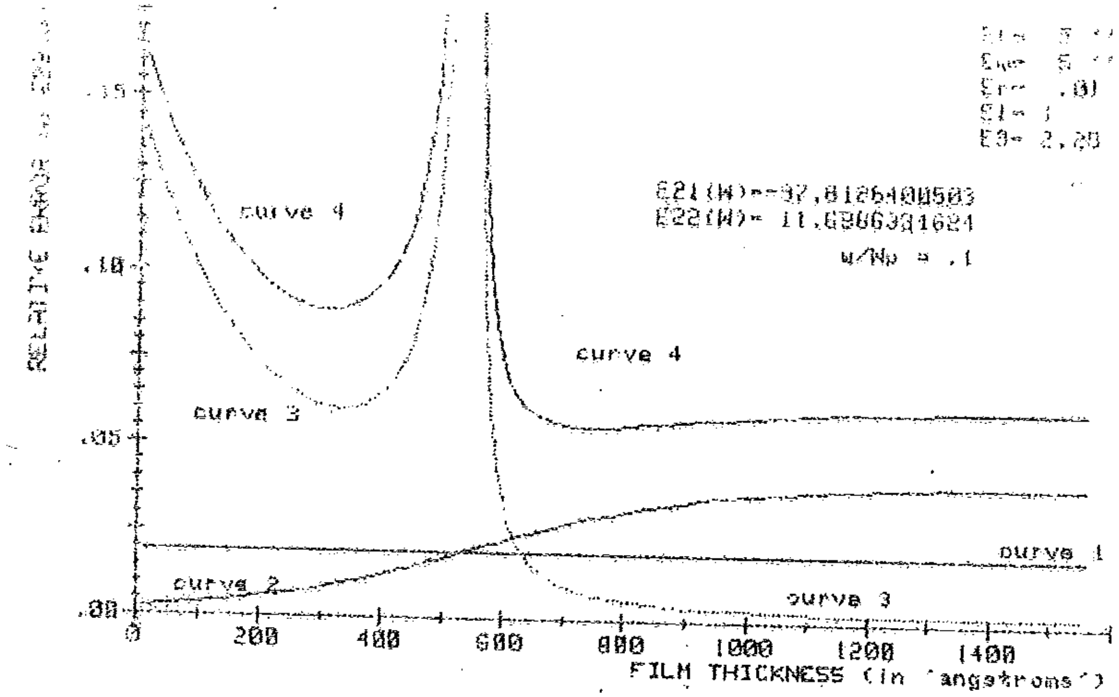

Fig.3.3b Dependence of relative error in determination of E22(w) versus thickness of metal film. Curve 1 gives a partial relative error due to finite accuracy in measuring the resonant angle, curve 2 – in half-width, curve 3 – in R min, curve 4 – the total relative error

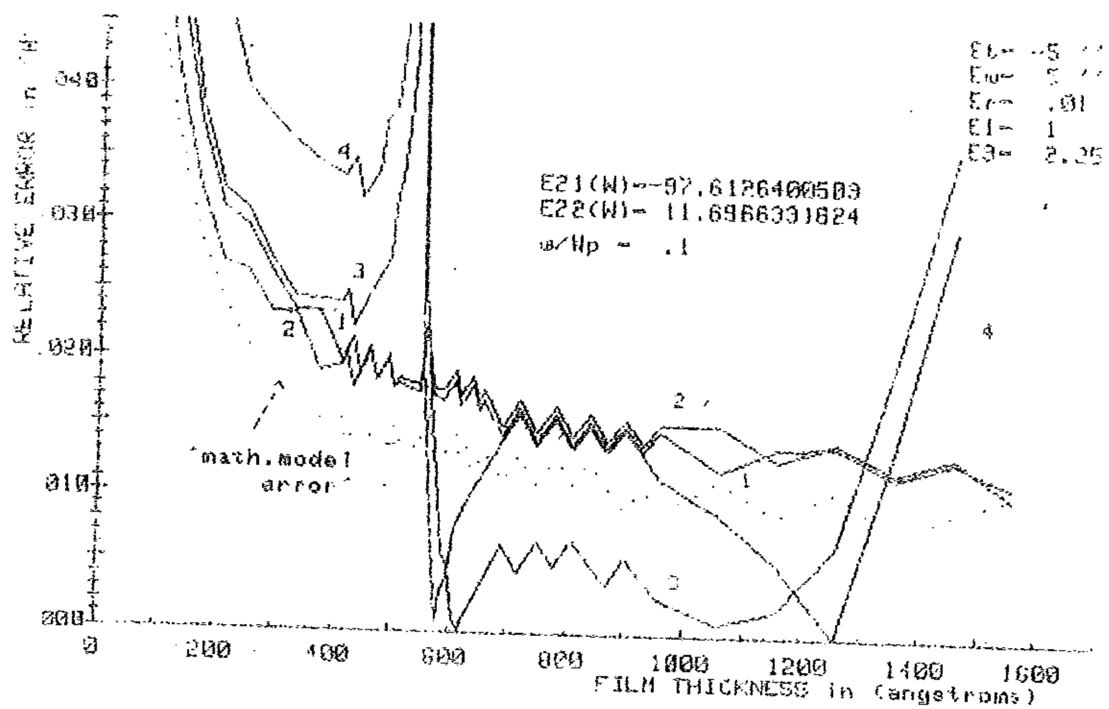

Fig. 3.4b Dependence of relative error in thickness on thickness of the metallic film. Curve 1 gives a partial relative error due to finite accuracy in measuring the resonant angle, curve 2 – in half-width, curve 3 – in Rmin, curve 4 – the total relative error

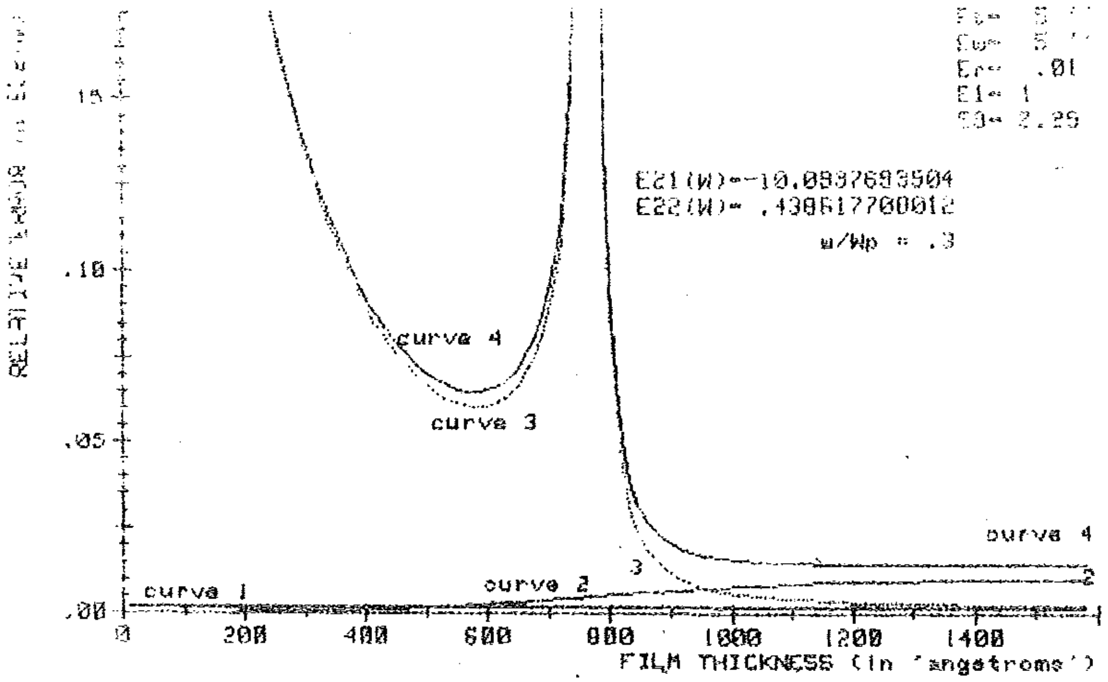

Fig.3.3c Dependence of relative error in determination of E22(w) versus thickness of metal film. Curve 1 gives a partial relative error due to finite accuracy in measuring the resonant angle, curve 2 - in half-width, curve 3 - in R min, curve 4 - the total relative error

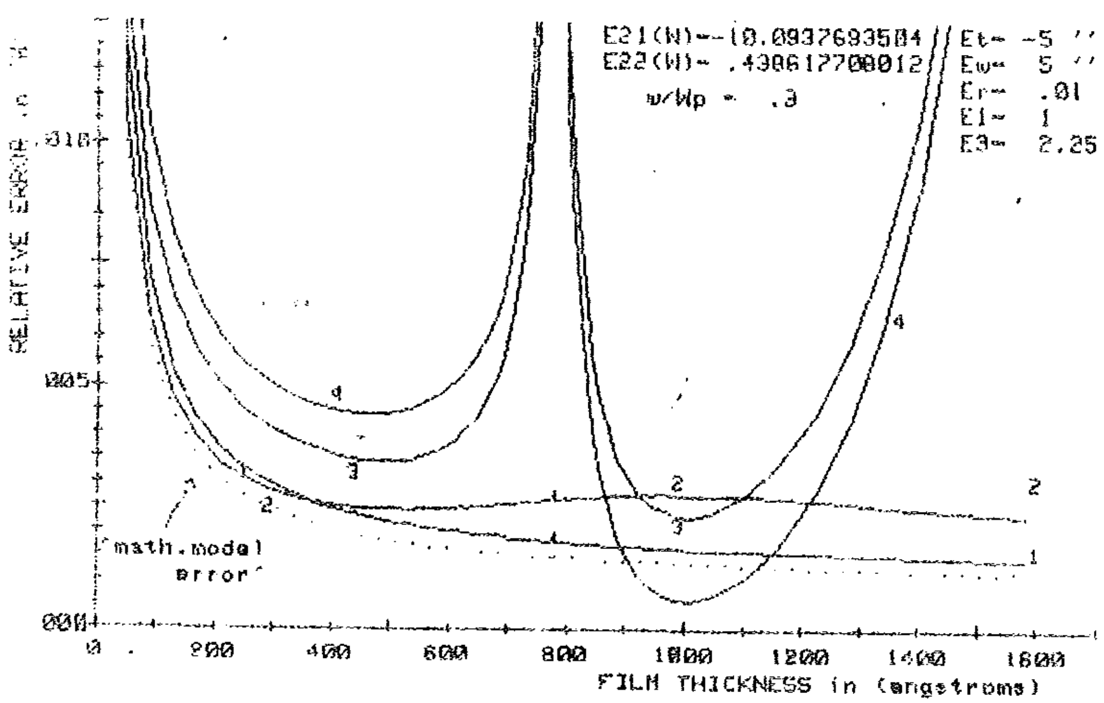

Fig. 3.4c Dependence of relative error in thickness on thickness of the metallic film. Curve 1 gives a partial relative error due to finite accuracy in measuring the resonant angle, curve 2 - in half-width, curve 3 - in Rmin, curve 4 - the total relative error

also supported by eqn. (3.18) which shows that $\left|\frac{\partial \varepsilon_2''}{\partial R_{min}}\right| \sim \frac{1}{\sqrt{R_{min}}}$.

The ' softwareerror' for the used frequencies has the following values

$$\frac{\Delta\varepsilon_2''}{\varepsilon''_{2\,theor.}} \left(\frac{W}{W_p} = 0.05\right) = 5.7\%$$

$$\frac{\Delta\varepsilon_2''}{\varepsilon''_{2\,theor.}} \left(\frac{W}{W_p} = 0.1\right) = 1.5\%$$

$$\frac{\Delta\varepsilon_2''}{\varepsilon''_{2\,theor.}} \left(\frac{W}{W_p} = 0.3\right) = 0.2\%$$

Conclusion 3

It is meaning less to perform the measurement for metal films with thickness values close to h_{opt}. The value of h_{opt} depends mostly upon $\frac{w}{W_p}$ and ranges from 400A^o-750A^o for $0.05 \le \frac{W}{W_p} \le 0.3$.

Conclusion 4

For metal films with thicknesses other than $h_{opt} \pm 100$ the relative error of determination of ε_2'' ranges from 17% at $W/_{Wp}$=0.05 to ~2% at $W/_{Wp}$ = 0.3 and h > 1000A^o only. For h< h_{opt}-100A^o and $W/_{Wp}$=0.3 the error has a minimum of ~ 7% at h ~ 600A^o and rapidly grows for less thicknesses.

At figs. (3.4a), (3.4b), and (3.4c) the relative error $\left(\frac{\Delta h}{h}\right)_{exp}$ as a function of h with normalized frequency as a parameter is shown.

Since h_{exp} is determined using $\varepsilon_{2\,exp}'$ and $\varepsilon_{2\,exp.}''$ it is the most affected because the errors made at all preceeding steps are accumulated now. In particular $(\Delta\varepsilon_2'')_{exp} \to \infty$ as $h \to h_{opt}$ cases. $\Delta h \to \infty$ as $h \to h_{opt}$.

Besides this we have a 'software error' (showing by a dotted line) growing to infinity as $h \to 0$. It happens because the assumption $|K_{xo}| << |K_{x1}|$ in the perturbation approach (see eqn. (2.13)) fails as $h \to \infty$. For thicknesses greater than $1500A^o$, $\frac{\Delta h}{h_{exp}}$ also grows due to the growth of the partial error in measuring R_{min}. At these big thicknesses $R_{min} \to 1$, which requires an accurate distinction from the unity.

Conclusion 5.

The measurement of the thickness of the metal film is reasonable to perform if $100A^o < h < 600A^o$, $850A^o < h < 1200A^o$ at $W/_{Wp} = 0.3$ with the relative error ~ 0.5,

if $250A^o < h < 500A^o$ with relative error $\sim 2.5\%$, and

$600A^o < h < 1250A^o$ with relative error $\sim 0.8\%$ at $W/_{Wp} = 0.1$

$480A^o < h < 1400A^o$ with relative error $\sim 3.5\%$ at $W/_{Wp} = 0.05$.

Summary

1. It is shown that radiative SPlP can exist at normalized frequencies higher than $\frac{W}{W_p}$ for strong absorbing media. Practically useful range of $W_p\tau$ might be $100<W_p\tau<5$.
2. The energy transportation performed by SPlP consists of two flows: one in the dielectric medium, the other in metal. It is shown that for $0<w<\frac{W_p}{\sqrt{\varepsilon_1+1}}$ the two flows have opposite directions with the net flow in the direction of the flow in the dielectric medium. For $w>w_p$, both flows have the same direction.
3. A dispersion equation for SPlP in thin metal films was derived. An approximate solution of this equation was suggested and tested.
4. The method of determination of complex $\varepsilon(w)$ and h of metal or semi-conductor film without a preset expression for $\varepsilon(w)$ was modified.
5. A frequency range $0.1\leq \frac{W}{W_p} \leq \frac{W^{**}}{W_p}$ in which the method is practically applicable is established.
6. It is found that the method diverges for ε_2'' and h determination in the vicinity of h_{opt}. For determination of h the method also diverges as $h\to 0$.
7. It is found that with in the specified frequency range $0.1\leq \frac{W}{W_p} \leq \frac{W^{**}}{W_p}$ the accuracy of determination ε_2' is not less than 2%. The accuracy of determination ε_2'' and h depends upon the thickness of the film and can range from 0.5% to 2.5%. Thickness less than 100A^o, greater than 1400A^o, and $h_{opt}\pm 100$A^o should be excluded reliable measurements.

8. Computer program capable of;

   - analysing dispersion properties of SP1P (semi-infinite case)
   - analysing power flows in SP1P (semi-infinite case)
   - simulating ATR model
   - finding an approximate solution of the dispersion equation of SP1P in a thin film
   - determining the values of ε_2', ε_2'', and h from experimentally measured θ_{ATR}, W_θ and R_{min}
   - assessing the accuracy of the method

   was designed.

References

[1] G.C. Aers and A.D. Boardman physics programs ed. by A.D. Boardman John Wiley and sons, 1980.

[2] Principles of optics M.Born, E. Wolf Pergamon Press, 1959.

[3] W.P. Chen, J.M. Chen "Use of surface plasma waves for determination of the thickness and optical constants of thin metallic film", J. Opt. Soc. Am/vol. 71, No.2 (189-191) February 1981.

[4] I. Pockrand "surface plasma oscillations at silver surfaces with thin transparent and absorbing coatings", Surf. Sci. 72, 577-588 (1978).

[5] C. Kunz, Z. Phys. V. 196, 311 (1966).

[6] G.R. Fowles, Introduction to modern optics.

[7] I Newton Optiks II, Book 8, 97 (1817).

[8] J. Fahrenfort, Spectrochim Acta, V.17, 698 (1961).

[9] N.J. Harrick, Phy.Rev., V.125, 1165, (1962),

[10] A Otto Z.Phys. V.216, 398 (1968).

[11] E. Kretschmann. Z.Phys. V.241, 313 (1971)

[12] F. Abels, ed. Optical properties and electronic structure of metals and alloys, (North Holland, Amsterdam, 1965).

[13] T. Lopez - Rios, G. Vuye "Use of surface plasmon excitation for determination of the thickness and optical constants of very thin surface layers," Surf. Sci. 81, 529-538 (1978).

Appendix A. Calculation of terms in the Taylor's series expansion of the dispersion eqn. (2.10)

From eqn. (2.14) it is clear that

$$f(K_{xo}) = \frac{1}{r^{\circ}_{21}} \cdot \frac{1}{r^{\circ}_{23}}\, e^{-2iK^{\circ}_{2y}h} \qquad \text{(A.1)}$$

where

$$\frac{1}{r^{\circ}_{21}} = \frac{\varepsilon_1 K^{\circ}_{2y} + \varepsilon_2 K^{\circ}_{1y}}{\varepsilon_1 K^{\circ}_{2y} - \varepsilon_2 K^{\circ}_{1y}} = \frac{\dfrac{i\varepsilon_1 K_o(-\varepsilon_2)}{\sqrt{-(\varepsilon_1+\varepsilon_2)}} + \dfrac{i\varepsilon_2 K_o \varepsilon_1}{\sqrt{-(\varepsilon_1+\varepsilon_2)}}}{\dfrac{i\varepsilon_1 K_o(-\varepsilon_2)}{\sqrt{-(\varepsilon_1+\varepsilon_2)}} - iK_o\varepsilon_2 \dfrac{\varepsilon_1}{\sqrt{-(\varepsilon_1+\varepsilon_2)}}} = 0 \qquad \text{(A.2)}$$

$$\frac{1}{r^{\circ}_{23}} = \frac{\varepsilon_3 K^{\circ}_{2y} + \varepsilon_2 K^{\circ}_{3y}}{\varepsilon_3 K^{\circ}_{2y} - \varepsilon_2 K^{\circ}_{3y}} = \frac{\varepsilon_3 + \sqrt{\varepsilon_1\varepsilon_3 + \varepsilon_2'(\varepsilon_3-\varepsilon_1)}}{\varepsilon_3 - \sqrt{\varepsilon_1\varepsilon_3 + \varepsilon_2'(\varepsilon_3-\varepsilon_1)}} \qquad \text{(A.3)}$$

$$K^{\circ}_{1y} = iK_o \frac{\varepsilon_1}{\sqrt{-(\varepsilon_1+\varepsilon_2)}} \qquad \text{------} \qquad \text{(A.4)}$$

$$K^{\circ}_{2y} = iK_o \frac{-\varepsilon_2}{\sqrt{-(\varepsilon_1+\varepsilon_2)}} \qquad \text{------} \qquad \text{(A.5)}$$

$$K^{\circ}_{3y} = \sqrt{K_o^2\varepsilon_3 - K^2_{xo}} = K_o \frac{\sqrt{-[\varepsilon_1\varepsilon_3 + \varepsilon_2'(\varepsilon_3-\varepsilon_1)]}}{\sqrt{-(\varepsilon_1+\varepsilon_2')}} \qquad \text{------} \qquad \text{(A.6)}$$

Note that K°_{3y} is real for $0 \le W \le W^*$ and is imaginary for $W^* \le W \le \frac{W_p}{\sqrt{\varepsilon_1+1}}$

Eqn. (A.2) shows that $f(K_{xo}) = 0$.

From eqn. (2.14) we have

$$\frac{\partial f}{\partial K_x}\Bigg|_{K_{xo}} = \frac{\partial}{\partial K_x}\left(\frac{1}{r_{21}}\cdot\frac{1}{r_{23}}\,e^{-2iK_{2y}h}\right)\Bigg|_{K_{xo}}$$

$$= \frac{\partial}{\partial K_x}\left(\frac{1}{r_{21}}\right)\Bigg|_{K_{xo}}\cdot\frac{1}{r_{23}}\,e^{-2iK^{\circ}_{2y}h} + \frac{1}{r^{\circ}_{21}}\,\frac{\partial}{\partial K_x}\left(\frac{1}{r_{23}}\right)\Bigg|_{K_{xo}}\cdot e^{-2iK^{\circ}_{2y}h} +$$

$$+ \frac{1}{r^{\circ}_{21}}\cdot\frac{1}{r^{\circ}_{23}}\,\frac{\partial}{\partial K_x}\left(e^{-2iK_{2y}h}\right)\Bigg|_{K_{xo}} \quad \text{-----} \qquad (A.7)$$

but from (A.2), $\frac{1}{r^{\circ}_{21}} = 0$ which results the second and the third terms of the right expression in (A.7) to be zero.

$$\frac{\partial f}{\partial K_x}\Bigg|_{K_{xo}} = \frac{\partial}{\partial K_x}\left(\frac{1}{r_{21}}\right)\Bigg|_{K_{xo}}\frac{1}{r^{\circ}_{23}}\,e^{-2iK^{\circ}_{2y}h} \quad \text{-----} \qquad (A.8)$$

where

$$\frac{\partial}{\partial K_x}\left(\frac{1}{r_{21}}\right) = \frac{\partial}{\partial K_x}\left(\frac{U}{V}\right) = \frac{\frac{\partial U}{\partial K_x}V - U\frac{\partial V}{\partial K_x}}{V^2} \quad \text{------} \qquad (A.9)$$

with $U = -\varepsilon_1\sqrt{K_o^2\,\varepsilon_2 - K_x^2} + \varepsilon_2\sqrt{K_o^2\varepsilon_1 - K_x^2}$

$$V = -\varepsilon_1\sqrt{K_o^2\varepsilon_2 - K_x^2} - \varepsilon_2\sqrt{K_o^2\varepsilon_1 - K_x^2}$$

$$\frac{\partial U}{\partial K_x}\Bigg|_{K_{xo}} = K_{xo}\left(\frac{-\varepsilon_1}{\sqrt{K_o^2\varepsilon_2 - K_o^2\,\frac{\varepsilon_1\varepsilon_2}{\varepsilon_1+\varepsilon_2}}} - \frac{\varepsilon_2}{\sqrt{K_o^2\varepsilon_1 - K_o^2\,\frac{\varepsilon_1\varepsilon_2}{\varepsilon_1+\varepsilon_2}}}\right)$$

$$= \frac{K_{xo}}{K_o}\left(\varepsilon_1^2 - \varepsilon_2^2\right)\sqrt{\frac{\varepsilon_1+\varepsilon_2}{\varepsilon_1\cdot\varepsilon_2}}$$

$$V \Big|_{K_{xo}} = -K_o \frac{\varepsilon_1 \varepsilon_2}{\sqrt{\varepsilon_1+\varepsilon_2}} - K_o \frac{\varepsilon_1 \varepsilon_2}{\sqrt{\varepsilon_1+\varepsilon_2}} = -2K_o \frac{\varepsilon_1 \varepsilon_2}{\sqrt{\varepsilon_1+\varepsilon_2}}$$

The term $\frac{\partial V}{\partial K_x} \Big|_{K_{xo}}$ vanishes

thus

$$\frac{U}{\partial K_x} \Big|_{K_{xo}} \cdot \frac{1}{V} \Big|_{K_{xo}} = \frac{(\varepsilon_1{}^{2-\varepsilon_2}\ \varepsilon_1+\varepsilon_2)}{2K_o\ \varepsilon_1 \cdot \varepsilon_2\ \varepsilon_1 \cdot \varepsilon_2}$$

$$\left(\frac{\partial V}{\partial K_x} \cdot \frac{1}{V}\right)\Big|_{K_{xo}} = \frac{\varepsilon_2-\varepsilon_1}{2K_o} \left(\frac{\varepsilon_1+\varepsilon_2}{\varepsilon_1 \cdot \varepsilon_2}\right)^{3/2} \text{------} \qquad (A.10)$$

equation (A.8), (A.10), (2.10) and (2.4) imply that

$$\frac{\partial f}{\partial K_x} \Big|_{K_{xo}} = \frac{(\varepsilon_2-\varepsilon_1)}{2K_o} \left(\frac{\varepsilon_1+\varepsilon_2}{\varepsilon_1 \cdot \varepsilon_2}\right)^{3/2} \frac{1}{r^0_{23}}\ e^{-2iK^0_{2y}h} \text{----} \quad (A.11)$$

which results in

$$K_{x1} = \frac{2K_o}{(\varepsilon_2-\varepsilon_1)} \left(\frac{\varepsilon_1 \cdot \varepsilon_2}{\varepsilon_1+\varepsilon_2}\right)^{3/2} r^0_{23}\ e^{-2iK_{2y}h} \text{------} \qquad (A.12)$$

```
2                       !APPENDIX -B-
3 !
4 !
10    ! PROGRAM which determines the accuracy of the SPIP method
20    !   This particular version is designed for normalized frequency w/Wp=.05
30    DIM Det22(300),Dew22(300),Der22(300),De22(300),Hh(300),Dl(300),Dr(300)
40    DIM Root(2),F_(2),Err(2),Dh(300),Dho(300),Dh1(300),Dh2(300),Dht(300)
50    DIM Ho(300),H1(300),H2(300),Ht(300)
60    INTEGER Screen(1:1024,1:36,1:3),Screen1(1:1024,1:32,1:3)
70    COM E3,E21,E22,E1
80    COM /Exp/ E21e,E22e
90    COM /H/ Teta,Wt,Rm
100   COM /Err/ Tetae,Wte,Rme
110   COM /H_opt/ Hoptmt                  ! Common Optimal thickness in 'meters'
120   COM /Wp/ Wp
130   COM /Tau/ Tau
140   COM /W/ W
150   COM /K/ Kx1iexp
160   C=2.998E+8                        ! Speed of light in m/s
170   Pi=3.14159265358979
180   !
190   Et=5/3600*Pi/180              ! Exp. error in measuring Teta  (in rad)
200   Ew=Et                        ! Exp. error in measuring half-width  Wt (in rad)
210   Er=.01                      ! exp. error in measuring Minimum Reflectivity
220   !
230   E1=1
240   E3=2.25                         ! Dielectric permittivity of the GLASS PRISM
250   Wp=8.30197252597E+15            !   Plasma Frequency for SODIUM
260   Tau=1.00583208114E-14           !   Relaxation Time  for SODIUM
270 !GOTO 3160  ! 1800  !3160         ! 2850      !  1800
280 ! LOADSUB E22accuracy FROM "E22acc1"
290 ! LOADSUB Filmdisp FROM "F1"
300 ! LOADSUB E21accuracy FROM "E21acc1"
310 !   LOADSUB E22accu FROM "E22acc2"
320 ! LOADSUB Refl FROM "RPMA3"
330 ! LOADSUB Fr12 FROM "RPMA3"
340 ! LOADSUB Fr23 FROM "RPMA3"
350 ! LOADSUB Fex FROM "RPMA3"
360 ! LOADSUB Opt_h FROM "Opt_h"
370 ! LOADSUB Bisect FROM "Bisect"
380 !LOADSUB FNMax FROM "Max"
390   !
400   M=1                                 ! Counts the number of attempt
410 ! INPUT "Normalized frequency   Wn =",Wn
420      Wn=.3
430   INPUT "No,N1,N2",No,N1,N2
431     PRINT No,N1,N2;"Attemt number = ";M
440   W=Wn*Wp
450   E21=1-Wp^2/(W^2+1/Tau^2)           ! E21 is needed for Filmdisp
460   E22=1/(W*Tau)*Wp^2/(W^2+1/Tau^2)
470       !
480       J=1                           ! Counts the array index
```

```
500      H=-30
510      H_exp=5
520     H=H+H_step
530   Hmt=H*1.E-10                                    !  thickness in meters
540   CALL Filmdisp(W,Wp,Tau,Hmt,E1,E3,Kxr,Kxi,Kxor,Kxoi,Kx1r,Kx1i)
550   ! For the given Hmt,E1,E2,W,,Wp,Tau              the subprogram 'Filmdisp'
560   !  Kxor - REAL part for semiinfinite case
570   !  Kxoi - IMAG. part for semiinfinite case
580   !  Kx1r - first order correction to Kxor for a metal film of finite thick-
590   !  Kx1i - first order correction to Kxoi for a film of given 'H'
600   !  Kxr  - REAL part of OX - wavevector for a metal film of thicness 'H'
610   !  Kxi  - IMAG. part of OX - wavevector for a metal film of thickness 'H'
620   !    NOTE !    ALL WAVEVECTORS ARE IN NORMALIZED FORM  !!!
630   Eta=Kxoi/Kx1i
640   Rm=1-4*Eta/(1+Eta)^2                 ! Expected experimental value of "Rmin"
650   Kxi=Kxi*Wp/C                                 ! Non- normalized values
660   Teta=ASN(Kxor/Wn/SQR(E3))   ! Expected experimental Resonant angle in rad
670   Wt=2*Kxi*COS(Teta)*C/W/SQR(E3)  !Expected Half-width of the resonant curve
680     ! In the preceeding part of the program the expected experimental values
690     !  of Teta,Wt,Rm were calculated. The following part of the program
700     !  is based exclusively on these experimentally determinerd values
710     !   NOTE, THAT THESE ARE EXACT EXPERIMENTAL VALUES
720     ! ***********************************************************************
730     ! ***********************************************************************
740     !
750    IF No=0 THEN Tetae=Teta             ! Experimental error is introduced
760    IF N1=0 THEN Wte=Wt                 ! in lines  1440 - 1520
770    IF N2=0 THEN Rme=Rm
780    IF No=+1 THEN Tetae=Teta+Et
790    IF N1=+1 THEN Wte=Wt+Ew                      ! in 'rad'
800    IF N2=+1 THEN Rme=Rm+Er
810    IF No=-1 THEN Tetae=Teta-Et
820    IF N1=-1 THEN Wte=Wt-Ew
830    IF N2=-1 THEN Rme=Rm-Er
840 !
850     IF Rme<0 THEN Rme=1.E-8
860    S2=SIN(Tetae)*SIN(Tetae)
870     E21e=E1*E3*S2/(E1-E3*S2)          ! Experimentally found E21(w)
880     K=-1
890     E22e=Wte*(1+K*SQR(Rme))*E1^2*E3*TAN(Tetae)/(2*(E1-E3*S2)^2)
900     E22o=Wte*E1^2*E3*TAN(Tetae)/(2*(E1-E3*S2)^2)              ! At H=Hopt
910     D1(J)=E22o-E22e                             ! Lines  1560 - 1670
920                                                 ! are a switch for Eta
930     Dr(J)=D1(J)-D1(J-1)                          ! as a function of R min
940     IF Dr(J)>0 AND J>1 THEN K=+1
950     IF Dr(J)<0 THEN K=-1
960     IF J=1 THEN K=-1
970     Prod=Dr(J)*Dr(J-1)
980     !
990     IF Prod<0 AND J>2 THEN Hopt1=H
1000    !
1010    !
1020    IF K=-1 THEN Hoptmt=1.E-6
1030    IF K=+1 THEN Hoptmt=Hopt1*1.E-10     ! Optimal thickness in 'meters'
1040    !
1050    E22e=Wte*(1+K*SQR(Rme))*E1^2*E3*TAN(Tetae)/(2*(E1-E3*S2)^2)
1060    !
1070  !  PRINT "E21-E21e =";E21-E21e,"E22-E22e =";E22-E22e,"Prod =";Prod
```

```
1080 IF K=-1 AND N1=1 AND N2=1 THEN CALL E22accu(Teta,Wt,Rm,Et,Ew,Er,E1,E21e,E2
1090 IF K=1 AND N1=1 AND N2=1 THEN CALL E22accuracy(Teta,Wt,Rm,Et,Ew,Er,E1,E21e
1100  !
1110                                                  ! Artificial correction
1120   Kx1exp=Wte*SQR(E3)*Wn*(1-K*SQR(Rme))/(4*COS(Tetae))
1130 ! PRINT "K=";Kx1i-Kx1exp,"        R min =";Rme
1140   !
1160 Acc=1.E-7
1170  IF H>775 AND H<790 THEN Acc=1.E-9
1180  CALL Bisect(H_exp-100,H_exp+400,6000,ABS(Kx1i)*Acc,50,Root(*),F_(*),Err(*)
1190   H_exp=Root(1)                     ! Expected experimentally determined 'H'
1200 !PRINT "H=";H,"H_exp=";H_exp,"H_opt =";Hopt1;"    K=";K;"      J= ";J
1210  Q=(H-H_exp)/H
1220  IF No<>0 AND N1<>0 AND N2<>0 THEN Dht(J)=Q            ! Total error
1230  IF No<>0 AND N1<>0 AND N2<>0 THEN Ht(J)=H
1240  IF No=0 AND N1=0 AND N2=0 THEN Dh(J)=Q            ! Error of the math. model
1250  IF No=0 AND N1=0 AND N2=0 THEN Hh(J)=H
1260  IF No<>0 AND N1=0 AND N2=0 THEN Dho(J)=Q           ! Partial error in 'Teta'
1270  IF No<>0 AND N1=0 AND N2=0 THEN Ho(J)=H
1280  IF No=0 AND N1<>0 AND N2=0 THEN Dh1(J)=Q        !Partial error in half-width
1290  IF No=0 AND N1<>0 AND N2=0 THEN H1(J)=H
1300  IF No=0 AND N1=0 AND N2<>0 THEN Dh2(J)=Q           !  Partial error in R min
1310  IF No=0 AND N1=0 AND N2<>0 THEN H2(J)=H
1320  J=J+1
1330     IF H>480 AND H<580 THEN H_step=20
1331     IF H>580 AND H<760 THEN H_step=10
1340     IF H>=775 AND H<790 THEN H_step=3
1350     IF Hopt1<>0 THEN H_step=3
1360     IF Hopt1=0 AND H>775 AND H<795 THEN H_step=.3
1370     IF H>800 AND H<950 THEN H_step=10
1380     IF H>=950 AND H<=1030 THEN H_step=30
1390    IF H>1030 THEN H_step=60
1400  IF H+H_step<1620 THEN 520
1401              M=M+1
1402  IF M<=5 THEN Hopt1=0
1403  BEEP
1404 !INPUT "SWITCH = ( if  ZERO  then the program is repeated for new No,N1,N2
1405  IF Sw<>0 THEN 1420
1410  IF M<=5 THEN 430
1420  BEEP 500,5
1430  PAUSE
1450  !222222222222222222222222222222222222222222222222222222222222222222222222222
1460  !222222222222222222222222222222222222222222222222222222222222222222222222222
1470  GINIT
1480  PEN 5
1490  DEG
1500  LDIR 90
1510  CSIZE 3
1520  MOVE 3,57
1530  LABEL "RELATIVE ERROR in E22(w)"
1540  LDIR 0
1550  MOVE 72,22
1560  LABEL "FILM THICKNESS (in 'angstroms')"
1570  MOVE 0,9
1580  LABEL "Fig.3.3  Dependence of relative error in determination of E22(w) ve
1590  MOVE 15,6
1600  LABEL "thickness of metal film. Curve 1 gives a partial relative error"
1610  MOVE 10,3
1620  LABEL "due to finite accuracy in measuring the resonant angle, curve 2 -"
```

```
1630  MOVE 4,0
1640  LABEL "in half-width, curve 3 - in R min, curve 4 - the total relative err
1650  MOVE 112,88
1660  LABEL "E1=";E1
1670  MOVE 112,85
1680  LABEL "E3=";E3
1690  !
1700  MOVE 112,97
1710  PEN 2
1720  LABEL "Et= ";Et*3600*180/PI;"''"
1730  MOVE 112,94
1740  PEN 3
1750  LABEL "Ew= ";Ew*3600*180/PI;"''"
1760  MOVE 112,91
1770  PEN 4
1780  LABEL "Er= ";Er
1790  MOVE 115,37
1800  PEN 7
1810  LABEL "curve 4"
1811  MOVE 46,60
1812  LABEL "curve 4"
1820  MOVE 16,30
1830  PEN 2
1840  LABEL "curve 1"
1850  PEN 3
1860  MOVE 56,31
1870  LABEL "curve 2"
1871  MOVE 128,32
1872  LABEL "2"
1880  MOVE 50,50
1890  PEN 4
1900  LABEL "curve 3"
1901  MOVE 73,33
1902  LABEL "3"
1910  PEN 5
1920  VIEWPORT 10,128,25,100
1930  WINDOW -50,1600,-.01,.175
1940  AXES 100,.005,0,0,2,5,2
1950  PEN -1
1960  VIEWPORT 9,12,28,32                    ! Horizontal deleting
1970  AXES 10,1,0,0,1,1,5
1980  VIEWPORT 12,15,24,28                   ! Vertical deleting
1990  AXES 1000,.005,0,0,1,1,5
2000  VIEWPORT 10,128,25,100
2010  PEN 5
2020  CLIP OFF
2030  LORG 6
2040  FOR I=0 TO 1450 STEP 200
2050  MOVE I,-.003
2060  LABEL USING "#,K";I
2070  NEXT I
2080  LORG 8
2090  FOR I=0 TO .5 STEP .05
2100  MOVE -25,I
2110  LABEL USING "#,.DD";I
2120  NEXT I
2130  MOVE 1400,.125
2140 LABEL "E21(W)=";E21
2150 MOVE 1400,.1175
```

```
2160 LABEL "E22(W)=";E22
2170  MOVE 1400,.1075
2180  LABEL "w/Wp =";Wn
2190  PEN 2
2200  FOR J=1 TO 300
2210  LINE TYPE 1
2220  IF Ht(J)=0 THEN 2240
2230  PLOT Ht(J),Det22(J)
2240  NEXT J
2250  PENUP
2260  PEN 3
2270  FOR J=1 TO 300
2280  LINE TYPE 1
2290  IF Dew22(J)=0 THEN PENUP
2300  PLOT Ht(J),Dew22(J)
2310  NEXT J
2320  PENUP
2330  PEN 4
2340  FOR J=1 TO 300
2350  LINE TYPE 4
2360 IF Der22(J)=0 THEN PENUP
2370  PLOT Ht(J),Der22(J)
2380  NEXT J
2390  PENUP
2400  PEN 7
2410  FOR J=1 TO 300
2420  LINE TYPE 1
2430  IF De22(J)=0 THEN PENUP
2440  PLOT Ht(J),De22(J)
2450  NEXT J
2460  PENUP
2470  PAUSE
2480  !3333333333333333333333333333333333333333333333333333333333333333333333333
2490  !3333333333333333333333333333333333333333333333333333333333333333333333333
2500  !3333333333333333333333333333333333333333333333333333333333333333333333333
2510  GINIT
2520  CSIZE 3
2530  PEN 5
2540  DEG
2550  LDIR 90
2560  CSIZE 3
2570  MOVE 3,61
2580  LABEL "RELATIVE ERROR in 'H'"
2590  LDIR 0
2600  MOVE 70,22
2610  LABEL "FILM THICKNESS in (angstroms)"
2620  MOVE 0,9
2630  LABEL "Fig. 3.4  Dependence of relative error in thickness on thickness of
2640  MOVE 18,6
2650  LABEL "metallic film. Curve 1 gives a partial relative error due to"
2660  MOVE 18,3
2670  LABEL "finite accuracy in measuring the resonant angle, curve 2 - in"
2680  MOVE 11,0
2690  LABEL "half-width, curve 3 - in Rmin, curve 4 - the total relative error."
2700  MOVE 112,88
2710  LABEL "E1= ";E1
2720  MOVE 112,85
2730  LABEL "E3= ";E3
2740  PEN 2
```

```
2750 MOVE 112,97
2760 LABEL "Et= ";(Tetae-Teta)*3600*180/PI;"''"
2770 PEN 7
2780 MOVE 112,94
2790 LABEL "Ew= ";(Wte-Wt)*3600*180/PI;"''"
2800 PEN 4
2810 MOVE 112,91
2820 LABEL "Er= ";Rme-Rm
2830 PEN 5
2840 MOVE 70,97
2850 LABEL "E21(W)=";E21
2860 MOVE 70,94
2870 LABEL "E22(W)=";E22
2880 MOVE 75,90
2890 LABEL "w/Wp = ";Wn
2900 MOVE 38,55
2910 PEN 7
2920 LABEL "4"
2930 MOVE 104,64
2940 LABEL "4"
2950 MOVE 40,46
2960 PEN 4
2970 LABEL "3"
2980 MOVE 78,40
2990 LABEL "3"
3000 MOVE 30,42
3010 PEN 3
3020 LABEL "2"
3030 MOVE 78,45
3040 LABEL "2"
3041 MOVE 120,45
3042 LABEL "2"
3050 MOVE 27,46
3060 PEN 2
3070 LABEL "1"
3080 MOVE 120,37
3090 LABEL "1"
3100 PEN 1
3110 MOVE 11,37
3120 LABEL "'math.model"
3130 MOVE 20,34
3140 LABEL "error'"
3150 MOVE 20,40
3160 DEG
3170 LDIR 60
3180 LABEL "--->"
3190 LDIR 0
3200 PEN 5
3210 VIEWPORT 10,128,29,100
3220 WINDOW -10,1700,-.0001,.0125
3230 AXES 100,.0005,0,0,5,5,2
3240 CLIP OFF
3250 LORG 6
3260 FOR I=0 TO 1600 STEP 200
3270 MOVE I,-.00025
3280 LABEL USING "#,K,";I
3290 NEXT I
3300 LORG 8
3310 FOR I=0 TO .05 STEP .005
```

```
3320 MOVE -10,I
3330 LABEL USING "#,.DDD";I
3340 NEXT I
3350 PEN 2
3360 FOR J=1 TO 300
3370                                                  ! Partial error in tet
3380 IF Ho(J)>0 THEN PLOT Ho(J),ABS(Dho(J))
3390 NEXT J
3400 PENUP
3410 PAUSE
3420 PEN 3
3430 FOR J=1 TO 300                                    ! Parial error in th
3440 IF H1(J)>0 THEN PLOT H1(J),ABS(Dh1(J))
3450 NEXT J
3460 PENUP
3470 PAUSE
3480 PEN 4
3490 FOR J=1 TO 300                                 ! Partial error in 6 mi
3500 IF ABS(Dh2(J))>1 THEN 3520
3501 IF ABS(Dh2(J))>.02 AND H2(J)>1350 THEN 3520
3510 IF H2(J)>0 THEN PLOT H2(J),ABS(Dh2(J))
3520 NEXT J
3530 PENUP
3540 PAUSE
3550 PEN 7
3560 FOR J=1 TO 300                             !  Total error
3570 IF ABS(Dht(J))>.02 AND H2(J)>1350 THEN 3590
3580 IF Ht(J)>0 THEN PLOT Ht(J),ABS(Dht(J))
3590 NEXT J
3600 PENUP
3610 PEN 1
3620 LINE TYPE 3
3630 FOR J=1 TO 300
3640 IF ABS(Dh(J))>1 THEN 3680
3650 IF Hh(J)>0 THEN PLOT Hh(J),ABS(Dh(J))   ! Indicates only the computationa
3660 NEXT J                                   !  error of the computer program
3670 PENUP
3680 PAUSE
3690 ! 44444444444444444444444444444444444444444444444444444444444444444444
3700 !4444444444444444444444444444444444444444444444444444444444444444444444
3710 !4444444444444444444444444444444444444444444444444444444444444444444444
3720 ! 44444444444444444444444444444444444444444444444444444444444444444444
3730 GINIT
3740 CSIZE 3
3750 PEN 5
3760 DEG
3770 LDIR 90
3780 CSIZE 3
3790 MOVE 3,61
3800 LABEL "RELATIVE ERROR in 'H'"
3810 LDIR 0
3820 MOVE 70,22
3830 LABEL "FILM THICKNESS in (angstroms)"
3840 MOVE 0,9
3850 LABEL "Fig. 3.4   (expanded scale)  Dependence of relative error in thick
3860 MOVE 18,6
3870 LABEL "on the thickness of the metallic film."
3880 MOVE 112,88
3890 LABEL "E1= ";E1
```

```
3900  MOVE 112,85
3910  LABEL "E3= ";E3
3920  PEN 2
3930  MOVE 112,97
3940  LABEL "Et= ";(Tetae-Teta)*3600*180/PI;"''"
3950  PEN 3
3960  MOVE 112,94
3970  LABEL "Ew= ";(Wte-Wt)*3600*180/PI;"''"
3980  PEN 4
3990  MOVE 112,91
4000  LABEL "Er= ";Rme-Rm
4010  PEN 5
4020  MOVE 90,81
4030  LABEL "E21(W)=";E21
4040  MOVE 90,79
4050  LABEL "E22(W)=";E22
4060  MOVE 100,74
4070  LABEL "w/Wp = ";Wn
4080  PEN 7
4090  MOVE 30,85
4100  LABEL "4"
4110  MOVE 85,48
4120  LABEL "4"
4130  PEN 4
4140  MOVE 32,73
4150  LABEL "3"
4160  MOVE 85,38
4170  LABEL "3"
4180  PEN 3
4190  MOVE 25,60
4200  LABEL "2"
4210  MOVE 85,69
4220  LABEL "2"
4230  PEN 2
4240  MOVE 42,65
4250  LABEL "1"
4260  MOVE 80,75
4270  LABEL "1"
4280  PEN 1
4290  MOVE 30,42
4300  LABEL "'math.model"
4310  MOVE 35,39
4320  LABEL "error'"
4330  MOVE 40,46
4340  DEG
4350  LDIR 45
4360  LABEL "--->"
4370  LDIR 0
4380  PEN 5
4390  VIEWPORT 10,128,29,100
4400  WINDOW 350,550,-.001,.152
4410  AXES 25,.01,355,0,5,5,2
4420  CLIP OFF
4430  LORG 6
4440  FOR X=355 TO 550 STEP 25
4450  MOVE X,-.002
4460  LABEL USING "%,K,";X
4470  NEXT X
4480  !
```

```
4490  LORG 8
4500  FOR Y=0 TO .15 STEP .01
4510  MOVE 350,Y
4520  LABEL USING "#,.DD";Y
4530  NEXT Y
4540  CLIP ON
4550  !
4560  PEN 2
4570  FOR J=2 TO 80
4580                                          ! Partial error in teta
4590  IF Ho(J)>0 THEN PLOT Ho(J),ABS(Dho(J))
4600  NEXT J
4610  PENUP
4620  PEN 3
4630  FOR J=2 TO 80                           ! Parial error in Wt
4640  IF H1(J)>0 THEN PLOT H1(J),ABS(Dh1(J))
4650  NEXT J
4660  PENUP
4670  PEN 4
4680  FOR J=2 TO 80                           ! Partial error in R min
4690  IF ABS(Dh2(J))>1 THEN 4710
4700  IF H2(J)>0 THEN PLOT H2(J),ABS(Dh2(J))
4710  NEXT J
4720  PENUP
4730  PEN 7
4740  FOR J=2 TO 80
4750  IF ABS(Dht(J))>1 THEN 4770
4760  IF Ht(J)>0 THEN PLOT Ht(J),ABS(Dht(J))
4770  NEXT J
4780  PENUP
4790  PEN 1
4800  LINE TYPE 3
4810  FOR J=2 TO 80
4820  IF ABS(Dh(J))>1 THEN 4840
4830  IF Hh(J)>0 THEN PLOT Hh(J),ABS(Dh(J))   ! Indicates only the computational
4840  NEXT J                                  !  error of the computer program
4850  PENUP
4860  END
4870  !
4800 SUB E22accuracy(Teta,Wt,Rm,Et,Ew,Er,E1,E21,E22,E3,H,Det22,Dew22,Der22,De22)
4890  ! This subprogram should be used for 'H' greater than 'Hopt'
4900  !  Et  - experimental accuracy of      "Teta" determination
4910  !  Ew  -                       of      "Wt"   determination
4920  !  Er  -                       of       "Ref" determination
4930  Ssq=SIN(Teta)*SIN(Teta)
4940  Rsq=SQR(Rm)
4950  Br=E1-E3*Ssq
4960  A=1+Rm+2*Rsq
4970  B=1+Rsq
4980  Dert=(Br+4*E3*Ssq)/Br/TAN(Teta)/(COS(Teta)^2)  !normalized Dert
4950  Derw=1/Wt                                      !normalized Derw
5000  Derr=(B^2-.5*A)/Rsq/A/B                        !normalized Derr
5010  Det22=ABS(Dert)*Et
5020  Dew22=ABS(Derw)*Ew
5030  Der22=ABS(Derr)*Er
5040  De22=Det22+Dew22+Der22
5050  SUBEND
5060  !
5070 SUB Cabs(X,Y,Cabs)
```

```
5080   X1=ABS(X)
5090   Y1=ABS(Y)
5100   IF X1<>0 THEN 5130
5110   Cabs=Y1
5120 SUBEXIT
5130   IF Y1<>0 THEN 5160
5140   Cabs=X1
5150 SUBEXIT
5160   IF X1>Y1 THEN Cabs=X1*SQR(1+(Y1/X1)^2)
5170   IF X1<=Y1 THEN Cabs=Y1*SQR(1+(X1/Y1)^2)
5180 SUBEND !

5190 SUB Csqrt(A,B,R,I)
5200   IF (A<>0) OR (B<>0) THEN 5240
5210   R=0
5220   I=0
5230 SUBEXIT
5240 CALL Cabs(A,B,Cabs)
5250   R=SQR((ABS(A)+Cabs)*.5)
5260   IF A<0 THEN 5290
5270   I=B/(R+R)
5280 SUBEXIT
5290   IF B<0 THEN I=-R
5300   IF B>=0 THEN I=R
5310   R=B/(I+I)
5320 SUBEND !

5330 SUB Cdivid(A1,B1,A2,B2,R,I)
5340   C=A2*A2+B2*B2
5350   IF C<>0 THEN 5390
5360   PRINT FNLin$(2);"ERROR IN SUBPROGRAM Cdivid."
5370   PRINT "DIVISOR IS ZERO.",FNLin$(2)
5380   PAUSE
5390   R=(A2*A1+B2*B1)/C
5400   I=(A2*B1-B2*A1)/C
5410 SUBEND !

5420 SUB Cexp(A,B,R,I)
5430   RAD
5440   R=EXP(A)*COS(B)
5450   I=EXP(A)*SIN(B)
5460 SUBEND !

5470 SUB Cmult(A1,B1,A2,B2,R,I)
5480   R=A1*A2-B2*B1
5490   I=A1*B2+B1*A2
5500 SUBEND !

5510 !
5520 SUB Filmdisp(W,Wp,Tau,H,E1,E3,Kxr,Kxi,Kxor,Kxoi,Kxir,Kxii)
5530   !  This subprogram calculates the OX - wavevector of a plasmon propagating
5540   !  The other interface of the metal film is with dielectric medium III,
5550   !      E1 - relative dielectric permittivity of the medium I (air)
5560   !      W  - is the frequency of the source of light in Hz
5570   !      H  - is the thickness of the metal film  in 'meters'
5580   !      Wp - is the plasma frequency in Hz
5590   !      Tau - is the relaxation time in seconds
5600   !      Kxr - REAL part of OX - wavevector of plasmon in metal film
5610   !      Kxi - IMAG. part of OX - wavevector of plasmon in metal film
5620   C=2.998E+8                                  ! Speed of light in vacuum in m/
```

```
5630  Ko=W/C                                        ! Wavevector of light in vacuum in 1/m
5640  E21=1-Wp^2/(W^2+1/Tau^2)                            ! REAL E2(w) of the metal film
5650  E22=Wp^2/(W^2+1/Tau^2)/W/Tau                         ! IMAG E2(w) of the metal film
5660  Dnm=(E1+E21)^2+E22^2
5670  Ao=(E1*E21*(E1+E21)+E1*E22^2)/Dnm
5680  Bo=(E22*E1^2)/Dnm
5690  A4=E1*E3+E21*(E3-E1)
5700  B4=E22*(E3-E1)
5710  A7=2*E1*E21
5720  B7=2*E1*E22
5730  A8=E21^2-E22^2-E1^2
5740  B8=2*E21*E22
5750! LOADSUB Cabs FROM "Complx"
5760! LOADSUB Csqrt FROM "Complx"
5770  CALL Csqrt(E1+E21,E22,A1,B1)
5780  CALL Csqrt(Ao,Bo,K1,K2)
5790  U=C/Wp                                            ! Normalizing factor
5800  Kxor=Ko*K1*U
5810  Kxoi=Ko*K2*U
5820! LOADSUB Cdivid FROM "Complx"
5830  CALL Cdivid(-2*Ko*H*E22,+2*Ko*H*E21,A1,B1,A2,B2)       ! Sign changed
5840! LOADSUB Cexp FROM "Complx"
5850  CALL Cexp(A2,B2,A3,B3)
5860  CALL Csqrt(A4,B4,A5,B5)
5870  CALL Cdivid(E3-A5,-B5,E3+A5,+B5,A6,B6)      ! A6,B6 - Real & Imag. parts of
5880  !                                          !                1/r32
5890  CALL Cdivid(A7,B7,A8,B8,A9,B9)            !
5900! LOADSUB Cmult FROM "Complx"
5910  CALL Cmult(A3,B3,+A6,+B6,A10,B10)
5920  CALL Cmult(A10,B10,A9,B9,A11,B11)
5930  CALL Cmult(Kxor,Kxoi,1+A11,B11,Kxr,Kxi)
5940  !
5950   Kxi1=Kxi-Kxoi
5960  SUBEND
5970  !
5980  SUB E21accuracy(Teta,Et,E1,E21,E22,E3,H,Det21,De21)
5990  !
6000  !
6010  ! Et=experimental accuracy of "Teta" determination
6020  Ssq=SIN(Teta)*SIN(Teta)
6030  Br=E1-E3*Ssq
6040  Dert=2*E1/Br/TAN(Teta)
      Det21=ABS(Dert)*Et
6060  De21=Det21
6070  SUBEND
6080  !
6090 SUB E22accu(Teta,Wt,Rm,Et,Ew,Er,E1,E21,E22,E3,H,Det22,Dew22,Der22,De22)
6100  !  This subprogram should be used for thicknesses  'H'  less than the
6110  !  optimal thicknes
6120  !  Et  - experimental accuracy of     "Teta" determination
6130  !  Ew  -                        of     "Wt"   determination
6140  !  Er  -                        of      "Ref" determination
6150  Ssq=SIN(Teta)*SIN(Teta)
6160  Rsq=SQR(Rm)
6170  Br=E1-E3*Ssq
6180  A=1+Rm-2*Rsq
6190  B=1-Rsq
6200  Dert=(Br+4*E3*Ssq)/Br/TAN(Teta)/(COS(Teta)^2)   !normalized Dert
6210  Derw=1/Wt                                       !normalized Derw
6220  Derr=(-B^2-.5*A)/Rsq/A/B                         !normalized Derr
```

```
6230  Det22=ABS(Dert)*Et
6240  Dew22=ABS(Derw)*Ew
6250  Der22=ABS(Derr)*Er
6260  De22=Det22+Dew22+Der22
6270  SUBEND
6280  !
6290  SUB Refl(Teta,W,Rr,Imr,Ref,R12,R23,D,E1,E3,E21e,E22e)
6300  ! Rr - is real part of the reflection coefficient of a single film
6310  ! Imr - is the imaginary part of the reflection coefficient
6320  ! Ref - is the reflectivity of a single film
6330  ! Note, E1 - stands for the prism
6340  !       E3 _ stands for the air
6350  E21=E21e
6360  E22=E22e
6370  Pi=3.14159265358979
6380  CALL Fr12(Teta,W,Rr12,Imr12,E1,E3,E21e,E22e)
6390  CALL Fr23(Teta,W,Rr23,Imr23,E1,E3,E21e,E22e)
6400  CALL Fex(Teta,W,D,R5,I5,E1,E3,E21e,E22e)
6410  R12=Rr12^2+Imr12^2
6420  R23=Rr23^2+Imr23^2
6430  R1=Rr12
6440  I1=Imr12
6450  R2=Rr23
6460  I2=Imr23
6470  R=R2*R5-I2*I5
6480  I=I2*R5+R2*I5
6490  A6=R1+R
6500  B6=I1+I
6510  A7=1+R1*R-I1*I
6520  B7=I1*R+R1*I
6530  GOTO 6580
6540  A6=Rr12+Rr23*R5-Imr23*I5
6550  B6=Imr12+R5*Imr23+I5*Rr23
6560  A7=1+Rr12*(Rr23*R5-Imr23*I5)-Imr12*(R5*Imr23+I5*Rr23)
6570  B7=+Imr12*(Rr23*R5-Imr23*I5)+Rr12*(R5*Imr23+I5*Rr23)
6580! PRINT Rr12;Imr12,Rr23;Imr23,R5;I5
6590! PRINT A6;B6;A7;B7
6600  CALL Cdivid(A6,B6,A7,B7,Rr,Imr)
6610  Ref=Rr^2+Imr^2
6620  SUBEND
6630  !
6640  SUB Opt_h(Tetae,W,Hinti,Hfnl,Hopt,Rmin,E3,E1,E21e,E22e)
6650  ! A subprogram for finding the optimal thickness of the metal film at
6660  ! whitch the coupling is maximum  (REFLECTIVITY - minimum)
6670  !    Teta - resonant angle in 'rad'
6680  !     w - frequency of the source in 'Hz'
6690  !     Hinti - initial thickness for the search  in 'angstroms'
6700  !     Hfnl  - final thickness for the search   in 'angstroms'
6710  !    Hopt  - determined by this subprogram the value of the optimal thick-
6720  !            ness in  'angstroms'
6730  !     Rmin  - the value of Reflectivity when H = Hopt
6740  !     E3 - is for the prism
6750  Rmin=1
6760  H_step=50
6770  IF Hinti>580 AND Hinti<640 THEN H_step=1
6780  FOR Ha=Hinti TO Hfnl STEP H_step              ! Thickness in angstroms
6790  Hmt=Ha*1.E-10                           ! Thickness in 'meters'
6800  CALL Refl(Tetae,W,Rr,Imr,Ref,R12,R23,Hmt,E3,E1,E21e,E22e)
6810  IF Ref<Rmin THEN Hopt=Ha
6820  IF Ref<Rmin THEN Rmin=Ref
```

```
6830  NEXT Na
6840  SUBEND
6850  !
6860  SUB Fr12(Teta,W,Rr12,Imr12,E1,E3,E21e,E22e)
6870            ! Teta - is the angle of incidence
6880            ! W    - is the frequency of the light source
6890            ! Rr12 - is the real part of the reflection coefficient  r12
6900            ! Imr12- is the imaginary part of the reflection coefficient  r12
6910  E21=E21e
6920  E22=E22e
6930  A1=E21
6940  B1=E22
6950  Q=E21^2+E22^2
6960  S=SIN(Teta)*SIN(Teta)
6970  A2=1-E1*E21*S/Q
6980  B2=E1*E22*S/Q
6990! LOADSUB Csqrt FROM "Complx"
7000! LOADSUB Cabs FROM "Complx"
7010  CALL Csqrt(A1,B1,R1,I1)
7020  CALL Csqrt(A2,B2,R2,I2)
7030  R1=R1*COS(Teta)
7040  I1=I1*COS(Teta)
7050  R2=R2*SQR(E1)
7060  I2=I2*SQR(E1)
7070  R12=R1-R2                                   !real part of numerator
7080  Im12=I1-I2                                  !imaginary part of numerator
7090  Rd12=R1+R2                                  !real part of denominator
7100  Imd12=I1+I2                                 !imaginary part of dinominator
7110! LOADSUB Cdivid FROM "Complx"  !
7120  CALL Cdivid(R12,Im12,Rd12,Imd12,Rr12,Imr12)
7130  SUBEND
7140  !
7150 SUB Fr23(Teta,W,Rr23,Imr23,E1,E3,E21e,E22e)
7160 E21=E21e
7170 E22=E22e
7180 S=SIN(Teta)*SIN(Teta)
7190 F=E3-E1*S
7200 A3=E21*E3^2-E1*S*E3^2
7210 B3=E22*E3^2
7220 IF F<0 THEN GOTO 7260
7230 R4=E21*SQR(F)
7240 I4=E22*SQR(F)
7250 GOTO 7280
7260 R4=-E22*SQR(-F)
7270 I4=+E21*SQR(-F)
7280 CALL Csqrt(A3,B3,R3,I3)
7290 R34=R3-R4
7300 Im34=I3-I4
7310 Rd34=R3+R4
7320 Imd34=I3+I4
7330 CALL Cdivid(R34,Im34,Rd34,Imd34,Rr23,Imr23)
7340 SUBEND
7350 !
7360 SUB Fex(Teta,W,D,R5,I5,E1,E3,E21e,E22e)
7370 E21=E21e
7380 E22=E22e
7390 RAD
7400 C=2.998E+8
7410 Pi=3.14159265358979
7420 K=W/C                              ! Vacuum wave vector magnitude in rad/m
```

16

```
8610   IF A8>Max THEN Max=A8
8620   IF NPAR=9 THEN RETURN Max
8630   IF A9>Max THEN Max=A9
8640   RETURN Max
8650 FNEND !


8660 !
8670  SUB Filmdisp2(W,Wp,Tetae,Wte,Rme,Hopt,H,E1,E3,Kxr,Kxi,Kxor,Kxoi,Kxir,K
8680  !  This subprogram calculates the OX - wavevector of a plasmon propaga
8690  !    for EXPERIMENTALLY MEASURED resonant angle Tetae, half-width Wte,
8700  !      minimum of reflectivity Rmin
8710  !  The other interface of the metal film is with dielectric medium III
8720  !     E1 - relative dielectric permittivity of the medium I (air)
8730  !     W  - is the frequency of the source of light in Hz
8740  !     H  - is the thickness of the metal film  in 'meters'  !!!!!!!!!
8750  !     Kxr - REAL part of OX - wavevector of plasmon in metal film
8760  !     Kxi - IMAG. part of OX - wavevector of plasmon in metal film
8770  C=2.998E+8                                ! Speed of light in vacuum in m.
8780  Ko=W/C                                   ! Wavevector of light in vacuum in
8790  S2=SIN(Tetae)*SIN(Tetae)
8800  E21=E1*E3*S2/(E1-E3*S2)           ! Exp-ly found REAL E2(w) of the metal
8810  IF H<Hopt THEN K=-1
8820  IF H=Hopt THEN K=0
8830  IF H>Hopt THEN K=+1
8840  E22=Wte*(1+K*SQR(Rme))*E1^2*E3*TAN(Tetae)/(2*(E1-E3*S2)^2)    ! IMAG. E:
8850  ! PRINT "E21_exp =";E21,"E22_exp = ";E22,"(line  8720)"
8860  Dnm=(E1+E21)^2+E22^2
8870  Ao=(E1*E21*(E1+E21)+E1*E22^2)/Dnm
8880  Bo=E22*E1^2/Dnm
8890  A4=E1*E3+E21*(E3-E1)
8900  B4=E22*(E3-E1)
8910  A7=2*E1*E21
8920  B7=2*E1*E22
8930  A8=E21^2-E22^2-E1^2
8940  B8=2*E21*E22
8950! LOADSUB Cabs FROM "Complx"
8960! LOADSUB Csqrt FROM "Complx"
8970  CALL Csqrt(E1+E21,E22,A1,B1)
8980  CALL Csqrt(Ao,Bo,K1,K2)
8990  U=C/Wp                                                        ! Normalizing fac
9000  Kxor=Ko*K1*U
9010  Kxoi=Ko*K2*U
9020! LOADSUB Cdivid FROM "Complx"
9030  CALL Cdivid(-2*Ko*H*E22,+2*Ko*H*E21,A1,B1,A2,B2)        ! Sign changed
9040! LOADSUB Cexp FROM "Complx"
9050  CALL Cexp(A2,B2,A3,B3)
9060  CALL Csqrt(A4,B4,A5,B5)
9070  CALL Cdivid(E3-A5,-B5,E3+A5,+B5,A6,B6)       ! A6,B6 - Real & Imag. part:
9080  !                                                 !              1/r32
9090  CALL Cdivid(A7,B7,A8,B8,A9,B9)          !
9100! LOADSUB Cmult FROM "Complx"
9110  CALL Cmult(A3,B3,+A6,+B6,A10,B10)
9120  CALL Cmult(A10,B10,A9,B9,A11,B11)
9130  CALL Cmult(Kxor,Kxoi,1+A11,B11,Kxr,Kxi)
9140 !
9150   Kxi1=Kxi-Kxoi
9160  SUBEND
9170  !
```

317

```
9180  SUB Opt_h_1(Tetae,Wte,Rme,E1,E3,Hopt1)
9190   S2=SIN(Tetae)*SIN(Tetae)
9200    E21e=E1*E3*S2/(E1-E3*S2)        ! Experimentally found E21(w)
9210    K=-1
9220    E22e=Wte*(1+K*SQR(Rme))*E1^2*E3*TAN(Tetae)/(2*(E1-E3*S2)^2)
9230    E22o=Wte*E1^2*E3*TAN(Tetae)/(2*(E1-E3*S2)^2)                ! At H=Hopt
9240    Delta=E22o-E22e                               ! Lines  1560 - 1670
9250    D1(J)=Delta                                   ! are a switch for Eta
9260    Dr(J)=D1(J)-D1(J-1)                            ! as a function of R min
9270    IF Dr(J)>0 AND J>1 THEN K=+1
9280    IF Dr(J)<0 THEN K=-1
9290    IF J=1 THEN K=-1
9300    Prod=Dr(J)*Dr(J-1)
9310    IF Prod<0 AND J>1 THEN Hopt1=H
9320    E22e=Wte*(1+K*SQR(Rme))*E1^2*E3*TAN(Tetae)/(2*(E1-E3*S2)^2)
9330    SUBEND
```